Modeling the Ignition of Soft Furnishings by a Cigarette

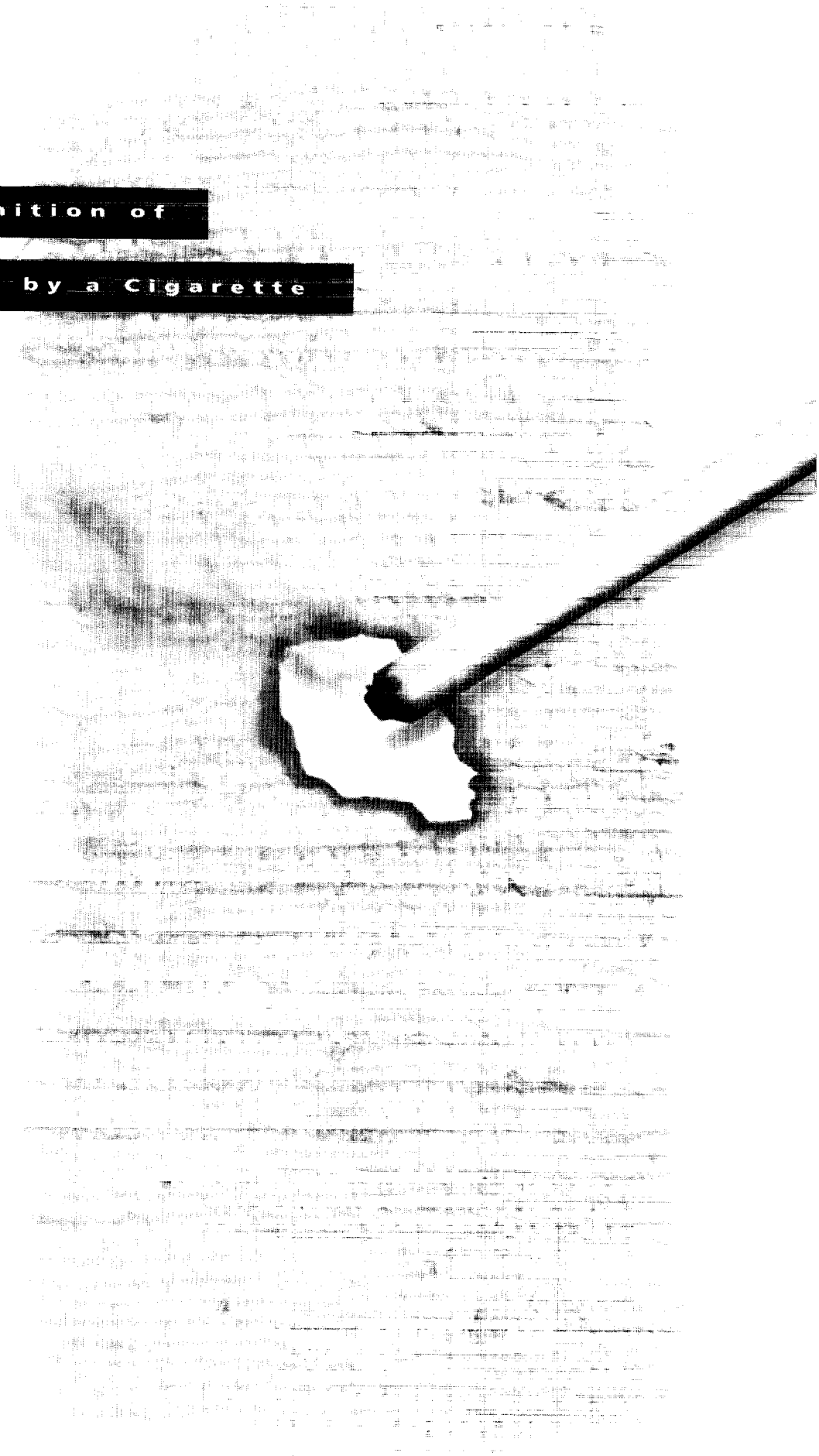

3

U.S. Department of Commerce

Technology Administration

National Institute of

Standards and Technology

August 1993

NIST Special Publication 852

NIST

Fire Safe Cigarette Act of 1990

Under the Cigarette Safety Act of 1984 (P.L. 98-567), the Technical Study Group on Cigarette and Little Cigar Fire Safety (TSG) found that it is technically feasible and may be commercially feasible to develop a cigarette that will have a significantly reduced propensity to ignite furniture and mattresses. Furthermore, they found that the overall impact of such a cigarette on other aspects of the United States society and economy may be minimal.

Recognizing that cigarette-ignited fires continue to be the leading cause of fire deaths in the United States, the Fire Safe Cigarette Act of 1990 (P.L. 101-352) was passed by the 101st Congress and signed into law on August 10, 1990. The Act deemed it appropriate for the U.S. Consumer Product Safety Commission to complete the research recommended by the TSG and provide, by August 10, 1993, an assessment of the practicality of a cigarette fire safety performance standard.

Three particular tasks were assigned to the National Institute of Standards and Technology's Building and Fire Research Laboratory:

- develop a standard test method to determine cigarette ignition propensity,
- compile performance data for cigarettes using the standard test method, and
- conduct laboratory studies on and computer modeling of ignition physics to develop valid, user-friendly predictive capability.

Three tasks were assigned to the Consumer Product Safety Commission:

- design and implement a study to collect baseline and follow-up data about the characteristics of cigarettes, products ignited, and smokers involved in fires,
- develop information on societal costs of cigarette-ignited fires, and
- in consultation with the Secretary of Health and Human Services, develop information on changes in the toxicity of smoke and resultant health effects from cigarette prototypes.

The Act also established a Technical Advisory Group to advise and work with the two agencies.

This report is one of six describing the research performed and the results obtained. Copies of these reports may be obtained from the **U.S. Consumer Product Safety Commission, Washington, DC 20207.**

3

Modeling the Ignition of Soft Furnishings by a Cigarette

Henri E. Mitler

George N. Walton

Building and Fire Research Laboratory

National Institute of Standards and Technology

Gaithersburg, MD 20899

U.S. Department of Commerce

Ronald H. Brown, Secretary

Technology Administration

Mary L. Good, Under Secretary for Technology

National Institute of Standards and Technology

Arati Prabakhar, Director

NIST Special Publication 852

August 1993

National Institute of Standards and Technology
Special Publication 852
Natl. Inst. Stand. Technol.
Spec. Pub. 852
169 Pages (Aug. 1993)
CODEN: NSPUE2

U.S. Government Printing Office
Washington: 1993

For sale by the Superintendent of Documents
U.S. Government Printing Office
Washington, DC 20402-9325

TABLE OF CONTENTS

LIST OF TABLES

LIST OF FIGURES

Certain commercial equipment, instruments, materials, or products are identified in this paper in order to specify the experimental procedure adequately. Such identification is not intended to imply recommendation or endorsement by the National Institute of Standards and Technology, nor is it intended to imply that the materials or equipment identified are necessarily the best available for the purpose.

MODELING THE IGNITION OF SOFT FURNISHINGS BY A CIGARETTE

Henri E. Mitler and George N. Walton

ABSTRACT

This paper describes the user-friendly computer models CIGARET and SUBSTRAT. CIGARET calculates the time-dependent behavior of a cigarette smoldering quietly in the air, away from surfaces. The model incorporates diffusion and convection of gases, as well as the kinetics of char oxidation. It calculates the internal heat fluxes, as well as the internal distributions of temperature, gas velocity, and oxygen concentration. SUBSTRAT determines whether a two-layer solid (with an air gap in between), exposed to a moving heating flux such as is produced by a cigarette, will ignite. Among the processes taken into consideration are three-dimensional heat conduction in the substrate and its pyrolysis. This model has successfully simulated the thermal runaway signifying smoldering ignition of the substrate when it is exposed to a set of external heating fluxes. SUBSTRAT and CIGARET have been designed to work in tandem to simulate the most frequent cause of fatal fires: cigarette ignition of upholstered furniture and bedding. Users' guides are included.

Key words: cigarettes; cigarette model; computer model; free smolder; furniture fires; ignition; mathematical modeling; modeling; pyrolysis; simulation; smoldering; substrates

I. INTRODUCTION

Lighted tobacco products (cigars, cigarettes, pipes) continue to be the leading ignition source for fatal fires in the United States (Miller, 1991). Most of those fires are established in soft furnishings: upholstered furniture and bedding. As a result, Congress passed the Cigarette Safety Act of 1984, with a goal to determine whether less fire-prone cigarettes were technically feasible. Under that Act, NIST developed prototype mathematical models of the components of this ignition scenario. The reason for having this capability is to "test" the effects that some particular change(s) in a cigarette will have on its propensity to ignite specified upholstered furniture quickly, cheaply, and repeatedly. The result was two prototype programs, TEMPSUB (for TEMPerature of a SUBstrate) and CIG25 (Gann *et al.*, 1988, Section 5).

Subsquent legislation, the Fire Safe Cigarette Act of 1990 (P.L. 101-352), mandated completion of such research, namely to:

> "(1) develop a standard test method to develop cigarette ignition propensity,
>
> (2) compile performance data for cigarettes using the standard test method developed under paragraph (1), and

(3) conduct laboratory studies on and computer modeling of ignition physics to develop valid, "user-friendly" predictive capability."

This publication describes the research performed and the results obtained in responding to the third task. The completion of the first two tasks is described in "A Computer Model of the Smoldering Ignition of Furniture," NISTIR 4973.

In this work, the ignition process is simulated using two computer codes, which are then used in tandem. While a single code of a fully interactive cigarette and substrate is ideal, the physical and numerical complexity of the combined burning near and at ignition renders it impossible to perform such computations on the personal computers of today.

Section II describes SUBSTRAT, a model of the time-dependent heating of substrate when subjected to a moving heat source, and establishes a criterion for its ignition. As in most soft furnishings, the substrate consists of a fabric layer over padding, with a potential air gap in between.

In order to examine how changing one or more properties of the cigarette will influence its ignition propensity, it is necessary to understand its behavior when smoldering. This includes knowing how its external heat flux and burning velocity depend on its various geometrical, physical, and/or chemical properties, and how these processes are modified when the cigarette lies on the substrate. Section III describes CIGARET, a model of a burning cigarette lying on a surface such as described above, describable by SUBSTRAT. Both the physics and chemistry of tobacco pyrolysis and simultaneous heat and gas transport in the cigarette are expressed by a set of coupled, nonlinear, partial differential equations with nonlinear boundary conditions. The model produces the time-dependent distributions of temperature, oxygen concentration, gas velocity, and burning rate in a freely smoldering cigarette which has user-prescribed properties.

In Section IV, we then describe how to use the two programs to simulate a burning cigarette on a susceptible substrate. SUBSTRAT reads an input file created by CIGARET, and also produces an output file which is used by CIGARET.

II. *SUBSTRAT*, A MODEL OF A SUBSTRATE SUBJECTED TO A MOVING HEAT SOURCE

A. Introduction

Consider what is involved in developing a computer model: we must simulate the behavior of a (typical) substrate when it is subjected to a heat flux. In order to do that, the physics and chemistry of the process must first be understood. It is then expressed as a set of equations describing the behavior; these equations must then be solved, with the appropriate data and boundary conditions. The solution method is numerical, and the data input is to a computer.

This program calculates the temperature of the upholstered furniture as a function of time and position, when it is exposed to a prescribed local heating flux. The furniture is simulated as a flat, horizontal cushioned seat; that is, a cushion consisting of fabric-covered foam padding. An air gap may be inserted between the two layers. The prescribed flux can be given either by a simple Gaussian function, or *via* an input file; if it is the former, the flux can be highly peaked at a point, vary with time, and move at a constant (specified) rate over the top surface of the furniture, assumed to be horizontal. The radiative and convective heat losses from the surface are given correctly. The temperature distribution within the substrate is calculated, since the temperature history will determine whether ignition takes place. If and when the temperature at a given location accelerates to a sufficiently high value ($\approx$ 500 °C), we can say that smoldering ignition has occurred. This is generally referred to as the **ignition** temperature, which is not unique, even for a well-defined material, depending also on the magnitude of the incident heat flux. The ambient oxygen level can be set at whatever value one wishes.

There are some limitations to this program. It will not tell whether **flaming** ignition takes place. It also does not treat the case where the flux is applied in a crevice, such as is formed between the seat cushion and the seat back. The program does not take oxygen diffusion within the cushion explicitly into account; hence in certain threshold situations, where a small change in oxygen concentration determines whether ignition does or does not take place, the results are ambiguous and not to be trusted. Note that it is often difficult to obtain the needed kinetic and/or thermophysical parameters for the materials; or, when available, to know how accurate they are. Therefore this caveat must also be made: even if the program were **perfect**, its results are only as good as the input parameters which are supplied. On the other hand, it should accurately reproduce or predict **trends**.

The first task is to examine the thermal response of the cushion to a specified flux distribution. This is done in Section II.B. [The flux data from the cigarette is described in Section III.] In Section II.C, the numerical solution method is presented, and some of the physics is revisited in this (numerical) context. In Section II.D we discuss a set of experiments where a mock-up was ignited, give the measured ignition times, and give the input data required to make computer runs. The results of these runs are given and then discussed in Section II.E, validating the model to some degree. Section II.F summarizes the work. For the reader interested in a more extensive discussion of this type of modeling, see the references cited here, especially the bibliography in Gann *et al.* (1988). A copy of the program on disk may be obtained from the authors, as well as a listing of the program and the program itself.

B. IGNITION DYNAMICS

The equations describing the relevant physical processes taking place in the substrate will be written in this Section. They will mostly be written in general form to start, and then particularized to our problem. The physical phenomena included in the model are summarized in Table 1 and discussed below.

Table 1. Features of the Substrate Model

Included	Not Included
two porous layers with an air gap	oxygen diffusion
3-d heat conduction	melting and/or regression of the foam
variable (prescribed) thermophysical properties	
correct (nonlinear) boundary conditions	
endothermic (non-oxidative) pyrolysis	
exothermic (oxidative) pyrolysis	
char oxidation	
arbitrary (prescribed) moving heat source	
variable grid on a moving coordinate system	
(approximate) radiative heat transfer within the material	
impinging air flow, when wanted	

1. Surface Heat Source

The potential ignition process is initiated by external heating of the surface. Thus, it is necessary to specify the heat gains at the bounding surfaces of the cushion. The cushion is assumed to be a rectangular parallelepiped, so a Cartesian coordinate system is employed. For the top surface, we first treat the localized heat flux from the glowing tip of the cigarette or other heat source. The flux consists of two parts, one due to convection (ϕ_c) and one due to radiation (ϕ_r):

$$\phi_{in} = \phi_c + \phi_r \tag{1}$$

ϕ_{in} is the heating flux reaching the surface. For a cigarette, these fluxes are strong functions of position, since the glowing tip is only a few millimeters in extent. With this formulation, ϕ_r can be expressed in the approximate form:

$$\phi_r \sim \Omega \epsilon_{cig} \sigma T_{cig}^4 + (1-\Omega)\sigma T_a^4 \tag{2}$$

where $\Omega = \Omega(\mathbf{r})$ is the shape, or view, factor of the cigarette as seen by the substrate at the point **r**. It is only approximate in this form, because the cigarette surface temperature, T_{cig}, varies strongly with position.

The convective flux is given by

$$\phi_c(x,y,t) = h[T_{cig}(x,y,t) - T_s(x,y,t)] \tag{3}$$

where h is the heat transfer coefficient, T_s is the surface temperature of the substrate, which is explicitly shown to be a function of position and time, and where T_{cig} is the cigarette surface temperature, also a function of position and time. It is important to point out here that in the TMPSUB2 version of the substrate model, the source flux must be specified by the user; in SUBSTRAT, on the other hand, the source flux can be either specified or it can be read in by the program, from a file produced by CIGARET.

It is equally necessary to specify the heat losses. If the existence of the cigarette is neglected for the moment, so that the view factors need not be considered, then

$$\phi_{out} = h(T_s - T_a) + \epsilon \sigma T_s^4 \tag{4}$$

where the first term is the convective cooling term and the second is the radiative cooling term. In contrast to the source term, these losses are explicitly included in the program. Here, the dependence of T_s on x, y, and t has not been shown explicitly. ϵ is the emissivity of the surface and σ is the Stefan-Boltzmann constant. (Note: we have used ε where sometimes α, the **absorptivity** of the surface, should be used. When there is thermal equilibrium between the radiation field and the hot surface, then $\alpha = \varepsilon$. We have assumed the latter, for simplicity). Evidently, the loss rate from the cushion surface increases as it heats up. h is determined by the laws of fluid flow, as well as the thermal properties of air; the simplest way to find h, however, is to use well-known expressions, usually derived from correlations. This will be further discussed below.

Along with the partial differential equation (12), we must have boundary conditions: for the top surface, the net flux entering the surface at each point is connected to the net flux according to

$$\phi_{net}(x,y,t) = -\kappa \left(\frac{\partial T(x,y,z,t)}{\partial z} \right)_{z=0} \qquad z=0, \quad t>0 \tag{5}$$

where

$$\phi_{net} \equiv \phi_{in} - \phi_{out} \cdot \tag{6}$$

When the cigarette lies on the substrate, the mean convective heating flux over the heating region is given by

$$\phi_c = h_{in}(\bar{T}_{cig} - T_s) \tag{7}$$

If h_q is the heat transfer coefficient for quiescent air, then the surface heat loss for the areas away from the cigarette is

$$\phi_{out} = h_q(T_s - T_a) \tag{8}$$

The boundary condition is greatly simplified if we can say that equation (8) is valid over the entire surface. That is readily achieved by using the **model** convective heating flux ϕ_c^*,

$$\phi_c^* = h_{in}(\bar{T}_{cig} - T_s) + h_q(T_s - T_a) \tag{9}$$

h_{in} is found as follows: the mean initial convective flux from a cigarette was measured to be 37 kW/m^2. Taking the mean value of the cigarette surface temperature to be about $<T>_{cig} \approx 450$ °C, the mean heat transfer coefficient in this area is $h_{in} \approx (37000/430) = 86$ W/m^2 K. h_q is found from Table 7-1 of Holman (1981): the Nusselt number for a heated, horizontal, upward-facing surface is

$$Nu = 0.54(Ra)^{1/4} \tag{10}$$

where Ra is the Rayleigh number. Since $h = \kappa Nu/L$, where L is the characteristic dimension of the surface, we find:

$$h = 0.54\,\kappa\left[\frac{g\beta(T_s - T_a)}{\alpha\nu L}\right]^{1/4} \tag{11}$$

where β is the volumetric coefficient of (gas) expansion. Taking the value for $T_s = 500$ K ≈ 227 °C as an approximate mean temperature of the surface, and L = 7 mm, we find:

$$h_q = 9.7 \text{ W/m}^2\text{-K}$$

For the other surfaces, the boundary conditions (b.c.) can be expressed in different forms, depending on whether the slab for which we are making calculations is exposed to the air, or is embedded within the cushion. If the slab were the entire cushion -- that is, the other five surfaces are exposed to the air, then the b.c. would be that the heat fluxes $\kappa\partial T/\partial x$, $\kappa\partial T/\partial y$, $\kappa\partial T/\partial z$, are given by terms of exactly the same form as (4), except that h is different for the vertical and the downward-facing horizontal surface. On the other hand, the numerical calculation we are using makes using the entire cushion prohibitively large. We therefore consider a subsection abstracted from the whole cushion, and the other five faces are surrounded by more foam. If that foam were a perfectly insulating material, then the b.c. at those faces is the adiabatic condition; that is, no flux crosses the surfaces: $\kappa\partial T/\partial x = \kappa\partial T/\partial y = \kappa\partial T/\partial z = 0$. This eliminates any heat losses from the slab, and makes the calculated temperatures somewhat higher than they really are. A simpler b.c. is to assume that the temperature at the five faces is constant and unchanging, remaining at the original (usually ambient) temperature. This produces a larger temperature gradient than actually prevails, and errs in the opposite direction. That is the default b.c. used in the calculation, but which of the two b.c.'s is used is determined by an input parameter.

2. Heat Transfer

The partial differential equation which describes the conduction of heat in a solid, when there is no radiation heat transfer, does so by giving the rate of change of temperature at every point within the solid. It is (see, *e.g.*, Carslaw and Jaeger (1959))

$$\rho\frac{\partial cT}{\partial t} = \text{div}(\kappa\,\text{grad}\,T) + S \tag{12}$$

where T, which is a function of position and of time, is the variable for which we are trying to find a solution. The other symbols in this equation are: ρ is the density of the solid, c its specific heat, κ its thermal conductivity, and S is any volumetric heat source or sink. ρ, c, κ, and S may vary with position and with T. Because these may vary in equation (12), it is conceptually simple to consider a substrate which consists of layers of material. Indeed, it will be straightforward to implement this in practice, as well. Note that because we only have derivatives of T, T need not be the absolute temperature: it may be taken to be that relative to a convenient reference temperature. In other places, such as in equation (2), it must be taken to be absolute (*i.e.*, in Kelvins).

The first term on the right-hand side describes the diffusion of heat in the solid. If there is any release of heat -- usually by combustion -- at the (interior) point in question, it is given by S(x,y,z,t). A general expression for S is

$$S = \sum_i R_i H_{ci} + L_v \frac{\partial \rho}{\partial t} \tag{13}$$

where R_i is the reaction rate (in kg/m^3-s) and H_{ci} is the heat of combustion (in J/kg), for the ith reaction. If there is endothermic pyrolysis or evaporation, we have the last term on the right-hand side as well, where L_v is the latent heat of evaporation or pyrolysis. An explicit expression for R_i will be given in Section II.B.4.

Since the furniture (apart from the frame) consists of a fabric-covered pad, it is clear that the program must take at least two layers (with different properties) into account. Therefore the program was written so as to permit different values for the relevant thermophysical constants ρ, c, and κ in each layer. In fact, generally there is not perfectly intimate thermal contact between the fabric covering and the padding; there is a small but sometimes significant intervening air gap. Normally, one would place a node within this gap, in order to take a third layer into account; because of the thinness of the gap, and other technical difficulties, however, a different treatment of the effect of this air gap has been devised: the gap can be represented in terms of its "thermal resistance." (See Section II.C.3.) This has been programmed and successfully tested.

In writing equation (12), we have made the simplifying assumption that the cushion is totally opaque; that is, there is no radiative transfer of heat through the cushion. If there were, the equation describing heat transfer through the solid would become still more complicated. However, the fabric and foam can each be thought of as porous, consisting of solid parts interspersed with void spaces. Then taking forward radiation transfer in those spaces, it is possible to incorporate a first approximation to (one-d) radiation transfer, as shown by Kunii (1961)

$$\kappa(T) = (1 - \Phi^{2/3})\kappa_s + \Phi^{1/3}(\kappa_g + 2h_r D_p/3) \tag{14}$$

where Φ is the void fraction, and κ_s and κ_g are the solid and gas-phase thermal conductivities, respectively; they are each functions of T. D_p is the mean pore diameter, and

$$h_r = 4\epsilon\sigma T^3 \tag{15}$$

Equation (14) was equation (5-50) in Gann *et al.* (1988). Finally, we must note that at a given temperature, the thermal conductivity is proportional to the density (also see Section II.C.5):

$$\kappa(\rho) = (\rho/\rho_a)\kappa(\rho_a) \tag{16}$$

3. Time to Ignition

An experimental test for the time to ignition is described in Section II.D. We can readily make an order-of-magnitude estimate for this time, based on equation (12). For the very special case that the substrate is initially at the uniform temperature T_o, that it is homogeneous, isotropic, inert, and semi-infinite, that the thermophysical characteristics ρ, c, and κ of the material are independent of the temperature, and that the problem is one-dimensional (*i.e.*, the incident flux is the same everywhere on the plane z = 0, resulting in the slab being subjected to the uniform net heating flux $\phi_{net}(t)$), then equation (12) can be solved analytically and explicitly, and it can be shown (Carslaw and Jaeger, 1959, p.76) that the surface temperature is given by

$$T_s(t) = T_o + \frac{1}{\sqrt{\pi\kappa\rho c}} \int_0^t \frac{\phi_{net}(t')\,dt'}{\sqrt{t-t'}} \tag{17}$$

For the still simpler (unrealistic) case ϕ_{net} = constant, this can be immediately integrated, and we obtain

$$T(t) = T_o + \frac{2\phi_{net}\sqrt{t}}{\sqrt{\pi\kappa\rho c}} \tag{18}$$

When the left-hand side reaches the ignition temperature T_{ig}, the time elapsed must be the time in the right-hand side of the equation, and may be called the ignition time:

$$t_{ig} = \frac{\pi\kappa\rho c}{4}\left(\frac{T_{ig}-T_o}{\phi_{net}}\right)^2 \tag{19}$$

Although not a single one of the simplifying assumptions required to obtain equation (19) is valid, this expression is nevertheless very useful as a guide to the form of the dependence of t_{ig}. In particular, we will use equation (19) in order to make sense out of the experimental observations, in Section II.E.1.

[We can, at some cost in computation time, get a somewhat more realistic result by relaxing one of the assumptions above: it is possible to write, starting with equation (17), an explicit expression for $T_s(t)$ for the case where the net flux is not constant, but results from some impressed external flux, diminished by a Newtonian (*i.e.*, linear) cooling loss; that is, where we can write $\phi_{loss} = h^*(T_s - T_s)$; see Quintiere (1988)].

4. Pyrolysis of the Substrate

As described above, we assume that the substrate consists of a thin fabric covering a relatively thick foam pad, with a very thin air gap between them. Each of the two materials will be heated and can pyrolyze. In this Section we describe how these reactions are calculated. Pyrolytic reactions can generally be expressed in the Arrhenius form

$$R_p(T,\rho_f,\rho_o) = A\,\rho_f^m\,\rho_{ox}^n\,e^{-E_A/RT} \qquad \mathrm{kg/m^3 \cdot s} \tag{20}$$

where ρ_f is the density of the fuel and ρ_{ox} that of oxygen; E_A is the activation energy for the reaction, and R is the universal gas constant (not to be confused with the reaction rate R_p in equation (20)). It is sometimes convenient to define an "activation temperature" T_A:

$$T_A \equiv E_A/R \tag{21}$$

In the remainder of the paper, R is used only to represent a reaction rate. All the quantities in equation (20) except the pre-exponential factor A are at the location (x,y,z) within the porous solid and at the time t; this dependence is not shown explicitly in order to minimize the complexity of the expression. Similarly, the subscript i, corresponding to ith "reaction" has been suppressed from R, A, ρ_f, m, n, and E_A. If the reactions were truly elemental Arrhenius reactions, then m = n = 1. However, equation (20) is really a model equation, and therefore m and n are purely empirical parameters (just as A and E_A are), and need not be integers.

Oxidative as well as non-oxidative pyrolysis (thermal decomposition) of materials have been included. The former reactions are generally exothermic, while the latter are generally endothermic. There may be several oxidative reactions as well as several non-oxidative ones; char oxidation, when it takes place, is the last step. In this model a maximum of three reactions is permitted for each material. The oxidative reactions are exothermic; we assume that the rate of each step (reaction) is adequately described by an Arrhenius equation of the form (20).

It had been hoped that the different pyrolysis steps take place at sufficiently different temperatures, that the reaction sequence for the ignition of the fabric could be taken to consist of a small number of steps which follow each other sequentially. That would correspond to the equations taking the form

$$R_p = \sum_i R_{p,i} = \sum_i A_i (\rho - \rho_i)^{s_i} \rho_{ox}^{n_i} \exp(-T_i/T) \tag{22}$$

where ρ_i is the density of the fuel at the end of the i^{th} reaction step. When the reaction produces a gaseous species which escapes, the reaction rate is given by

$$R_p = -\frac{\partial \rho}{\partial t} \tag{23}$$

More generally, if species i is reacting and producing species j, then

$$\frac{\partial \rho_i}{\partial t} = -R_i = -\frac{\partial \rho_j}{\partial t} \tag{24}$$

We will here discuss only the pyrolysis of the fabric, which is of principal interest: when smoldering ignition is produced, it is almost always first initiated in the fabric. Pyrolysis of the foam is discussed briefly in Section II.D.2. The fabric of particular interest is cotton duck; cotton is principally cellulose.

Analysis of the reaction kinetics of a cellulosic paper by Kashiwagi and Nambu (1992) showed that it could be described by three reactions, all of which will proceed simultaneously (though obviously at different rates). That means that the equations describing the creation and destruction of different fuel species must be included. Virgin material goes to char, *via* two pathways: degradation and oxidative pyrolysis. Each gram produces n_c grams of char. The char then goes to ash, *via* char oxidation. Each gram of char produces n_a grams of ash. Thus one gram of material produces $n_a n_c$ grams of ash. The governing equations are

$$\dot{\rho}_v = -R_d - R_{op} \tag{25a}$$

$$\dot{\rho}_c = n_c(R_d + R_{op}) - R_{co} \tag{25b}$$

and

$$\dot{\rho}_a = n_a R_{co} \tag{25c}$$

The density of the solids is

$$\rho_s = \rho_v + \rho_c + \rho_a \tag{25d}$$

Hence

$$\dot{\rho}_s = -(1 - n_c)(R_d + R_{op}) - (1 - n_a)R_{co} \tag{25e}$$

The subscripts denote:

a = ash	op = oxidative pyrolysis
c = char	s = solid
co = char oxidation	v = virgin material
d = degradation	

Besides the surface heat source described in Section II.B.1, there are also internal heat sources (and sinks), given by equation (13). The heats of combustion must be supplied by the user of the model; those for cotton are given in Section II.D. The global kinetic constants given by Kashiwagi and Nambu are also listed in Section II.D. If the reaction rate of one or more exothermic reactions becomes high, for any reason, the rate at which energy is being generated will exceed the rate at which it is lost, and a "thermal runaway" will ensue, very similar to a chain reaction. During the runaway, the rate of pyrolysis (and of heating) is limited by the availability of oxygen. Since O_2 has 0.001 times the density of the local fuel, it would immediately be exhausted, but for the supply which (a) diffuses in from adjoining cells, and that which (b) diffuses in (or is convected in) from the surface.

5. Gas Diffusion

As oxygen is depleted in the regions where combustion (oxidative pyrolysis, char oxidation) is taking place, the concentration gradient which results will induce diffusion of oxygen into those regions, from the surface as well as from adjacent, oxygen-rich regions, assuming the medium is porous and permits diffusion. Similarly, the gaseous (and other) products which are generated -- mainly CO_2 -- build up in local concentration, and diffuse away.

The equations which describe the rate of change of species concentration are analogous to equation (12) for the diffusion of heat; assuming no convection, the ith species density is governed by

$$\frac{\partial \rho_i}{\partial t} = \mathrm{div}(D_{io} \,\mathrm{grad}\, \rho_i) + S_i \tag{26}$$

where D_{io} is the diffusion coefficient for species i in the background "o," and S_i is the source/sink term. If the diffusion coefficient increases with T, as it normally does, then the CO_2 diffusion, for example, will take place preferentially towards the hot regions, *i.e.*, towards the surface. The migration of gases is expected to have a minor effect on the heat transfer, and hence on the temperature distribution, from

this effect. However, the diffusion of oxygen is important: the rate at which oxygen enters the reacting region sets the limit on the reaction rate.

A porous medium is one consisting of solid particles embedded in a gaseous medium. Put in a different way, a gas molecule cannot penetrate any of the solid phase, but is able to traverse the entire medium, either because of a pressure difference, or merely from the "random walk" which constitutes diffusion. The diffusivity of a gas species in such a medium is really the diffusivity of those gas molecules through a gaseous medium consisting of the same or some other gas, where the solid volumes are excluded. That is the **effective** diffusivity.

It has been found experimentally (Szekely *et al.*, 1976) that, approximately,

$$D_{eff} = D_o \Phi^n \tag{27}$$

where Φ is the fractional void space; this is also referred to as the "porosity" in the literature. The relationship is strongly dependent on the structure of the (granular) material; thus, Figure 2.4 from Szekely *et al.*, 1976, shows that for particles of mica,

$$D_{eff}/D_o = \Phi^{10.3} \tag{27a}$$

whereas for sand, a bed of glass spheres, carborundum powder, and table salt,

$$D_{eff}/D_o = 0.677\,\Phi^{1.18} \tag{27b}$$

for $\Phi < 0.7$. As shown in Appendix E, $\Phi \approx 0.6$ for the cotton fabric that will be our main focus of interest; hence equation (27b) is the relationship to be used.

Here D_o is the diffusivity of O_2 in N_2. From equation (16.3-1) of Bird *et al.* (1960), we find that for O_2 in N_2, the temperature dependence is

$$D_o(T) = 0.199\left(\frac{T}{293.16}\right)^{1.823} \quad \text{cm}^2/\text{s} \tag{28}$$

6. Boundary Conditions for Gases

There are two cases of interest: first, when the air above the substrate is quiescent, and second, when -- as was the case in the experiment to be described in Section II.D -- there is a stream of air impinging on the substrate. We first obtain a general expression:

When the air above the substrate is quiescent, and there are oxidative reactions taking place in the substrate, the concentration of oxygen molecules in the air decreases towards the surface, through a boundary layer. The maximum possible reaction rate is obtained by assuming $y_s = 0$, as can be seen from equation (29). On the other hand, this is clearly not possible, since we must have a finite concentration at the surface in order to get any reactions at all. It is possible to obtain a value for y_s analytically, if one makes the simplifying assumptions of an isothermal substrate and a first-order reaction rate (Ohlemiller, 1991).

Mass transfer is a (molecular) transport phenomenon, just as is heat (momentum) transfer. Thus, analogous to the first term on the right-hand side of equation (4), the mass transfer of oxygen across the surface of the solid can be written as

$$\dot{m}''_{O2}(x,y) = k_{gas}[Y_a - Y_s(x,y)] \tag{29}$$

where Y_a is the ambient oxygen mass fraction and Y_s that at the solid surface; the x,y dependence of the latter has been put in explicitly in order to emphasize the origin of the spatial dependence of $\dot{m}_{02}$". This is the boundary condition.

Note: The **velocity** at which oxygen enters the surface is

$$V_o = D\left(\frac{\partial Y}{\partial x}\right)_s = \gamma(Y_a - Y_i) \tag{30}$$

(see Gann *et al.*, 1988, pp. 159-160) where D is the diffusion coefficient inside the solid. Thus

$$k_{gas} = \rho_a \gamma \tag{31}$$

where γ is the normalized mass transfer coefficient for oxygen traversing the boundary layer above the substrate. In SUBSTRAT (see Gann *et al.* (1988), equation (5-64) (from Muramatsu, 1981)), the following equation was used for γ:

$$\gamma_b = 6.38x10^{-3}\left[\frac{T^{2.75}(T - T_a)(T + 123.6)}{R T_a}\right]^{1/4} \quad \text{cm/s} \tag{32}$$

where the subscript "b" refers to "boundary layer". On the other hand, in this paper we obtain γ in a different way; we will afterwards use equation (32) in order to compare the results. The way γ is obtained is as follows: Because of the similar origin of mass and heat transfer, one can often use the Reynolds-Colburn analogy. It is not difficult to show, from the treatment in Chapter 3 of Treybal (1955), that the Reynolds-Colburn analogy leads to

$$\gamma = \frac{h\,Pr^{2/3}}{\rho\, c_p\, Sc^{2/3}} \quad \text{m/s} \tag{33}$$

where h is the heat transfer coefficient appropriate to the problem, Pr is the Prandtl number, Sc is the Schmidt number (Sc = ν/D), and ν is the kinematic viscosity. Once we have γ_b, equation (31) gives k_{gas}, to be used in equation (29).

Case A. Quiescent air

Here we have

$$h = \kappa\, Nu / l_c \tag{34}$$

where κ is the thermal conductivity, l_c is a characteristic dimension for the problem, and Nu is the Nusselt number. We can thus rewrite equation (33) as

$$\gamma = \frac{\alpha}{l_c} Nu \left(\frac{Pr}{Sc}\right)^{2/3} \tag{35}$$

In quiescent air, there is a constant movement of molecules in all directions; the flow in any one direction is exactly compensated by the flow in the opposite direction, normally. If, however, the gas is near a boundary which "absorbs" some of these molecules (as is the case for oxygen impinging on a reactive substrate) then evidently the return flow is smaller, and hence the impinging flow is not completely nullified. The result is that there is a gradual decrease in the concentration of those molecules as the surface is approached. This region is referred to as the "boundary layer."

The quantities in equation (35) are to be evaluated at some characteristic (mean) temperature of the boundary layer. That temperature can be taken to be the mean between T_a and T_s. For quiescent air, with the surface horizontal and facing upward, l_c is the boundary layer thickness. The expression for the Nusselt number is given in Section II.B.1.

Case B. Impinging Air

The Nusselt number for this case is given by equation (D10), Appendix D. Inserting that into equation (35), we obtain

$$\gamma \approx 0.767 \frac{\alpha}{l_c} \sqrt{Re}\, Pr^{1.07} Sc^{-2/3} \tag{36}$$

where α is the thermal diffusivity of air, $Re \equiv u_o l_c/\nu$ is the Reynolds number and u_o is the incoming velocity of the impinging flow.

We now show that when oxygen consumption is significant, it takes place in a very narrow layer; this is analogous to the flame sheet approximation for combustion in air. As a result, we may take the concentration of oxygen in that layer to be some appropriate average value, rather than having to actually program in the species diffusion equations, *via* equation (26).

7. Oxygen Diffusion

In this Section, it is shown that a reasonable approximation to the overall reaction rate can be obtained without explicitly solving the gas diffusion equation, equation (26), for the diffusion of oxygen in the substrate. This is the approximation made in the model.

In the experiment to be discussed in Section II.D, a jet of air is directed downward at the substrate. Hence there is no boundary layer in this case, and the oxygen concentration just outside the surface is 21%. When the reaction rate is low, the oxygen concentration in the top of the substrate will not be much affected by the slow reactions. When the reaction rate becomes high, on the other hand, the mean oxygen concentration in that thin layer becomes low. It cannot get too low, however, since (as discussed in Section II.B.6), the reaction rate would then fall. Hence a quasi-steady state is established. Thus, in the "runaway" phase, the reaction rate must be given by the boundary condition equation (29).

We will now argue that when significant oxidative pyrolysis is taking place,

(a) taking a constant value for the oxygen concentration ($[O_2]$) in the substrate is a valid approximation,

(b) most of the pyrolysis occurs in the surface layer, and therefore

(c) we obtain an adequate approximation to the pyrolysis rate, without explicitly including the oxygen diffusion equations.

When the surface temperature is relatively low, there is negligible pyrolysis, and the oxygen distribution $[O_2](x)$ in the substrate is approximately uniform. When T_s has risen to the point that perceptible pyrolysis is taking place at and near the surface, the $[O_2]$ profile in the substrate dips as the surface is approached from below (*i.e.*, from within);it must reach a minimum and then rise again at the surface, because of the diffusion of oxygen from outside. When the temperature reaches values so high that $[O_2]$ is pulled down to negligible values near (but not at) the surface, the principal source of oxygen in the reaction zone is from the air diffusing in from the surface; the region where there is significant oxidative reaction is then highly localized near the surface, with $[O_2]$ being highest at the surface, and falling rapidly until it reaches negligible values. The characteristic oxygen penetration distance is δ, and it is clear that δ is a steeply falling function of T. [At some further distance in, the oxygen must diffuse towards the surface from other (deeper, or peripheral) parts of the porous substrate, because of the concentration gradient, so that the profile must rise again as we go deeper. It can do so because at that depth the temperature has fallen sufficiently to "freeze out" the (oxidative) reaction rate, *i.e.*, it is negligibly small].

Suppose that T_s is high enough to drive $[O_2]$ to near-zero at some depth. Then we may write, crudely,

$$Y(x) \sim Y_s e^{-x^2/\delta^2} \tag{37}$$

with Y_s = surface value of $[O_2]$, and δ = characteristic penetration depth. If we write the reaction rate in the form

$$R[x,T(x)] = Y(x)^n F[x,T(x)] \equiv Y^n G(x) \tag{38}$$

then the total reaction rate per unit area is

$$\dot{m}'' = \int_o^\infty Y(x)^n G(x)\, dx \tag{39}$$

where G(x) is a fairly steep (decreasing) function of x. We may thus further write (still very crudely)

$$G(x) \sim G_o e^{-x^2/\theta^2} \tag{40}$$

Then

$$\dot{m}'' \sim \int_o^\infty Y_s^n e^{nx^2/\delta^2} G_0 e^{-x^2/\theta^2}\, dx = G_0 Y_s^n \frac{\sqrt{\pi}}{2}\left(\frac{1}{\theta^2} + \frac{n}{\delta^2}\right)^{-1/2} \tag{41}$$

We use the mean-value theorem, and write the integral in equation (41) as

$$\int_o^\infty \bar{Y}^n G_o e^{-x^2/\theta^2}\, dx = \bar{Y}^n G_o \theta\sqrt{\pi}/2 \tag{42}$$

Then

$$\bar{Y}^n = Y_s^n \left(1 + \frac{n\theta^2}{\delta^2}\right)^{-1/2} \tag{43}$$

We now need an estimate for θ/δ. Clearly, the reaction rate must be significant for a distance comparable to the penetration depth δ: else, if the reactions "froze" before $[O_2]$ becomes negligible, $[O_2]$ would not fall below some appreciable value. Moreover, the reaction rate cannot be significant below that depth, precisely because there is so little oxygen below. Thus $\theta \approx \delta$. For n, we take $n_o = 0.5$, as given in Kashiwagi and Nambu (1992). Then equation (43) yields

$$\bar{Y} = 2Y_s/3 \tag{44}$$

Next, consider the effect of discretizing the equations (Section II.C). If $\delta > \Delta x$, then assuming that the reaction takes place in the top cells only, clearly underestimates the reaction rate. However, when δ is large, the total reaction rate is very low. That is, while the fractional error is large, the absolute error is small, and (we shall show) typically negligible.

Assume, for the sake of simplicity, only one oxidation reaction. Assume, also, that the temperature and reaction rate are uniform in a thin sheet of depth δ at the surface, where T is maximum. (This is essentially what is implicitly assumed in the numerical calculation.) Then if the stoichiometric fuel/oxygen ratio is r, the fuel burnup rate is

$$R\delta = \dot{m}_f'' = r\,\dot{m}_{ox}'' \tag{45}$$

where R is the reaction rate (g/cm^3s or kg/m^3s). If δ is greater than the thickness of the surface cell, then evidently the reaction rate in the top layer is limited to $R\Delta z$; whereas if $\delta < \Delta z$, equation (45) gives the limit. Thus the reaction rate in the top cell is

$$R_{top}\Delta z = \min[R\Delta z,\ r\,\dot{m}_{ox}''] \quad g/cm^2\text{-}s \tag{46}$$

Note that when the reaction rate is so high that $\delta < \Delta z$, the concentration at the bottom face of the top cell(s) is close to zero; therefore a reasonable value to take for $[O_2]$ in the cell is on the order of the mean value, 11%, (or 0.12 for the mass fraction); or, according to equation (44), $\langle Y \rangle \approx \frac{2}{3}(0.2318) = 0.15$.

We now make a calculation to find a typical value for δ. As is clear from equation (45), we must begin by calculating a reaction rate R. In order to find R, we must anticipate some results from Section II.D.2. Using equations (79) and (80), we find that

$$R_{op} = \rho_v k_{op} = \rho_v\ 1.5\text{x}10^{14}\ Y^{0.5}\ (W_d/W_o)^{1.3}\ \exp(-160/RT)$$

and

$$R_{co} = \rho_c k_{co} = \rho_c\ 3.4\text{x}10^{11}\ Y^{0.78}\ (W_c/W_o)\ \exp(-160/RT)$$

The meaning of the subscripts is made clear in the list below equation (25e). These rates are in kg/m^3 min. We must choose characteristic values for ρ_v, Y, W_d/W_o, ρ_c, W_c/W_o, and T, in order to get estimates. Reasonable values are:

$$W_d = W_o/2,\ W_c = W_o/4,\ \text{and}\ Y \approx 0.11$$

For ρ_v and ρ_c, we assume that the volumes are unchanged, so that

$$\rho_v/\rho_o = W_d/W_o \quad \text{and} \quad \rho_c/\rho_o = W_c/W_o$$

Finally, we take $\rho_o = 1560$ kg/m^3. We then find that

$$k_{op} = 2.02\text{x}10^{13} \exp(-160/RT) \ \text{min}^{-1}$$

and

$$k_{co} = 1.52\text{x}10^{10} \exp(-160/RT) \ \text{min}^{-1}$$

The universal gas constant R = 8.31447 J/mol-K, so that the activation temperature for both reactions is

$$T_A = 160{,}000/R = 19244 \text{ K}.$$

For a temperature in the vicinity of the ignition temperature, say, 400 °C = 673.16 K, we then have

$$k_{op} = 7.77 \text{ min}^{-1} \quad \text{and} \quad k_{co} = 0.00584 \text{ min}^{-1},$$

yielding

$$R_{op} = \rho_v k_{op} = 101 \text{ kg/m}^3 \text{ s}$$

and

$$R_{co} = \rho_c k_{co} = 0.038 \text{ kg/m}^3 \text{ s}.$$

Thus at 400 °C, with these assumptions for ρ_v and ρ_c, oxidative pyrolysis takes place more than 2600 times faster than does char oxidation, and we may therefore take

$$R = R_{op} = 101 \text{ kg/m}^3 \text{ s}$$

Next, we need to have the rate at which oxygen enters the medium, $\dot{m}''_{ox}$. Equations (29) and (31) give the required value. For the ignition experiment, the appropriate expression to use to find γ is equation (36). The temperature at which the various quantities must be evaluated is that of the purging gas. Examination of Table D-1 in Appendix D shows that T_g is quite high. Assume $T_g = 800$ K. Equation (28) yields $D_o(800) = 1.24$ cm^2/s. Then the Schmidt number is Sc = 0.663, and

$$\gamma \approx 8.10\text{x}10^{-5} \sqrt{\text{Re}} \, / \ell_c \ \text{m/s}$$

(with ℓ_c in meters). The characteristic air velocity for calculating Re is given by eauation (D15) in Appendix D. Finally, the characteristic length ℓ_c is the standoff distance, δ. With $\delta = 5.4$ mm, we find Re = 11.06 and $\gamma = 4.99$ cm/s. (Incidentally, if we had quiescent air at 800 K, Muaramatsu's expression, equation (32), yields $\gamma_b \approx 2.35$ cm/s).

Finally, taking $Y_a = 0.232$ and $Y_s = 0$, equations (29) and (31) then yield

$$\dot{m}''_{ox} \approx 13.6 \text{ g/m}^2\text{s}$$

We must also have r (the stoichiometric fuel/oxygen ratio) in order to use equation (45) to get the penetration depth δ. The stoichiometric air/fuel mass ratio for wood is S = 5.78, close enough to that for cellulose. Hence r $\approx$ 0.746, and we find $\delta = 0.10$ mm. Thus the penetration depth δ is indeed much smaller than the layer thickness Δx (which is of the order 0.5 mm).

For T_s = 300 °C, on the other hand, we find k_{op} = 0.053 min^{-1}, so that R_{op} = 1.38 kg/m^3 s. Then $\delta \approx$ 7.3 mm, several times Δx, but the resulting mass-loss rate is only 0.043 g/m^2 s, which is indeed negligible.

For the case of quiescent air above the substrate, the mean value for the oxygen concentration to be used in the top cell during the runaway, is midway between the value at the top surface (*i.e.*, at the bottom of the boundary layer), and at the bottom of the top cell (presumably, close to zero).

The only time that we cannot justifiably make the simplification that the oxygen concentration in the top layer is either that at the top surface or half (or 2/3) that value (during runaway), is when the reaction rate is intermediate between the very low values and the runaway value. This period should be relatively short, and the error introduced by these simplifications should not be large.

C. NUMERICS

In general, it is not possible to solve equation (12) analytically, in spite of the simplifying assumption of no radiation heat transfer, and even for the case S=0. That is, to write down an explicit expression which gives T in terms of the inputs. This is so, because of the nonlinear and nonuniform boundary conditions. It is therefore necessary to resort to a numerical procedure, which is that incorporated in TMPSUB2 and SUBSTRAT. Hereafter, we shall only refer to the latter, when something applies to both, as is the case here).

1. Introduction

The development of TMPSUB2 centers around the capability to simulate transient heat transfer. A one-dimensional heat conduction problem provides the simplest example to illustrate transient simulation methods. Figure 1 shows a portion of a one-dimensional conduction problem in which the material has been divided into thin layers. This example will be described by physical instead of mathematical arguments following the description given by Clausing (1969, pp.157-213).

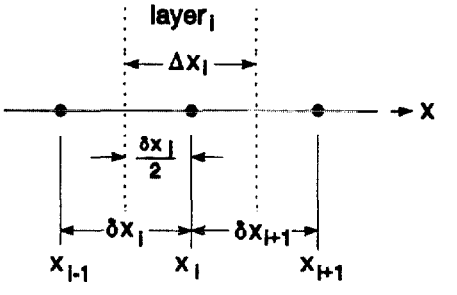

Figure 1. One-dimensional conduction

The figure focuses on a representative layer of material of thickness Δx_i centered in a node at coordinate x_i. This material layer is represented by a single temperature T_i and a corresponding thermal conductivity κ_i, density ρ_i, and specific heat c_i. Assume this layer has a surface area of magnitude A in the Y-Z plane. The distance between nodes i and i-1 is given by δx_i (= $x_i - x_{i-1}$). Subscripts i and n refer to positions in space and time, respectively. Subscript n is temporarily suppressed until it becomes necessary to consider time, in the following equations.

The instantaneous internal energy of layer i is given by

$$U_i = \rho c \Delta V T_i = \rho c \Delta x_i A T_i = C_i T_i \tag{47}$$

where T is the absolute temperature. This equation also serves to define the heat capacity, C, assigned to node i. Heat is transferred to and from layer i by three methods:

(1) conduction from layer i-1 at the rate

$$q_{i-} = (T_{i-1} - T_i)\,\kappa_{i-} A / \delta x_i = K_{i-}(T_{i-1} - T_i) \tag{48}$$

(2) conduction from layer i+1 at the rate

$$q_{i+} = (T_{i+1} - T_i)\,\kappa_{i+} A / \delta x_{i+1} = K_{i+}(T_{i+1} - T_i) \tag{49}$$

(3) internal heat generation or radiation absorbed within the layer, S_i.

Equations (48) and (49) define the thermal conductance, K, in each direction. The possibility of a thermal conductivity which varies with position is explicitly taken into account here using labels + and —: κ_{i-} and κ_{i+}. A good first order approximation for κ_{i-} is the harmonic average of κ_i and κ_{i-1}:

$$\kappa_{i-} \approx \frac{2\kappa_i \kappa_{i-1}}{\kappa_i + \kappa_{i-1}} \tag{50}$$

with a similar expression for κ_{i+}.

The change in internal energy of this layer between time t_n and time t_{n+1} is given to first order in Δt by

$$\Delta U_{i,n-n+1} \equiv C_{i,n+1}T_{i,n+1} - C_{i,n}T_{i,n} = \Delta t\,(q_{i-} + q_{i+} + q_i) \tag{51}$$

where the time dependence has now been put in explicitly. There are several common solutions to equation (51) depending on when the heat gains are evaluated. One solution involves evaluating at time n

$$C_{i,n+1}T_{i,n+1} = C_{i,n}T_{i,n} + \Delta t\,[K_{i-}(T_{i-1,n} - T_{i,n}) + K_{i+}(T_{i+1,n} - T_{i,n}) + S_{i,n}] \tag{52}$$

which is the standard Euler explicit time integration formula. "Explicit" means that $T_{i,n+1}$ can be directly computed from values known at time n. On the other hand, evaluating at time n+1 gives

$$C_{i,n+1}T_{i,n+1} = C_{i,n}T_{i,n} + \Delta t\,[K_{i-}(T_{i-1,n+1} - T_{i,n+1}) + K_{i+}(T_{i+1,n+1} - T_{i,n+1}) + S_{i,n+1}] \tag{53}$$

which is Euler's standard implicit time integration formula. "Implicit" means that $T_{i,n+1}$ is computed from other values also evaluated at time n+1. These values depend implicitly on each other and must be computed by a solution of simultaneous equations.

Clausing (1969, p.190) also gives a discussion of stability in terms of thermodynamic laws. Rearranging equation (52) to solve for $T_{i,n+1}$ gives

$$T_{i,n+1} = (K_{i-,n}T_{i-1,n} + K_{i+,n}T_{i+1,n} + S_{i,n})\,\Delta t / C_{i,n+1} + T_{i,n}[C_{i,n} - (K_{i-,n} + K_{i+,n})\,\Delta t] / C_{i,n+1} \tag{54}$$

where the time subscript, n, has been added to the K terms to indicate exactly when these values are evaluated. For the sake of argument, assume $C_{i,n+1} = C_{i,n}$ ($=C_i$) for simplicity. There is no solution if $C_i = 0$. If C_i is sufficiently small or Δt sufficiently large, then $(K_{i-,n} + K_{i+,n})\,\Delta t / C_i > 1$, and

as $T_{i,n}$ increases $T_{i,n+1}$ must decrease, and vice versa. This is thermodynamically impossible. It shows up in a numerical solution as oscillations, *i.e.*, "instability," in the node temperatures at each time step. These oscillations tend to quickly increase to totally meaningless values. In general, the smaller the thermal mass of the element, the smaller the time step needed for a stable explicit solution. This suggests a simple technique to determine the minimum stable time step for any element in the system.

Thus, rearranging the implicit (53) to solve for $T_{i,n+1}$ gives

$$T_{i,n+1} = \frac{C_{i,n}T_{i,n} + \Delta t\,(K_{i-,n+1}T_{i-1,n+1} + K_{i+1,n+1}T_{i+1,n+1} + S_{i,n+1})}{C_{i,n+1} + \Delta t\,(K_{i-,n+1} + K_{i+,n+1})} \tag{55}$$

This equation shows none of the computational or thermodynamic problems of equation (54), indicating that the standard implicit method is stable for all time steps.

The spatial discretization error (for a uniform grid) for the standard explicit and standard implicit methods is proportional to $(\Delta x)^2$ (for a variable grid, the accuracy is reduced somewhat; see Section II.C.4). The time discretization error is proportional to Δt.

The standard explicit and standard implicit methods err in opposite directions. Therefore, a more accurate solution can be obtained by combining the two methods. Expressing this combination generally in terms of a parameter β gives

$$\Delta U_{i,n\to n+1} = \Delta t\,[(1-\beta)(q_{i-,n} + q_{i+,n} + S_{i,n}) + \beta(q_{i-,n+1} + q_{i+,n+1} + S_{i,n+1})] \tag{56}$$

where $0 \le \beta \le 1$.

$\beta = 0$ corresponds to the standard explicit method,
$\beta = 1/2$ corresponds to the Crank-Nicholson method,
$\beta = 2/3$ corresponds to the Galerkin method, and
$\beta = 1$ corresponds to the standard implicit method.

For $\beta \ge 1/2$ this method is unconditionally stable, although the solution may be oscillatory. For $\beta > 3/4$ (approximately) the solution is stable and non-oscillatory. For $\beta = 1/2$, the time discretization error is proportional to $(\Delta t)^2$.

The methods presented above extend directly into three dimensions. For a Cartesian coordinate system and a cell of dimensions Δx_i by Δy_j by Δz_k, equation (51) can be rewritten to account for conduction from the six adjacent cells in the 3-D system:

$$\Delta U_{i,j,k} = \Delta t\,(q_{i-,j,k} + q_{i+,j,k} + q_{i,j-,k} + q_{i,j+,k} + q_{i,j,k-} + q_{i,j,k+} + S_{i,j,k}) \tag{57}$$

where

$$q_{i-} = (T_{i-1,j,k} - T_{i,j,k})\,\kappa_{i-}\,\Delta y_j\,\Delta z_k / \delta x_i$$

$$q_{i+} = (T_{i+1,j,k} - T_{i,j,k})\,\kappa_{i+}\,\Delta y_j\,\Delta z_k / \delta x_{i+1}$$

$$q_{j-} = (T_{i,j-1,k} - T_{i,j,k})\,\kappa_{j-}\,\Delta x_i\,\Delta z_k / \delta y_j$$

$$q_{j+} = (T_{i,j+1,k} - T_{i,j,k})\,\kappa_{j+}\,\Delta x_i\,\Delta z_k / \delta y_{j+1}$$

$$q_{k-} = (T_{i,j,k-1} - T_{i,j,k})\,\kappa_{k-}\,\Delta x_i\,\Delta y_j / \delta z_k$$

$$q_{k+} = (T_{i,j,k+1} - T_{i,j,k})\,\kappa_{k+}\,\Delta x_i\,\Delta y_j / \delta z_{k+1}$$

and $S_{i,j,k}$ represents other heat added directly to the cell.

2. Boundary Conditions

Special treatment is required for cells on the boundaries of the region being modeled. In particular, the nodes which represent the cells are placed on the boundary, rather than at the center. Referring to the one-dimensional example in Figure 1, the surface layer is only half as thick as the others.

An adiabatic boundary condition (b.c.) is handled by setting the appropriate heat flux terms in equation (45) to zero. A constant temperature (isothermal) b.c. is handled by leaving the temperature unchanged.

The surface of the substrate (z=0 plane; see Figure 3) transfers heat to the environment by convection and by radiation. The convective heat gain for cell i,j,1 is given by

$$(S_c)_{i,j,1} = (T_a - T_{i,j,1})h\,\Delta x_i \Delta y_j \tag{58}$$

where T_a is the temperature of the surrounding (ambient) air, and h is the heat transfer coefficient.

A positive value of S_c represents a heat gain by the cell. The radiative heat gain is given by

$$(S_r)_{i,j,1} = \sigma\epsilon(T_a^4 - T_{i,j,1}^4)\,\Delta x_i \Delta y_j \tag{59}$$

where

T_a is the temperature of the surrounding surfaces,
σ is the Stefan-Boltzmann constant, and
ϵ is the emissivity of the fabric (assuming that α, the absorptivity, $= \varepsilon$).

The temperatures in equation (59) must be absolute (Kelvin) temperatures. In TMPSUB2 the temperature of the surrounding surfaces is assumed equal to the air temperature. (Note that equation (59) can be rewritten in an apparently linear form similar to equation (58):

$$(S_r)_{i,j,1} = [\sigma\epsilon(T_a + T_{i,j,1})(T_a^2 + T_{i,j,1}^2)](T_a - T_{i,j,1})\,\Delta x_i \Delta y_j \tag{59a}$$

This form will be useful further on.

The heat flux from a smoldering cigarette to the fabric is, for the "prescribed flux" choice of input, represented by the following pair of equations:

$$\phi_s(x,y,t) = \phi_{max}\exp\left[-\left(\frac{x - x_o - vt}{\sigma_{x+}}\right)^2 - \frac{y^2}{\sigma_y^2}\right] \qquad (x \geq x_o + vt) \tag{60a}$$

and

$$\phi_s(x,y,t) = \phi_{max}\exp\left[-\left(\frac{x-x_o-vt}{\sigma_{x-}}\right)^2 - \frac{y^2}{\sigma_y^2}\right] \qquad (x<x_o+vt) \tag{60b}$$

This heat flux is converted to a heat gain, S_g, by multiplying the flux at the position of the node by the cell surface area. These values are adjusted slightly so that their (discrete) sum is equal to the total heat flux represented by equations (60a,b):

$$\int_{-\infty}^{\infty}\int_{-\infty}^{\infty}\phi_s\,dx\,dy = \frac{\pi}{2}\phi_m\sigma_y[\sigma_{x+}+\sigma_{x-}] \tag{60c}$$

3. Air Gap

Since the furniture (apart from the frame) consists of fabric-covered padding, it is clear that the program must take at least two layers (with different properties) into account. Therefore the program was written so as to permit different values for the relevant thermophysical constants ρ, c, and κ at each node. In fact, generally there is not perfectly intimate thermal contact between the fabric covering and the padding: there is a small but sometimes significant intervening air gap. Normally, one would place a node within this gap, in order to take a third layer into account; because of the thinness of the gap, and other technical difficulties, however, a different treatment of the effect of this air gap has been devised: the gap can be represented in terms of its "thermal resistance."

The optional air gap between the fabric and the padding is modeled by assuming one-dimensional heat transfer. Figure 2 shows the basic configuration and nomenclature for an air gap of thickness s between cells i,j,k and i,j,k+1. s is small relative to the separation between the cells, δ_{k+1}. Although pyrolysis of the fabric and the possible melting and/or pyrolysis of the padding may well change the dimensions of the air gap, the simplifying assumption is nevertheless made here that the air gap has fixed and uniform dimensions. The heat transfer between these cells is given by

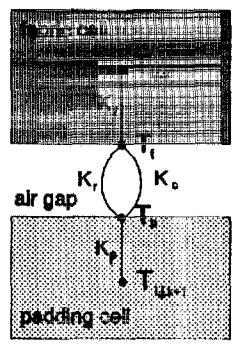

Figure 2. Air gap heat transfer model

$$q_{i,j,k+} = K(T_{i,j,k}-T_{i,j,k+1}) \tag{61}$$

where K is an implicit function of $q_{i,j,k+}$, $T_{i,j,k}$, and $T_{i,j,k+}$.

The overall heat transfer coefficient is given by

$$K = \frac{1}{\frac{1}{K_f} + \frac{1}{K_p} + \frac{1}{K_r + K_c}}$$

where the fabric conductance is

$$K_f = 2\Delta x_i \Delta y_j \kappa_{i,j,k} / \delta_{k+1} \ ,$$

the padding conductance is $K_p = 2\Delta x_i \Delta y_j \kappa_{i,j,k+1} / \delta_{k+1}$,

the fabric (bottom) surface temperature is $T_f = T_{i,j,k} - q_{i,j,k+} / \kappa_{i,j,k}$,

the padding surface temperature is $T_p = T_{i,j,k+1} + q_{i,j,k+} / \kappa_{i,j,k+1}$,

the radiant conductance is

$$K_r = \frac{\sigma \Delta x_i \Delta y_j (T_f + T_p)(T_f^2 + T_p^2)}{\frac{1}{\epsilon_f} + \frac{1}{\epsilon_g} - 1} \ ,$$

and the convective conductance is

$$K_c = \Delta x_i \Delta y_j \kappa_{air} / s \ .$$

The conductance of the air, κ_{air}, is evaluated at the average of T_f and T_p. These equations are solved to give K and $q_{i,j,k+}$ during the overall process used to compute cell temperatures.

4. Variable Grid

The heat from the cigarette spreads into the substrate by conduction. In order to correctly estimate the temperatures near the peak, it is important that conduction to the outer boundaries (at $x=0$, $x=x_{max}$, $y=y_{max}$, and $z=z_{max}$) be negligible, since it cannot be known *a priori*. This requires a relatively large region relative to the size of the cigarette heat flux pattern. However, setting Δx, Δy, and Δz sufficiently small to achieve the desired accuracy in the conduction calculation can result in an extremely large number of cells ($N = (x_{max}/\Delta x) \cdot (y_{max}/\Delta y) \cdot (z_{max}/\Delta z)$) with correspondingly large memory requirements and computation time.

The heating flux from a smoldering cigarette rises from negligible values to a high peak, on the order of 60 kW/m^2 over a region only a few millimeters in extent. In order to follow this faithfully, the region must be covered by a mesh which is fine enough so that there are no changes from one mesh point to another large enough to produce numerical inaccuracies or instabilities. Thus, the required size of the grid is inversely proportional to the temperature gradient, where steep temperature gradients occur only near the point of peak heat flux. Therefore, a variable grid is used. This grid consists of a few constant-width cells near the peak followed by cells of regularly increasing size to the outer boundaries. The increase in cell size is based on geometric progression, and can be different for each axis. Thus, for example, $\Delta y_{j+1} = R_y \Delta y_j$ ($R_y \geq 1$). The general effect of this variable grid is shown in Figure 3. This is easy to implement in equation (45) which explicitly incorporates the grid sizes. The variable grid gives

results which are less accurate than a constant grid. A benchmark test indicates that the results for R = 1.23 differ by < 0.11% at t = 100 s. from those obtained for the constant grid case, with still smaller errors for R closer to unity. (See Table A-1, Appendix A.)

Note: In choosing a grid, the user determines four items, in each coordinate direction: the width of the constant-width cells in the fine-grid region, the number of such cells, the total number of nodes along that axis, and the total width in that direction. The program then does the arithmetic, and finds the corresponding value of R_i. If that is < 1, an error message will be returned. Likewise, if too many grid points result from the attempted selection, an error message will result.

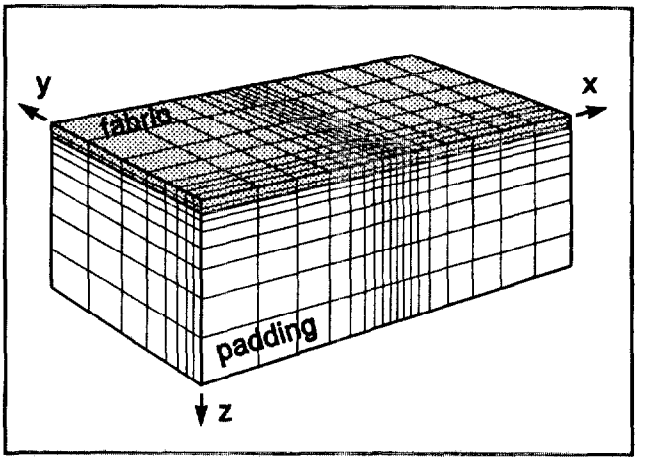

Figure 3. Substrate coordinate system

The point of peak heat flux moves as the cigarette smolders. TMPSUB2 adjusts the x-coordinates to keep the fine grid region centered on that peak. This adjustment is made by

(1) computing the new x-coordinates of the shifted grid,
(2) computing a cubic spline curve for the temperature in each row of cells in the old grid, and
(3) using the curve to compute the cell temperatures in each row at the new grid positions.

The standard explicit algorithm for solving equation (12), without pyrolysis included, was checked in several ways, principally by comparing its predictions against known analytical solutions. (See Appendix A.) These checks showed that the numerical procedure, and the computer program for implementing it, are correct, effective, and accurate.

5. Variable Thermal Properties

The conductivity and specific heat of the substrate materials are known to vary with temperature. TMPSUB2 allows the user to describe this variation. The values entered for κ and c are converted to cubic spline curves giving $\kappa(T)$ and c(T). The conductivity is further adjusted within the program to take into account the fact that the thermal conductivity is proportional to the density:

$$\kappa = \rho\, \kappa(T) / \rho_o, \tag{62}$$

where ρ_o is the original density (recall that the assumption of constant κ, ρ, and c, in Section II.B.3, was a special case used only in order to obtain equations (17) to (19)).

6. Pyrolysis

Consider pyrolysis from the finite difference viewpoint. We begin with a cell having constant volume, ΔV (= $\Delta x\, \Delta y\, \Delta z$) and temporarily ignore the subscripts i,j,k. This cell contains a mass $\rho_v\, \Delta V$ of virgin (unpyrolyzed) material, a mass $\rho_c\, \Delta V$ of char, and a mass $\rho_a\, \Delta V$ of ash. The numerical method must

keep track of the density of each material as a function of time; in this program, this is done *via* the difference equation

$$\rho_{x,n+1} = \rho_{x,n} + \Delta t\, \dot{\rho}_{x,n+\beta} \tag{63}$$

where the subscript x may be v, c, or a, and β indicates the type of time integration, as discussed above. $\dot{\rho}_x$ is modeled using equations (25a,b,c). Note that $\rho_a = \rho_c = 0$ and $\rho_s = \rho_v = \rho_o$ at t = 0.

Some material is converted to gases during pyrolysis; the rate as which gases are created is given by equation (25e). The gases are lost from the cell, and they carry away all the energy they contain, *i.e.*, there is an enthalpy loss which does not affect the temperature of the remaining mass. Moreover, since the gas diffusion equations have not been explicitly included, any possible loss of heat from the escaping hot gases to the cooler solid in other regions of the substrate is ignored. Thus, the rate of heat gain in the cell due to pyrolysis is (almost exactly) given by

$$S_p = \Delta V(R_d H_d + R_{op} H_{op} + R_{co} H_{co} + \dot{\rho}_s c T) \qquad \text{Watts} \tag{64}$$

The R_i are given in Section II.B.3, and $d\rho_s/dt$ is given by equation (25e).

7. Time Integration

A choice must be made for the time integration method. Following the discussion of Belytschko (1983, pp. 55, 419, 445), the advantages of explicit time integration are:

(1) fewer calculations per time step;
(2) simple algorithm logic and structure are simple, implying that it is good for testing new ideas;
(3) ease of handling complex nonlinearities;
(4) requirement of little core storage compared to implicit methods using direct elimination procedures; and
(5) high reliability in terms of accuracy and completing the computation.

The only notable disadvantage is that explicit time integration is only conditionally stable so that a very large number of time steps may be required.

With regard to accuracy, since implicit methods are unconditionally stable, they can easily be used with too large a time step, leading to significant time integration errors. The stability requirements for explicit time integration force the time step to be so small that the time integration error is almost always smaller than the spatial discretization error. Of course, it is also possible to use a spatial discretization that is much too large.

The addition of pyrolysis to the model required significantly smaller cells in the region of interest, and therefore required significantly longer execution time. Hence a better method than explicit time integration was required. The following method attributed to Saul'yev as described by Larkin (1964) and Clausing (1969) was adopted:

Again consider the one-dimensional presentation of Figure 1. Assume that the calculation of cell temperatures is proceeding in the positive x direction. Then at cell i, $T_{i-1,n+1}$ is a known quantity and can be used in computing $T_{i,n+1}$. Equation (51) becomes

$$\Delta U_{i,n\to n+1} \equiv C_{i,n+1}T_{i,n+1} - C_{i,n}T_{i,n} = \Delta t(q_{i-,n+1} + q_{i+,n} + S_{i,n+\beta}) \tag{65a}$$

During the next time step, calculate cell temperatures in the negative x direction. In that case equation (51) becomes

$$\Delta U_{i,n\to n+1} \equiv C_{i,n+1}T_{i,n+1} - C_{i,n}T_{i,n} = \Delta t(q_{i-,n} + q_{i+,n+1} + S_{i,n+\beta}) \tag{65b}$$

Both equations (65a) and (65b) are unconditionally stable because of the inclusion of the implicit terms; operating together, the truncation errors during successive time steps tend to cancel leading to an $O(\Delta t^2)$ algorithm. This method is directly expanded into 2 or 3 dimensions by adding the j and k position indices and the q_{j-}, q_{j+}, q_{k-}, and q_{k+} heat gains. The key factor is that it is only necessary to solve implicitly for one cell temperature at a time. There are no time-consuming simultaneous equations to be solved. Tests indicate that this method is very accurate except for the possibility of some small oscillations as with the Crank-Nicholson method.

A question remains on when to evaluate S_i, C_i, and κ_i (which is implicit in the q's) in equation (65a). Numerical errors are minimized by evaluating S_i at time step $n+\frac{1}{2}$. These terms are all functions of temperature in the SUBSTRAT program. Furthermore, they are such complicated functions that the equations cannot be solved directly. The following equation must be solved implicitly for $T_{i,j,k,n+1}$:

$$\begin{aligned} U_{i,j,k,n+1} = U_{i,j,k,n} + \Delta t\,(& q_{i-,j,k,n+1} + q_{i+,j,k,n} + q_{i,j-,k,n+1} + q_{i,j+,k,n} \\ & + q_{i,j,k-,n+1} + q_{i,j,k+,n} + S_{i,j,k,n+\beta}\,) \end{aligned} \tag{66}$$

where

$$U_{i,j,k,m} = \rho_{i,j,k,m}\,\Delta V_{i,j,k}\,c_{i,j,k,m}\,T_{i,j,k,m}$$

with m = n and n+1. The total solid density in the cell is the sum of the virgin, char, and ash densities [equation (25d)] and is a function of time due to the pyrolysis reactions:

$$\rho_{i,j,k,n+\beta} = (\rho_v + \rho_c + \rho_a)_{i,j,k,n} + \beta\,\Delta t\,(\dot{\rho}_v + \dot{\rho}_c + \dot{\rho}_a)_{i,j,k,n+\beta} \tag{67}$$

The cell pyrolysis for the time step is evaluated at $T = (T_n + T_{n+1}) / 2$, and component densities also at $\beta = \frac{1}{2}$. Equation (66) was rewritten in a form allowing numerical solution by a standard secant method (Conte, 1972, pp. 299-306). This completes the outline of Larkin's method. The net result of using Larkin's method is that the time step is no longer limited by grid size, and pyrolysis is modeled with a reasonable execution time.

D. EXPERIMENTS

1. Experimental Arrangement

The next step is to compare the results predicted by SUBSTRAT with experimental results, in which an electrical heater was substituted for a cigarette. The schematic of an experiment designed to measure time to ignition is shown in Figure 4. This consists of the heater element from an automobile cigarette lighter, fitted with a concentric jacket to permit an air purge. The purpose of the air purge is to keep evolved products from the sample from being ignited to flaming, rather than to merely smolder. The heating element is raised to varying temperatures, all of them high enough for the element to be glowing (500 - 900 °C). The purging jet comes through the jacket, past the face of the element, and then out normal to it, toward the sample. It picks up a good deal of heat as it travels through the device. The resulting flux distribution beneath the heating element is shown in Figure 5. As we would expect, it is axially symmetric; it is well fitted by a Gaussian profile. Note that the higher the temperature the disk is heated to, the higher is the peak flux.

The measured flux to the gauge is not the same as what the substrate sees, however, because the latter heats up, whereas the flux gauge does not; call the former ϕ_g and the latter, ϕ_s. It follows from equation (3) that

$$\phi_g = \phi_{rad} + \phi_c = \phi_{rad} + h(T_g - T_c) \tag{68}$$

where T_g is the temperature of the hot purging gas, T_c that of the (cold) gauge, and $\phi_s \equiv \phi_{in}$. For the case where the substrate is being heated, however, the convective contribution goes down:

$$\phi_s = \phi_{rad} + h[T_g - T_s(t)] \tag{69}$$

where $T_s(t)$ is the temperature of the substrate, which increases continuously. Thus the total flux decreases monotonically. Although we do not know the gas temperature T_g, we do not need it; for, we can combine equations (68) and (69) to obtain

$$\phi_s(t) = \phi_g - h[T_s(t) - T_c] \tag{70}$$

The heat transfer coefficient h was discussed in Section II.B. It is found for this experimental configuration in Appendix D. Analysis of the experimental results, given in Appendix D, yields a number of values important for this experiment, including h and the disk temperatures; the results are shown in Table D-1; h is found to be a weak function of ϕ_{ext}.

When a mock-up consisting of flexible PU foam covered by #12 cotton duck was placed in position under the heat source, smoldering ignition occurred after a certain amount of time; the ignition delay depends on the intensity of the flux, as indicated qualitatively by equation (19), Section II.B.2. The experimentally obtained ignition delays are plotted in Figure 6 as a function of the peak heat flux.

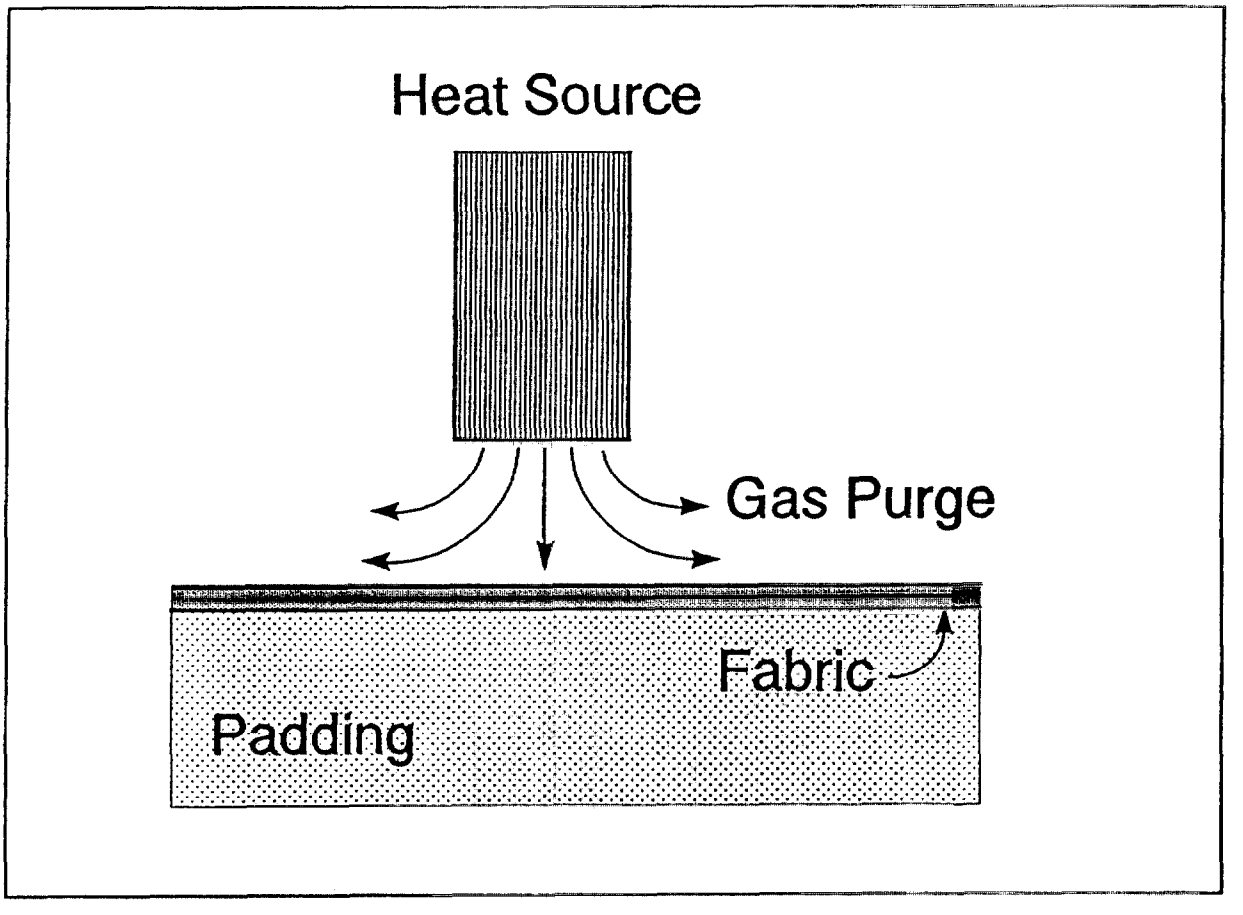

Figure 4. Schematic of heat source for ignition tests

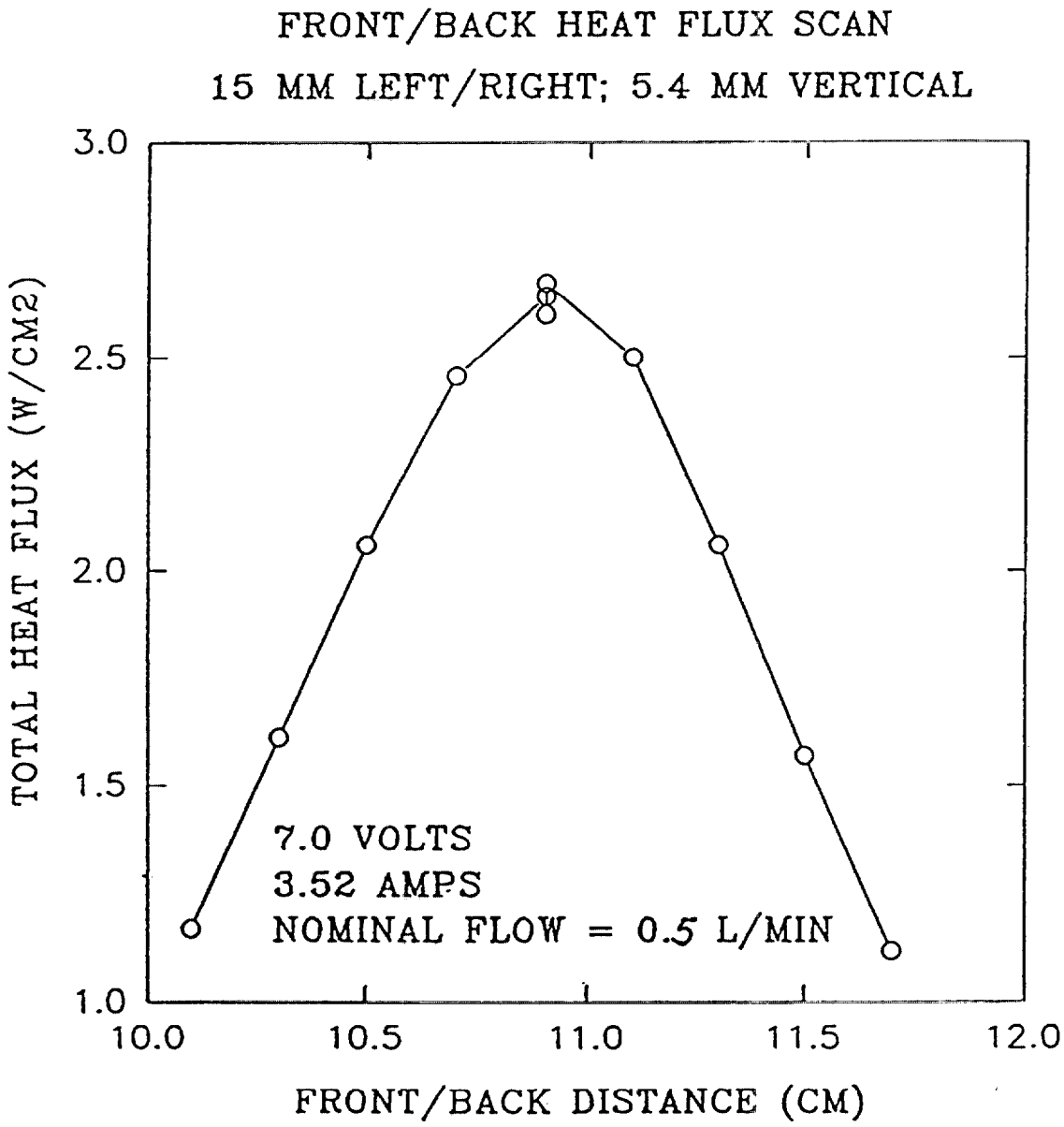

Figure 5. Flux profile from heat source, as measured by a total heat flux gauge

The ignition delay times as a function of the external flux are given in Table 2.

Table 2. Substrate Ignition Delay Times

$\phi_{ext}(kW/m^2)$	18	25	34.5	44
$t_{ig}(s)$	472	70	37	22

Since ϕ_{net} is constant for each run, then according to equation (19), a plot of ϕ_{ext} versus $t_{ig}^{-1/2}$ should yield a straight line whose intercept is the critical flux, ϕ_{crit}. When this is done, however, the result is not a straight line. More generally, then, we assume that the relationship has the form

$$\Delta\phi \equiv \phi_{ext} - \phi_{crit} = A\, t_{ig}^{-p} \tag{71}$$

Only the correct choice for ϕ_{crit} will yield a straight line in a logarithmic plot of $\Delta\phi$ *vs* t_{ig}. When that is obtained, the slope of the line is -p; it was found that $\phi_{crit} \cong 16.9$ kW/m^2 and that $p \cong 1.087$, with A varying from 757 to 816; the average value is 798. If we take $p = 1$, A increases slowly with ϕ_{ext}.

The fact that $p \approx 1$, rather than 1/2, indicates that the substrate behaves like a **thermally thin** material; that, in turn, suggests that it is principally the fabric which is involved in the heating and ignition. If we assume that the principal cooling mechanism is radiation, then $\phi_{crit} \cong 16.9$ kW/m^2 implies that if the radiative absorption coefficient of the fabric is $\alpha = 0.9$, then $T_{ig} = 759$ K ≈ 485 °C -- a remarkably high value. Even with $\alpha = 1.0$, $T_{ig} = 739$ K = 466 °C, considerably greater than the 400 °C measured independently. This shows that there is substantial convective cooling during the heating/ignition process.

2. Material Data

In order to see whether the program can calculate t_{ig} correctly, it is necessary to calculate the surface temperature under the heater. In order to do that, however, it is necessary to have correct input data. Among these data are the thermophysical data, $\kappa\rho c$.

Fabric. First, consider the fabric. The fabric that was used in the experiment was #12 cotton duck. Material data for cotton, especially as a function of temperature, are surprisingly difficult to find, even though it is a common and long-used material.

In Appendix E, we find that reasonable values for the thermophysical constants for this particular cotton fabric (#12 cotton duck) are

$$\rho = 620\ kg/m^3$$

and

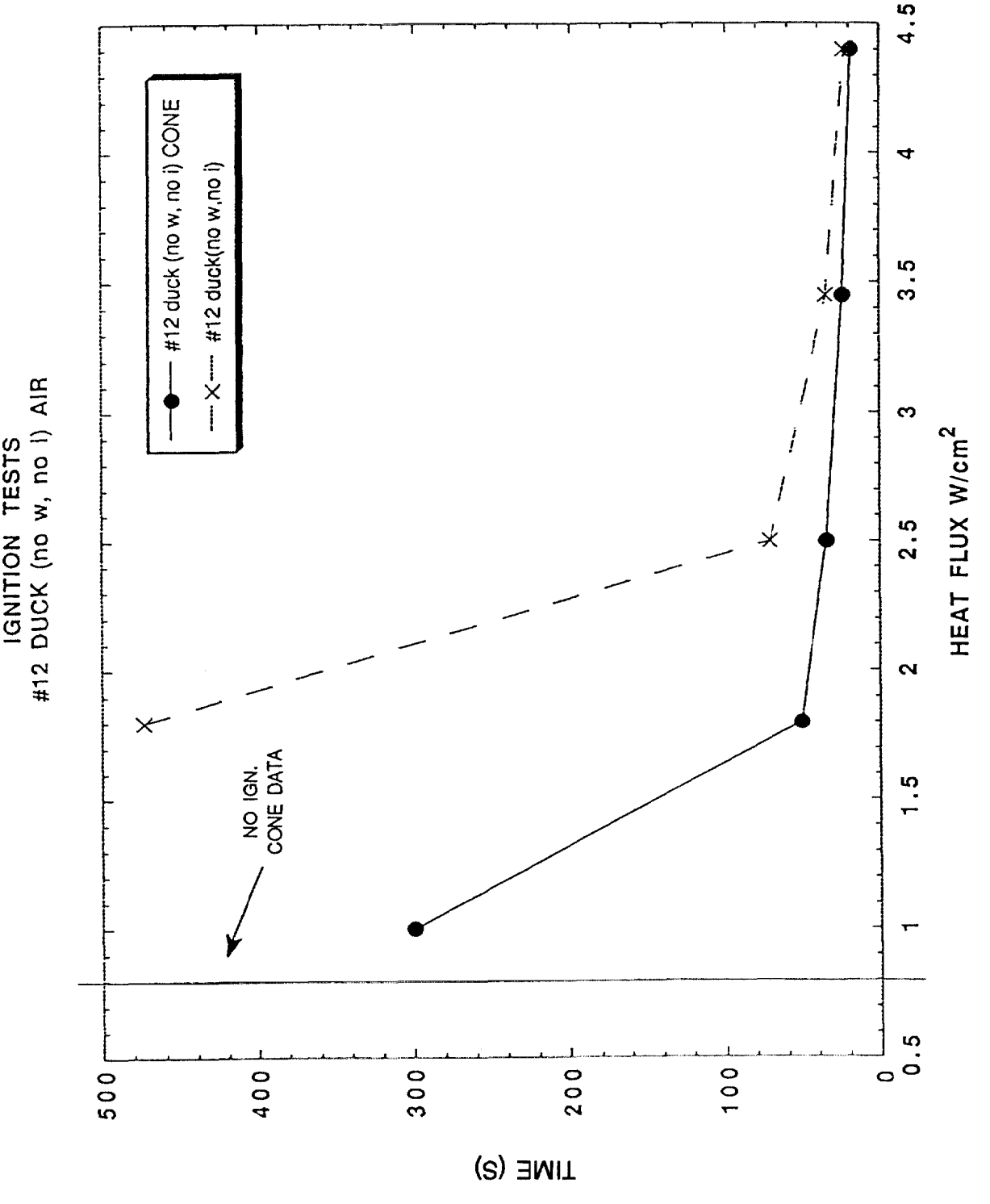

Figure 6. Time required to ignite the fabric, for different (initial) heat flux exposures. Crosses correspond to the discussion in the text. Filled circles correspond to a different set of experiments.

$$\kappa(T) = 0.28505\,\kappa_s(T) + 0.84554\,\kappa_{gas}(T) \qquad W/m\text{-}K \tag{72}$$

where

$$\kappa_s(T) = \kappa_s(T_a)\,(T/T_a) = 1.242\times10^{-3}\,T \quad W/m\text{-}K \tag{73}$$

(with T in Kelvins) and $\kappa_{gas} = 1.7\,\kappa_{air}$, with

$$\kappa_{air} = \frac{a\sqrt{T}}{1 + \dfrac{b\times10^{-c/T}}{T}}\ , \tag{74}$$

The constants are: a = 2.6464x10^{-3}, b = 245.4, and c = 12. Then κ(25 °C) = 0.1435 W/m-K and c(T) = κ(T)/$\rho\alpha$ ≈ 7819κ(T); thus, c ≈ 1122 J/kg K at 300 K.

Char. The cotton decomposes and pyrolyses to form char. According to Parker (1985, 1988), the specific heat of char is just about that of carbon:

$$c_c(T) = 1.43 + 3.55\text{x}10^{-4}T - 7.32\text{x}10^{4}/T^2 \qquad J/g\text{-}K, \text{ with T in K} \tag{75}$$

The thermal diffusivity of wood char is approximately constant:

$$\alpha_c \approx 2.1\text{x}10^{-7}\ m^2/s \tag{76}$$

The density of the char depends on whether the fibers contract while pyrolyzing, or not. Finally, the thermal conductivity of char is found from

$$\kappa_c(T) = \alpha_c\rho_c c_c(T). \tag{77}$$

Reaction Kinetic Parameters. When the analysis of a pyrolyzing material is carried out, it is done for a thin layer, in order to ensure uniformity of temperature and of oxygen concentration throughout the sample. It is then simplest to find the reaction rate in the form

$$k_d = \frac{d(W_d/W_o)}{dt} = A_d\left(\frac{W_d}{W_o}\right)^{n_d}\exp(-E_d/RT) \quad min^{-1} \tag{78}$$

for the degradation reaction, rather than as in equation (20); here $W_d = W_d(t)$ is the (instantaneous) weight of the remaining (virgin) material = weight of sample minus weight of char and ash, and W_o is the original weight. Note that A_d is commonly given in reactions/minute. The actual reaction rate is given by

$$R_d = \rho_o k_d.$$

The relationship between (20) and (78) is simple: since $\rho_d = W_d/V_d$ and $\rho_o = W_o/V_o$, then as long as V_o/V_d = const, $W_d/W_o = \rho_d/\rho_o$, and, as in equations (20),

$$R_d = A_d'\,\rho_d^n\exp(-...)$$

where

$$A_d' = A_d \rho_o^{1-n}$$

(in the appropriate units). For pyrolysis in pure nitrogen, Ohlemiller (1991) found:

$A_d = 7.49 \times 10^{14}$ min^{-1}, n = 0.60, and $E_A = 182.4$ kJ/mol

Instead of these parameters, however, we shall use the results of Kashiwagi and Nambu (1992) for a cellulosic paper pyrolyzed in air; that will maintain internal consistency in the reaction set. The global kinetic constants given by Kashiwagi and Nambu for the thermal degradation reaction of their cellulosic paper are

$E_d = 220$ kJ/mole $\quad n_d = 1.8$
$A_d = 1.2 \times 10^{19}$ min^{-1} $\quad H_d = -570$ J/g

The parameters for the other two reactions are given in their Tables 1 and 2, reproduced below. For the oxidative pyrolysis reaction,

$$k_{op} = A_{op} X_{ox}^{n_{op}} \left(\frac{W_d}{W_o}\right)^{n_{fop}} \exp\left(-\frac{E_{op}}{RT}\right) \tag{79}$$

where X_{ox} is the **volume fraction** of oxygen. The kinetic constants are:

$E_{op} = 160$ kJ/mol $\quad n_{op} = 0.5$
$A_{op} = 1.5 \times 10^{14}$ min^{-1} $\quad n_{fop} = 1.3$

and: $H_{op} = 5.7$ kJ/g

For the char oxidation reaction,

$$k_c = A_c X_{ox}^{n_{co}} \left(\frac{W_c}{W_o}\right)^{n_c} \exp\left(-\frac{E_c}{RT}\right) \tag{80}$$

with the kinetic constants

$E_c = 160$ kJ/mol $\quad n_{co} = 0.78$
$A_c = 3.4 \times 10^{11}$ min^{-1} $\quad n_c = 1.0$

and $H_c = 25$ kJ/g

The fraction of ash which remains is 9% by mass. Equations (79) and (80) transform to the standard form in the same way that (78) does. Thus

$$A_{op}' = A_{op} \rho_o^{1-n_{fop}} \rho_a^{-n_{op}}$$

$$A_o' = A_c \rho_o^{1-n_c} \rho_a^{-n_{co}}$$

Heats of Combustion. Brandrup and Immergut (1989) give the heat of combustion from several measurements; as expected, the results vary:

H_c(cotton) $\approx$ 18850 J/g
H_c(fabric1) $\approx$ 15450 J/g
H_c(fabric2) $\approx$ 16700 $\pm$ 250 J/g (fabric weight was 180 g/m^2)

Note: as material pyrolyzes, we should take c(T) and κ(T) for the combination of materials; for the sake of simplicity, however, we assume that the virgin fuel, the pyrolyzed material, the char, and even the ash, all have the same specific heat. Then the appropriate density to use in equation (12), for example, is the density of the solid, ρ_s, which is the sum of the bulk densities of all the components of the solid (see equation (25d)). As pyrolysis and combustion proceed, ρ_s decreases monotonically, assuming no fabric shrinkage.

Foam. For the padding component of the substrate, we have PU foam, for which we have the following data (Ohlemiller, 1991):

$$\rho = 0.032 \text{ g/cm}^3 = 32 \text{ kg/m} \tag{81a}$$

$$c_p = 1.46 \text{ J/g K} \tag{81b}$$

and $$\kappa(T) = 0.03613 + 2.003\text{x}10^{-4}\, T, \tag{81c}$$

with T in °C.

There is one other datum for PU foam: $<\kappa\rho c>$, the mean value of the thermal inertia, was measured in the LIFT apparatus (Quintiere *et al.*, 1983, Quintiere and Harkleroad, 1985, Quintiere, 1988). However, the foam melts before it ignites, so that ρ (and, consequently, κ) go up substantially; moreover, the measurement entails all the other model approximations. Hence the measurement is not directly useful.

Foam Kinetic Parameters. The first pyrolysis reaction, which results in the collapse of the foam structure, yields 0.7 g of liquid and 0.3 g of vapor for every gram of foam which pyrolyzes. The reaction rate, RR_1 = (mass gasified/min)/(mass of foam), is given by

$$RR_1 = 0.30B\left(\frac{\rho - \rho_R}{\rho_o - \rho_R}\right)^m \exp\left(-\frac{E_B}{RT}\right) \tag{82}$$

where m = 1.5
B = 3.36x10^{17}, and
E_B = 187 kJ/mol.

Also, ρ_0 = starting density,
ρ = current density, and
ρ_R = density of residue $\approx 0.70\rho_0$.

These densities are those of the **solid phase** (ρ_0 of order 1g/cm^3), rather than that of the foam ($\rho_0 \approx 0.03$ g/cm^3). The **total** heats of pyrolysis of PU foams range between 400 and 800 J/g; for this foam, it is closer to the upper value. Assuming it varies linearly with the mass loss, we can estimate 30% of 800, or

$$H_p \sim 240 \text{ J/g}$$

Finally, for the diffusion coefficient for O_2 in the fabric, see equation (28).

E. RESULTS AND DISCUSSION

Rather than give the final results immediately, it was decided to describe the evolution of our thinking, including some of the false steps we took, because a good deal can be learned that way, and it could be instructive for anyone else who might work on this problem in the future. With that in mind, we first consider the results of calculations made assuming an inert substrate.

1. Inert Substrate

First, the computer program was used to calculate the peak surface temperature under the heater as a function of time for several peak fluxes. The results are shown in Figure 7.

The ignition temperature of cotton was measured to be 390-400 °C (Ohlemiller, 1991). According to Figure 7, if $T_{ig} \approx 400$ °C, then ignition is attained for the 44 kW/m^2 exposure at $t \approx 18$ s, and for the 34.5 kW/m^2 exposure at $t \approx 50$ s. These values compare very favorably with experimental values of 22 and 37 s, respectively.

On the other hand, ignition is not attained at all for the 25 and 18 kW/m^2 cases, while the calculation predicts the substrate will reach the ignition temperature, albeit at long exposure times. A conceivable reason might be that the ignition temperature given above was overestimated. In order to intersect the $\phi = 18$ kW/m^2 curve at $t \approx 472$ s, the ignition temperature would have to have been about 290 °C; it is very unlikely that such a large error in the measurement of T_{ig} would have been made. Even if it were, that would yield ignition times of 7, 12, and 25 s, respectively, much shorter than the measured times of 22, 37, and 70 s.

[Three possible reasons why the calculated ignition times might be so short are:

(a) endothermic pyrolysis taking place, which slows the temperature rise;

(b) Significant radiative heat transfer within the material, so that the flux is absorbed in depth, rather than mainly at the surface; and/or

(c) $T_{ig} = 290$ °C and the estimates of $\kappa\rho c(T)$ were in error, the actual value being larger.

Now, if we consider endothermic pyrolysis, then we must also consider exothermic pyrolysis. Second, the effect of radiative heat transfer will be small when T is near T_a, and small in comparison with the effects of pyrolysis when $T >> T_a$. Finally, consider item (c): If $\kappa\rho c$ were larger, then the rate of rise of T_s would be smaller, as can readily be seen from equations (17)-(19). The final temperature, however, is independent of $\kappa\rho c$. Hence not only would T_{ig} have to be much smaller, but the estimates of $\kappa\rho c$ would have to have been 9 times too small. This is all possible, but extremely unlikely.]

2. Results with Pyrolysis

On the other hand, we know that pyrolysis must take place. Figure 8 shows the effect of including pyrolysis for the Q = 25 kW/m^2 case. Curve a indicates what the temperature of the fabric surface would be if the fabric (and foam) were inert. Curve b is the result of "turning on" the (endothermic) degradation reaction. Note that although the rate of growth of temperature is slowed down quite perceptibly, as expected, the temperature the surface reaches asymptotically is exactly the same (assuming the same surface absorptivity/emissivity as before).

However, the exothermicity of the oxidative pyrolysis and of char oxidation are far greater than the endothermicity of thermal decomposition, and should overwhelm it. We cannot, therefore, consider thermal decomposition alone: if we consider pyrolysis, we must include all the major reactions. Another way of seeing this is to note that in order to have ignition, we must have a "thermal runaway," where exothermic pyrolysis heats up the material faster than heat diffusion and surface losses can carry the heat away.

Curve c indicates what takes place when the oxidative pyrolysis reaction is included, as well: it is exothermic, and adds a great deal more energy than the degradation reaction removes. The result is, logically, that the temperature rises rapidly, almost like a thermal run-away. However, the temperature reaches a peak, than declines. The reason is simple: the fuel is rapidly exhausted. Once that happens, the heat source is reduced to the original external flux. This is clearly depicted in Figure 9, which shows the fuel density as a function of time. The ordinate is temperature, in °C, and density in kg/m^3. The curves marked T_0 and ρ_0 correspond to the cell with the highest temperature. Those marked T_1 and ρ_1 correspond to the (laterally) adjacent cells, and those marked T_2 and ρ_2 to the next ring of cells. These calculations were carried out assuming no char oxidation. We see that as the reaction accelerates, T_s "runs away" and the density plummets from its virgin value to that of char. Most significantly, the peak temperatures develop just after the density falls.

Finally, curved of Figure 8 shows the result of adding the char oxidation reaction as well: that additional heat source takes the pyrolysis "over the top." The temperature **continues** to run away. (We have arbitrarily cut off the calculation at 600 °C, here.) The question then arose: why was there an oscillation in T_s? The qualitative explanation is that if a cell is too large, then the surface/volume ratio is small, and the heat cannot diffuse away rapidly enough. This is confirmed by Figure 10. With a cell size taken to be a bit less than half as large, the amplitude of the oscillation declined considerably, and with the cell size halved again, the oscillations have almost disappeared.

Presumably, as we continue to decrease the cell size, the numerical errors should become progressively smaller, until a further decrease in cell size would make no further difference in the results. However, it was found that the results were apparently not converging with decreasing Δx, and that the sensitivity varied with Q. Investigation of the reason for this great sensitivity revealed that it lay in our use of a variable grid size: whereas for grids of constant spacing, the numerical approximations are correct to second order in Δx, that accuracy drops to somewhere between first and second order. Indeed, if the numerical error is proportional to $(\Delta x)^n$, then n is given by a complex formula (Torrance, 1985, pp. 43 and 51). The "flavor" of that expression is given by $n \sim (2+a)/(1+a)$, where $a \equiv \partial \Delta x/\partial x$. That is, the accuracy depends inversely on the rate of growth of the grid size. An explicit calculation is given in Appendix A; see Table A-1 there.

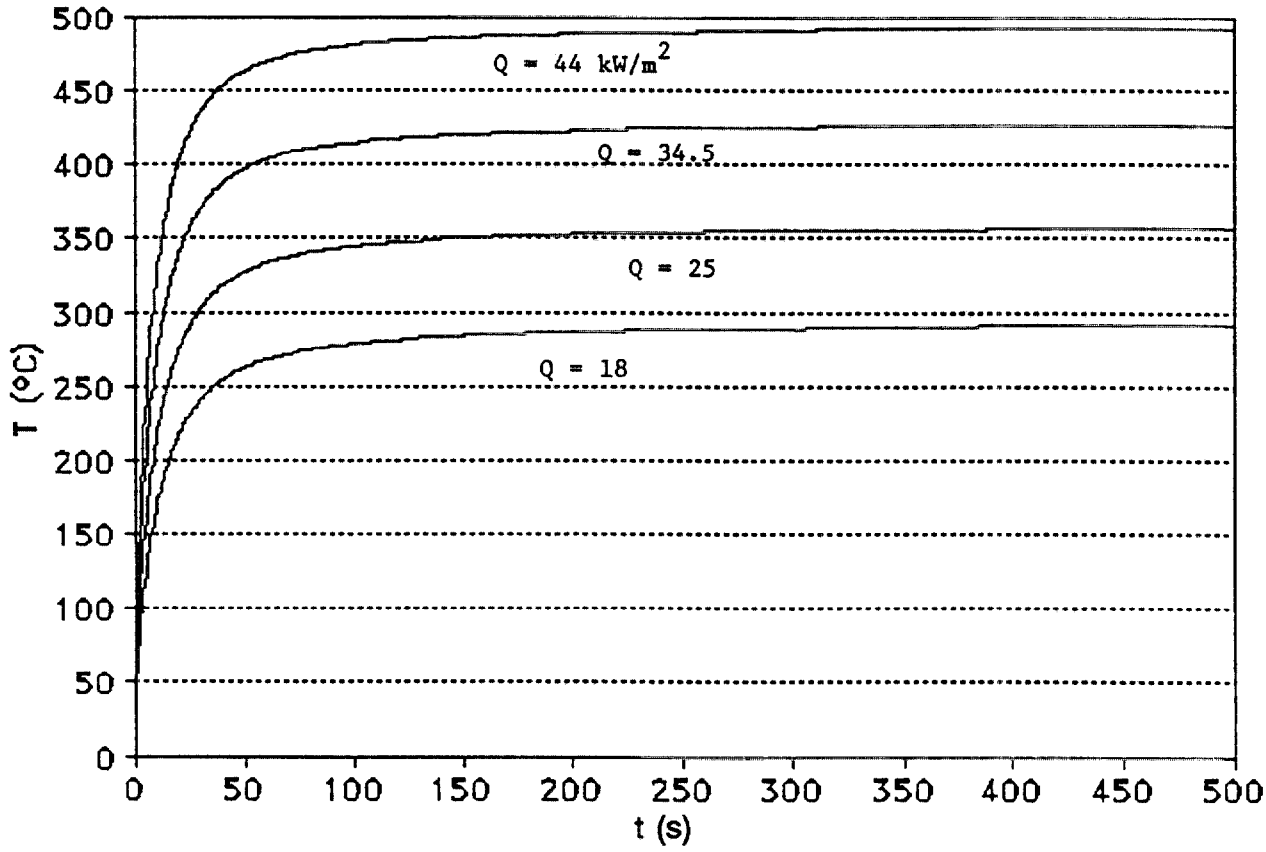

Figure 7. Peak surface temperatures of substrate as a function of time, for the four exposures

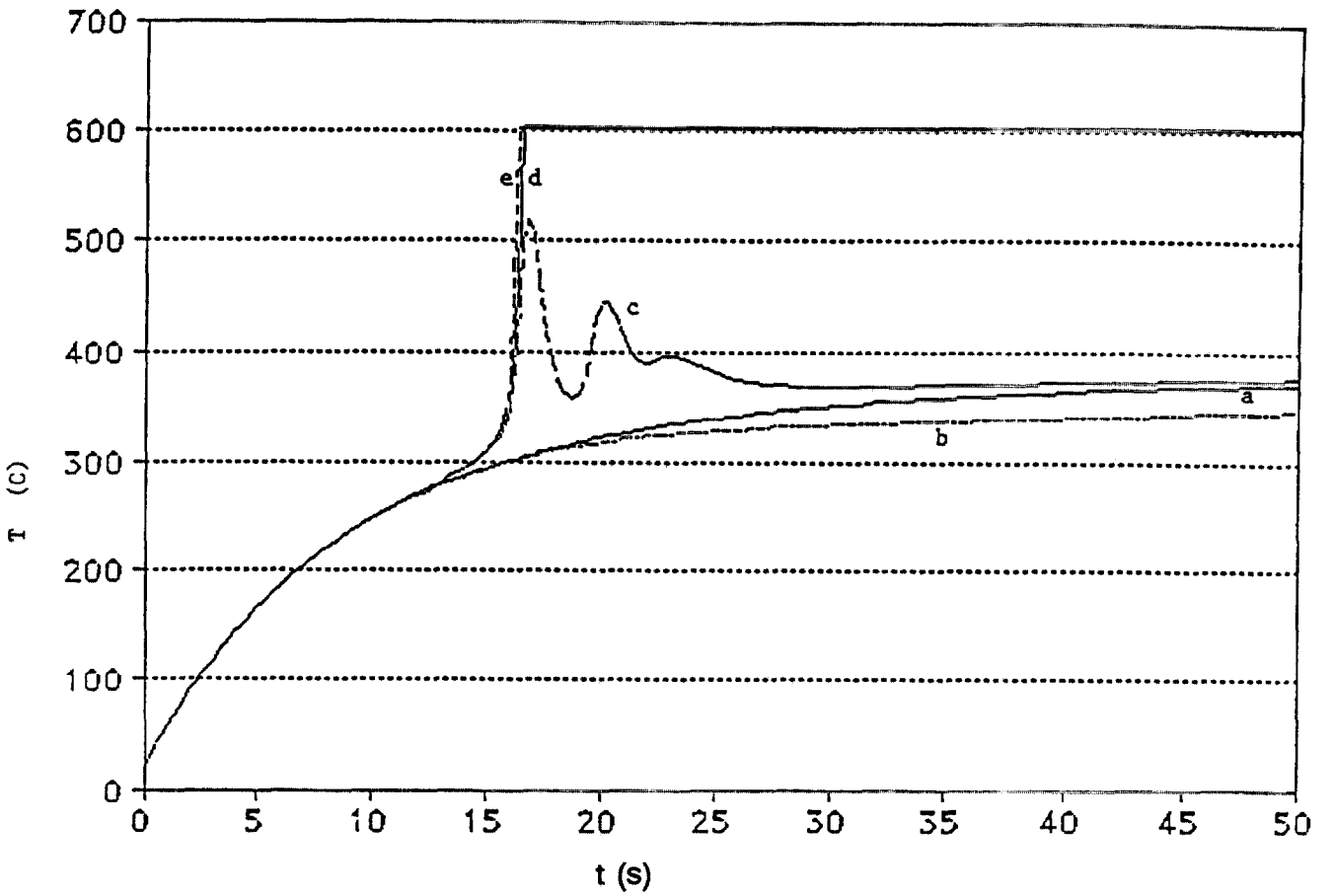

Figure 8. Peak surface temperatures of substrate exposed to Q = 25 kW/m^2, as a function of t, for
a. Material assumed to be inert
b. Thermal degradation only
c. Oxidative pyrolysis as well
d. Char oxidation also included, as well
e. Only <u>one</u> reaction: oxidative pyrolysis

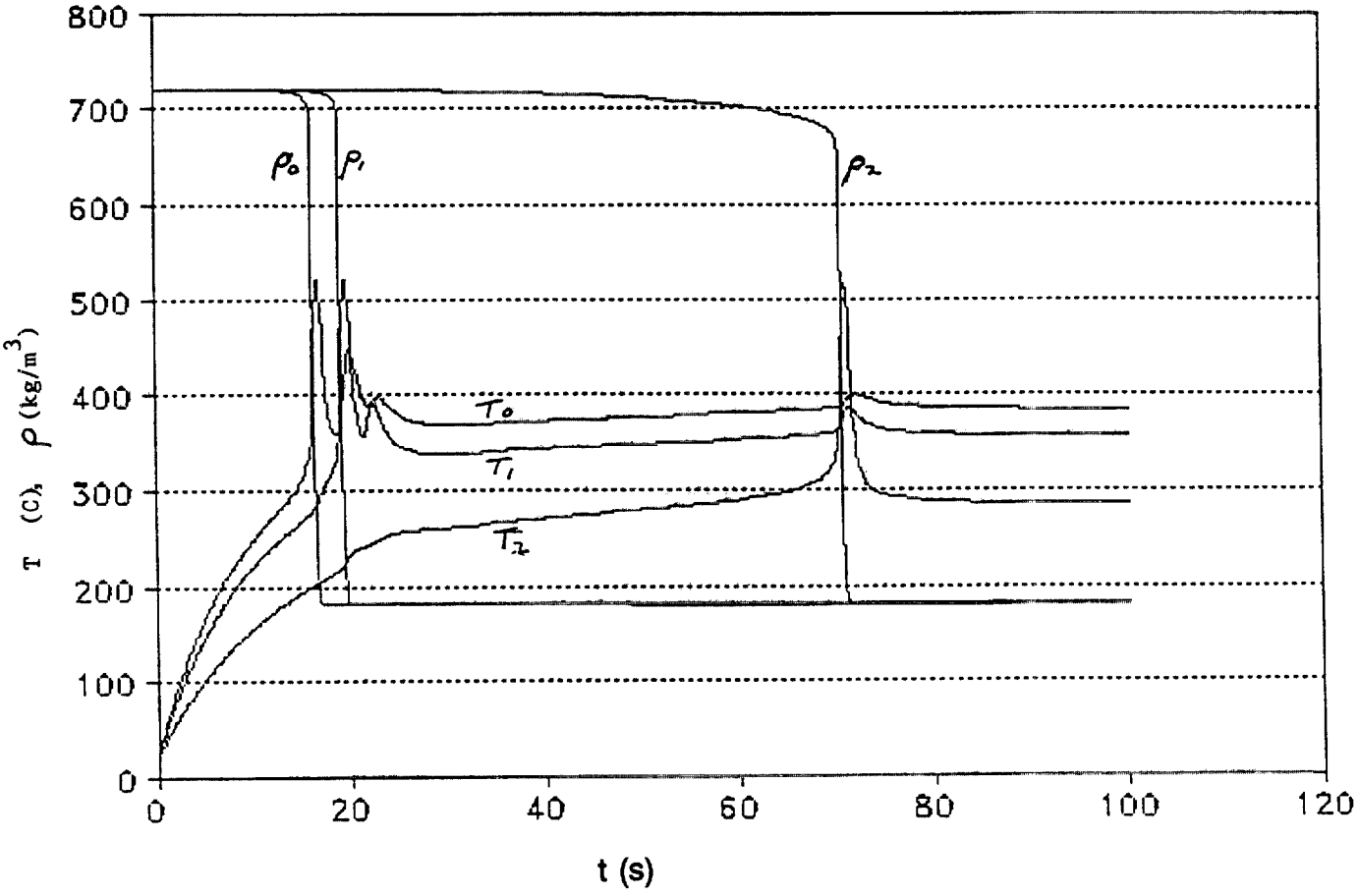

Figure 9. Temperature and density of central cell (subscript 0), adjacent cells (subscript 1), and cells in next ring around center (subscript 2), as functions of time

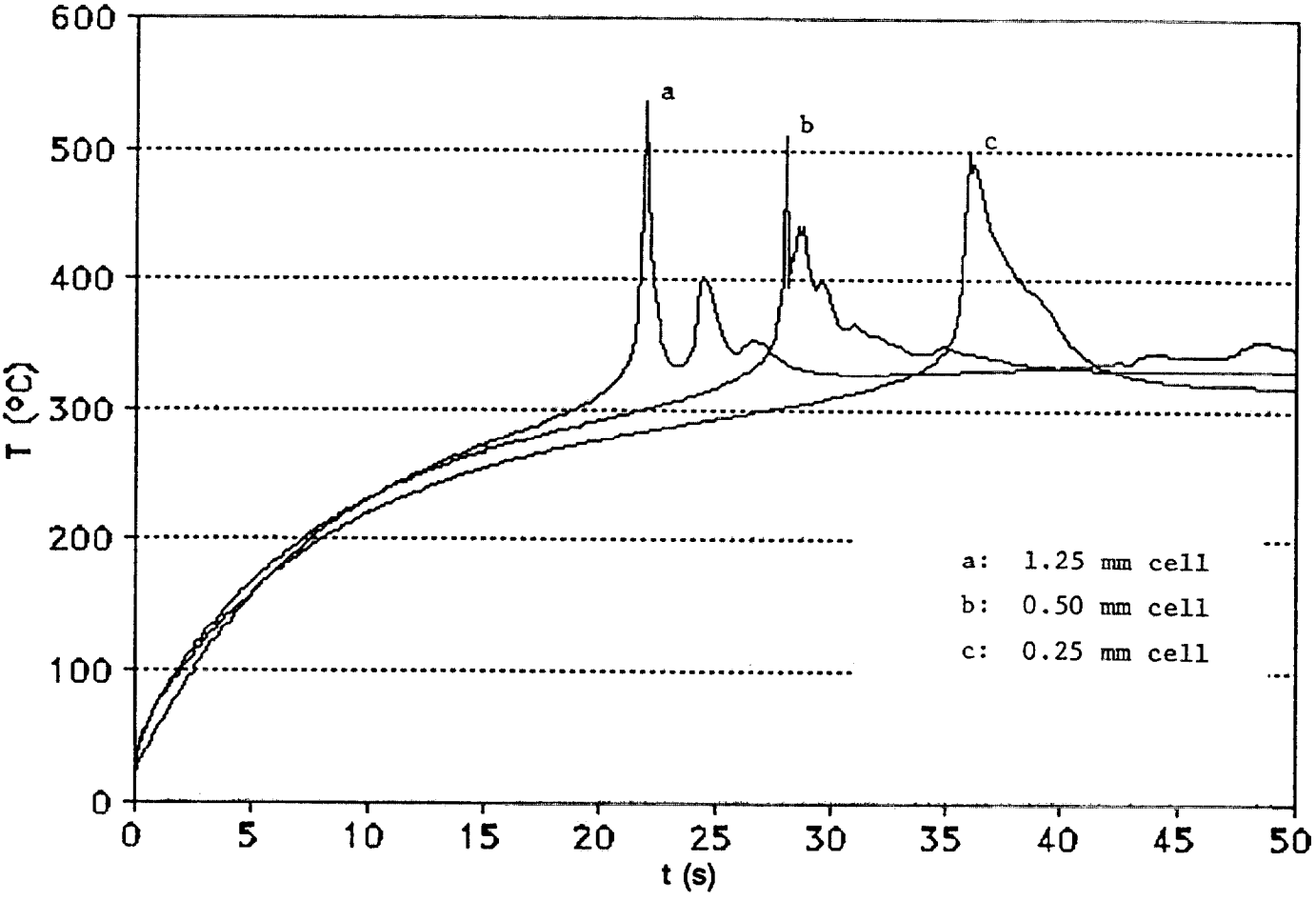

Figure 10. Temperature of central surface cell (i.e., peak temperature) for three different grid sizes: 1.25, 0.50, and 0.25 mm cubes. Char oxidation was purposely left out

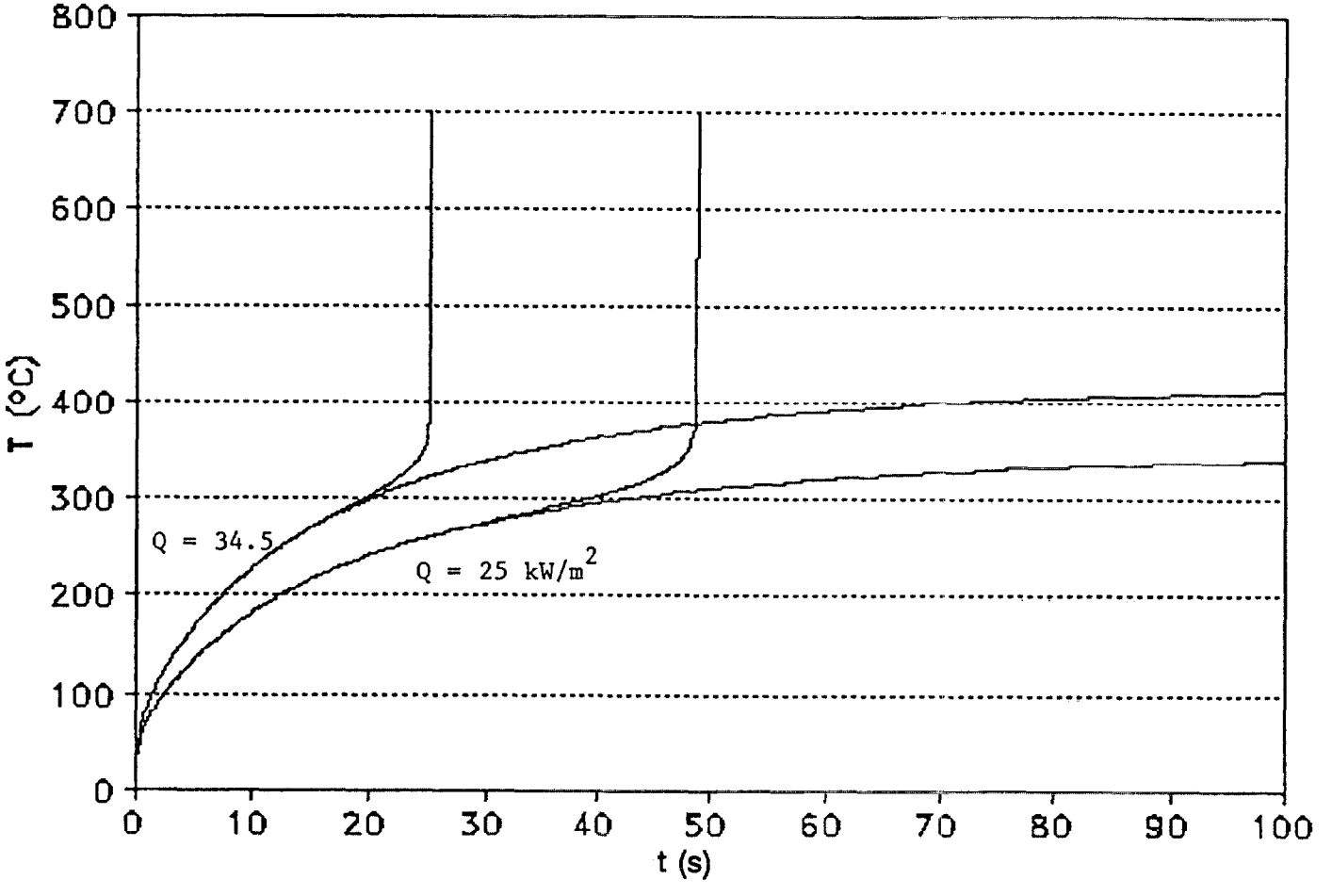

Figure 11. Peak temperature for the 25 and 34.5 kW/m^2 cases, assuming (a) no pyrolysis, and (b) all three pyrolytic reactions

By reducing the rate of increase of grid size, therefore, the accuracy was increased, and the results made to converge better. Moreover, it was decided to switch from an explicit solution method to Larkin's semi-implicit method (see Section II.C). After those changes, we arrived at the results shown. The results of four calculations are shown in Figure 11. These were made
with an assumed heat transfer coefficient h = 20, and an assumed oxygen concentration of 20%. For initial fluxes with peak values of 25 and 34.5 kW/m^2, calculations are first made assuming that the substrate is inert, and then pyrolysis is "turned on." We see that for the 34 kW case, the asymptotic temperature lies at about 430 °C, and that a thermal runaway begins at about 300 °C, at $t \approx 20$, and is completed at $t \approx 25$ s; that would then be the ignition time. It is difficult to state precisely what "the ignition temperature" is, in this case (but see below).

For the 25 kW case, the asymptotic temperature lies at about 360 °C. The first perceptible deviation of the curve for the reactive case from that for the inert material occurs at $T \approx 280$ °C, and is clearly established at 300 °C. The thermal runaway takes place at $t \approx 48$ s. These times may be compared with the experimentally-established ignition times, which were about 22 and 70 s, respectively. Thus we have achieved semi-quantitative agreement. In Figure 12, on the other hand, we see that a thermal runaway, and therefore ignition apparently did not take place for the 18 kW case. Here, the asymptotic temperature is about 290 °C; this is apparently not high enough to produce a runaway.

Wherein lies the difficulty? Most likely, one or more of the input values is incorrect. Altering $\kappa\rho c$ would principally change the time scale. Figure 13 shows the effect of changing the assumed oxygen concentration: the highest curve reproduces the upper curve in Figure 12. The next two curves show what happens when $<Y>$ is assumed to be 0.15 and 0.11, respectively. Finally, the bottom curve (again) corresponds to the inert case. Thus, it is not $[O_2]$ having been chosen too low that prevents ignition, and one or more of the kinetic parameters is probably in error. In Figure 14, curves a and b again reproduce Figure 12 (on a different scale). For curve c, the char oxidation rate was doubled. It is apparent that the curves overlap completely. A preliminary conclusion inferred from this was that the observed result was due to all the char that is produced already being oxidized. Observation of the kinetic constants for oxidative pyrolysis and char oxidation, however, makes it clear that the latter is three orders of magnitude slower than the former. Therefore merely doubling the char-oxidation rate will only perturb the energy output slightly -- so slightly that it will not even show up in the figure.

For curve d, the oxidative pyrolysis rate was doubled (the pre-exponential factor A was doubled), doubling the char-production rate through this branch; this indeed produced a thermal runaway. Curves e and f are the results of increasing A by 20% and 10%, respectively. Thus, a quite modest increase in A predicts ignition, although at 230 s, rather that the measured 472 s. Such an increment is not only well within experimental error, but is entirely plausible, when the likely differences between the cellulosic paper and a cotton fabric (with different impurities) are considered. On the other hand, it was assumed that y = 0.20. For y = 0.15, A must be increased by 30% in order to get ignition (the resulting T(t) curve is very similar to the "best" one). Although this is greater than the 10% increase found above, it is still entirely plausible.

We have so far considered the sensitivity of the results to the oxygen concentration, the thermophysical constants of the fabric, and its kinetic parameters. Surprisingly, there are two other significant parameters: first, if we use h = 22 for the heat transfer coefficient in equation (69) (as suggested by the results of Appendix D, shown in Table D-1), rather than the assumed h = 20, the "asymptotic" temperature (that at t = 500 s) reaches only 272 °C, rather than 292 °C, and there is not the faintest possibility of achieving ignition, unless E_A is substantially smaller than 160 kJ/g. One solution is to assume that h = 20 is the correct value to use, since the theoretical calculations in Appendix D could

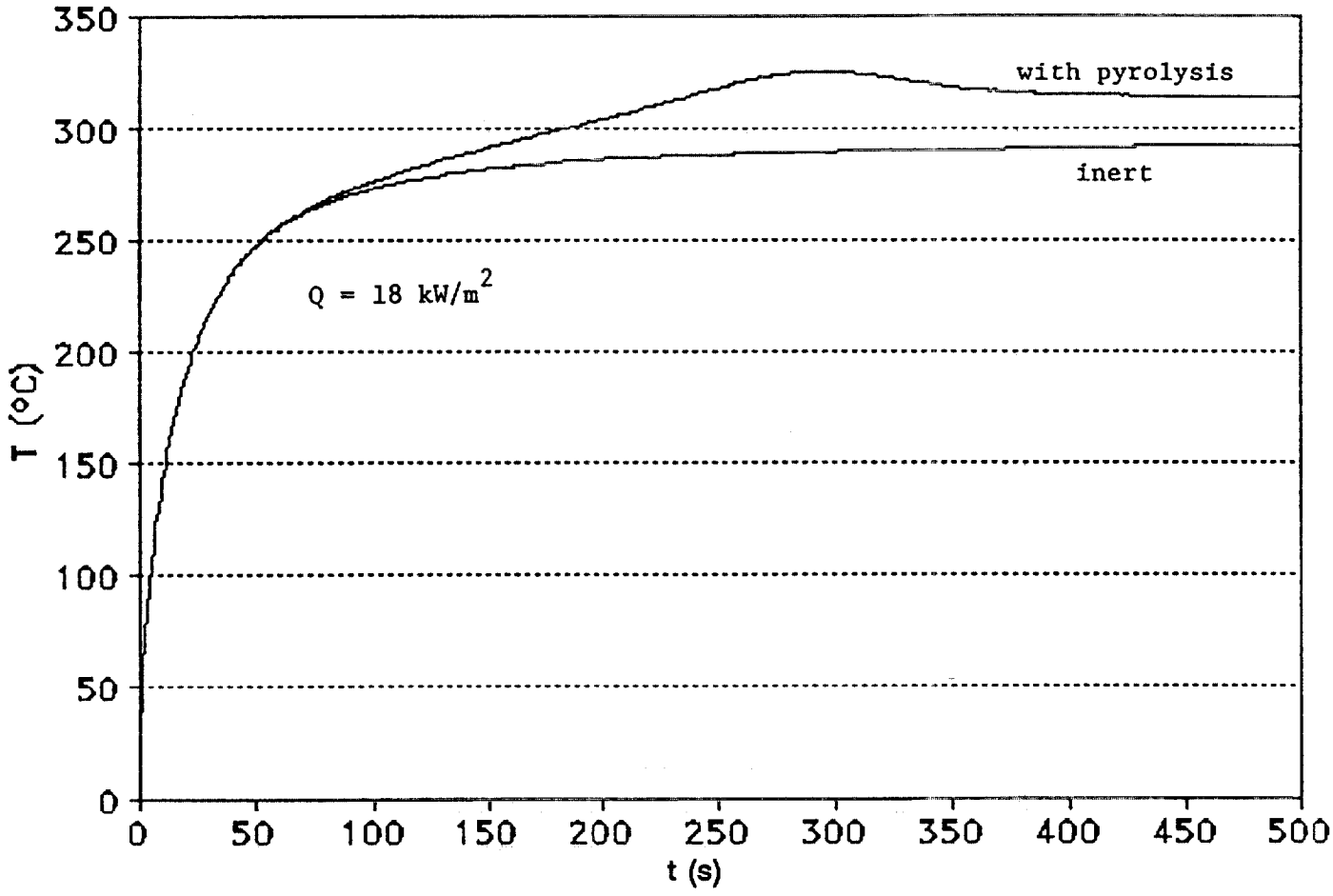

Figure 12. Peak temperature for the 18 kW/m^2 case, with the same assumptions as in Fig.11

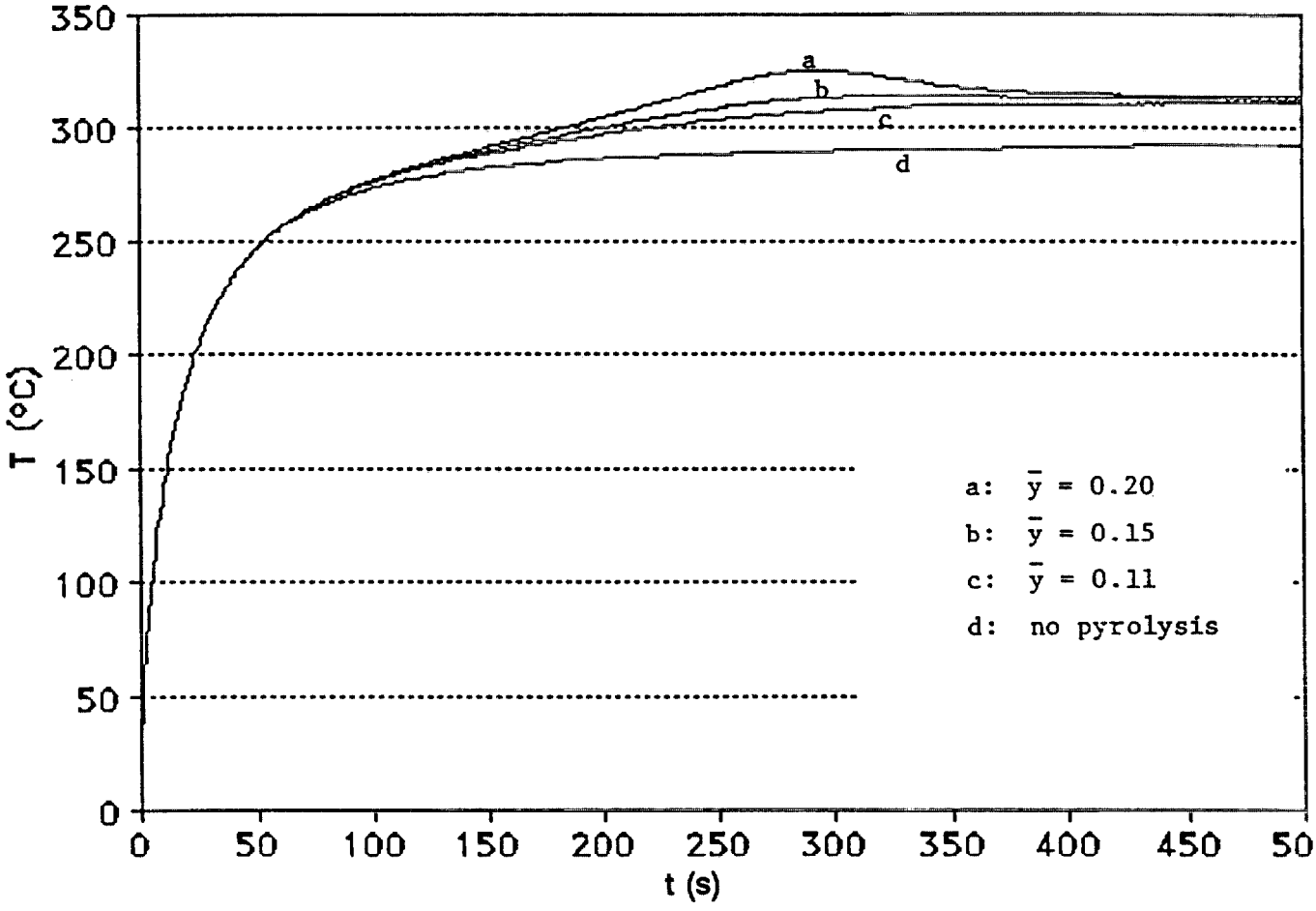

Figure 13. Peak temperature for the 18 kW/m^2 case, for several values of mean O_2 mass fraction, <y>

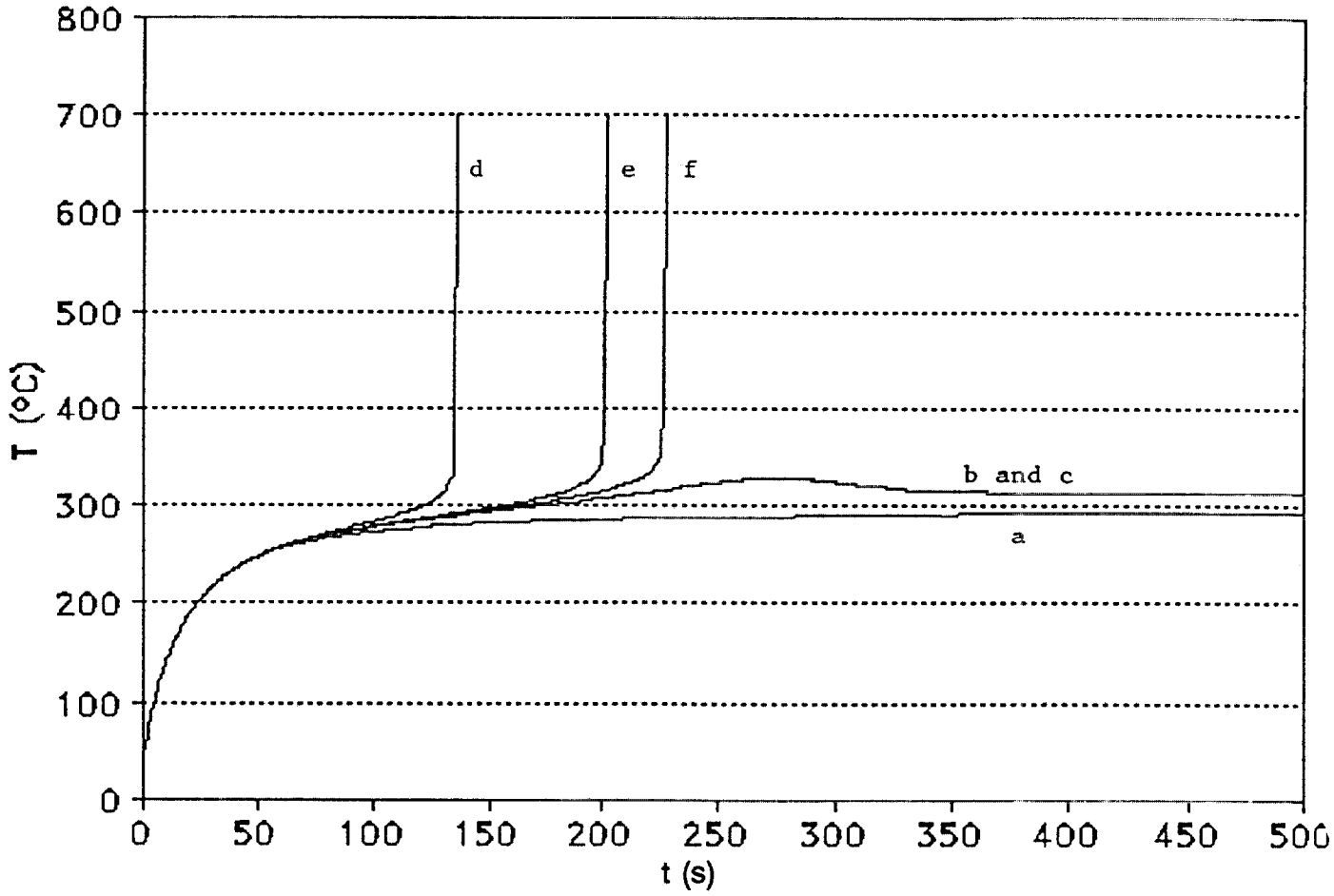

Figure 14. Peak temperature for the 18 kW/m^2 case, with various assumptions for the pyrolysis: Curve a, no pyrolysis; curve b, "standard" pyrolysis; curve c, double the char oxidation rate; Curve d, double the oxidative pyrolysis rate; Curve e, 1.2 times the oxidative pyrolysis rate; Curve f, 1.1 times the oxidative pyrolysis rate

easily be off by 10% or more. Another resolution is possible, too: the second parameter which is important in this threshold region ("threshold," because 18 kW/m^2 is close to the critical flux, 16.9 kW/m^2) is the thermal conductivity of the foam padding. In all the runs made above, it was assumed that κ = 0.056 J/m K and c = 1.9 J/g K, for the foam at T = 20 °C. If it were assumed that κ = 0.096, instead, then the foam would act as a more efficient heat sink, and the surface temperature could be expected to drop; indeed, a calculation showed that the peak surface temperature at t = 500 s fell to 272 °C for the inert fabric. In fact, however, the value 0.056 for the thermal conductivity was for a foam of density 48 kg/m^3! Transforming that for a 32 kg/m^3 foam, according to equation (62), yields 0.036, almost exactly what is given in the present test (see equation (81c)). This **reduces** the heat sink, and must yield an increased asymptotic surface temperature. Using the foam parameters given by equations (81), and h = 20, the t = 500 temperature indeed rises, from 292 °C to 300 °C; with h = 22, it is 294 °C, and we only need to increase A by 10% to get runaway.

The "best" set of parameters for the fabric and foam, then, is given in Section II.D.2. For the heat transfer coefficient, use the values in Table D-1. With that set, we obtain the curves shown in Figure 15. The corresponding calculated ignition times are given in Table 3. The calculated values are all about half the measured values, and the trend is well-predicted.

Note that the polyurethane foam begins to melt and recede from the fabric when its temperature reaches about 300 °C, thereby decreasing the heat-sink effect of the padding, and accelerating the heating of the fabric. This effect has not been included in the model.

Table 3. Comparison of Substrate Ignition Delay Times

	Ignition delay, t_{ig} (s)	
Q (kW/m^2)	Calculated	Measured
18	209	472
25	37	70
34	19	37
44	13	22

It has been suggested that we might avoid the necessity of explicitly including the pyrolysis reactions by choosing some effective ignition temperature. This is not, in fact, feasible: if we take the measured ignition times and mark them on the four curves in Figure 7, corresponding to the inert assumption, we find that they intersect these curves at widely varying temperatures; see Table 4. It is apparent that this "ignition temperature" is a strong function of the external flux.

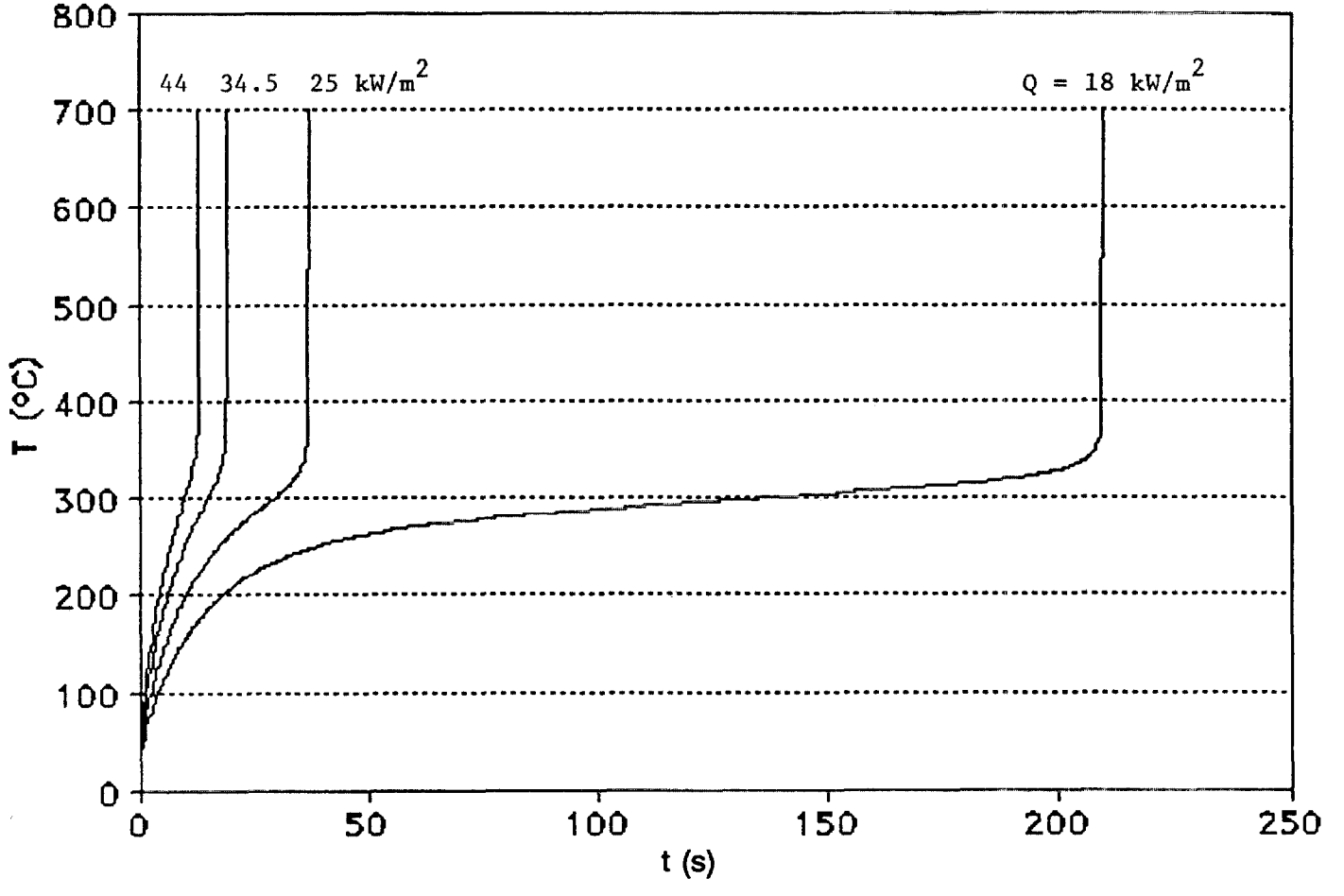

Figure 15. Peak temperature as a function of time, for all four cases, using the best set of input data

Table 4. Surface Temperatures Which Would be Attained by the Substrate at the Measured Ignition Times If the Substrate Were Inert

ϕ_{ext} (kW/m^2)	18	25	35	44
T_{ig} (°C)	291	342	380	400
T_{ig} (K)	564	615	653	673

On the other hand, if we define "the ignition temperature" as the point on the $T_s(t)$ curve where the temperature is rising at some rapid rate, *e.g.*, 100 °C/s, then from Figures 11 and 13 we see that that gradient is attained at the approximate temperatures shown here:

Table 5. Surface Temperatures at a 100°C/s Rate of Rise (Data From Figures 11 and 13)

ϕ_{ext} (kW/m^2)	18	25	35
T_{ig} (°C)	390	390	380
T_{ig} (K)	663	663	653

These calculated temperatures are close to each other, and close to the 390-400 °C which has been measured.

F. SUMMARY FOR SECTION II

We have created several computer programs, of which the central one is SUBSTRAT2. This program calculates the temperature history at every point in a substrate (the upholstered furniture) which is subjected to a strongly localized heating flux on its top surface (assumed to be horizontal). The (solid) substrate consists of two layers, the top one being a fabric and the lower a foam pad; there may be a thin intervening air gap. The substrate is taken to be a rectangular parallelepiped, and it is broken up into several thousand cells. The ambient oxygen level can be set at whatever value one wishes.

The solid is subjected to a nonuniform and time-varying heating flux at its top surface, and (simultaneously) experiences convective and radiative heat losses. Moreover, the solid can undergo pyrolitic reactions; we consider three, here: one endothermic step (thermal degradation to char), one oxidative pyrolysis to char, and oxidation of the char (to ash). The way T(r,t) is found is by solving the PDE which describes the diffusion of heat in a solid, equation (12), numerically. The equation set is very stiff, because of the highly nonlinear form of the (Arrhenius) reactions. We have therefore used a semi-implicit method to solve the equation set.

If and when the temperature rate of rise at some location suddenly "accelerates" to a value high enough that the surface glows (that is, T > 500 °C or so), we can say that smoldering ignition has occurred. The program will not tell us whether flaming ignition takes place. It also does not treat the case where the flux is applied in a crevice, such as is formed between the seat cushion and the seat back. The

program does not take into account the effect(s) of the foam possibly melting and receding away from the fabric. Finally, it also does not take oxygen diffusion within the cushion explicitly into account; hence in certain threshold situations, where a small change in oxygen concentration determines whether ignition does or does not take place, the results are ambiguous. What is and is not in the program is listed in Table 1, section II.B.

It is important to note that it is often difficult to obtain the needed kinetic and/or thermophysical parameters for the material; or, when available, to know how accurately they are known. Therefore this *caveat* must also be made: even if the program were perfect, its results are only as good as the input parameters which are supplied. On the other hand, it should accurately reproduce (or predict) **trends**.

There is a user-friendly front end for the input, described in Section II.C. The program runs well on a 386-level computer with a math co-processor, and faster on a 486-chip computer.

An experiment was carried out to ignite the substrate. In trying to reproduce those experimental results, it was found that the calculated results are sensitive to the input values chosen, especially the kinetic parameters. It was found that the preexponential factor found by Kashiwagi and Nambu (1992) for the oxidative pyrolysis reaction in a cellulosic paper had to be increased by **10%** for the cotton duck fabric in order to get ignition for the lowest of a set of heating fluxes to which the substrate was exposed. The result was semi-quantitative agreement with the observed ignition times.

III. *CIGARET*, A MODEL OF A QUIETLY SMOLDERING, ISOLATED CIGARETTE

A. GENERAL DESCRIPTION

A cigarette consists of small strands of cured tobacco leaf (varying in length from about 0.5 to 12 mm, with the average about 3-4 mm), held in place by a paper wrapping. The shape is usually cylindrical; the radius of the cross-section is R. The circumference, $2\pi R$, generally lies between 17 and 25 mm. There is usually a filter at one end.

A schematic illustration of a smoldering cigarette in its quiescent phase is given in Figure 16. The section marked C in this figure is char, most of which is oxidizing at a rate sufficient to make it glow. The peak temperature in this region is some 800 to 850 °C; that is, about 1100 ± 25 K. The glowing coal is shaped approximately like a thick cone. The cone length varies; it is usually on the order of 1 cm.

The heat created by the char oxidation diffuses, convects *via* hot gases, and radiates away in all directions. Part of this heat is carried back towards the virgin tobacco, the zone marked VT in the figure. The tobacco just behind the burning coal then dehydrates and decomposes; this is the region marked P in the figure (P for "pyrolyzing"). This is the region from which a visible plume of smoke rises. At the front of the cigarette is the residual ash, marked A in the figure. EA stands for "evanescent ash"; that is the ash which generally falls off a cigarette, or is flicked off by the smoker. Since we will eventually assume that the cigarette rests on a substrate, the part EA might not, in fact, disappear.

We will see in Section III.C that a good deal of detail is lost when the model is assumed to be one-dimensional. Therefore the present model is two-dimensional; *i.e.*, cylindrical symmetry is assumed. This is not a bad assumption for the cigarette freely smoldering in air, but is not so good when the cigarette lies on a substrate. We nevertheless assume that whatever asymmetries are produced by that interaction can be simulated by spreading the effects of the substrate out evenly over the circumference.

B. DYNAMICS OF A SMOLDERING CIGARETTE

A good deal of effort, both experimental and theoretical, has gone into understanding the (isolated) smoldering cigarette. In this Section, a brief, qualitative discussion of the dynamical processes which occur will be presented and the salient results from earlier experiments noted. It is not intended to be an exhaustive review. For a more detailed description of cigarettes, see Gann *et al.* (1988).

1. Pyrolysis Rates

There have been many careful studies of the pyrolysis of tobacco; we will only consider some global results here. A detailed description of cigarettes can be found, for example, in Section 2 of Gann *et al.* From Table 2-3 there, it is found that for those experimental cigarettes, the average mass, exclusive of the filter, is 870 ± 470 mg. The variation for commercial cigarettes is lower. The mean mass loss rate is 60 ± 20 mg/min, corresponding, on average, to some 14 min of smolder time. This agrees with the common observation that an unattended cigarette will smolder for 10 to 20 min.

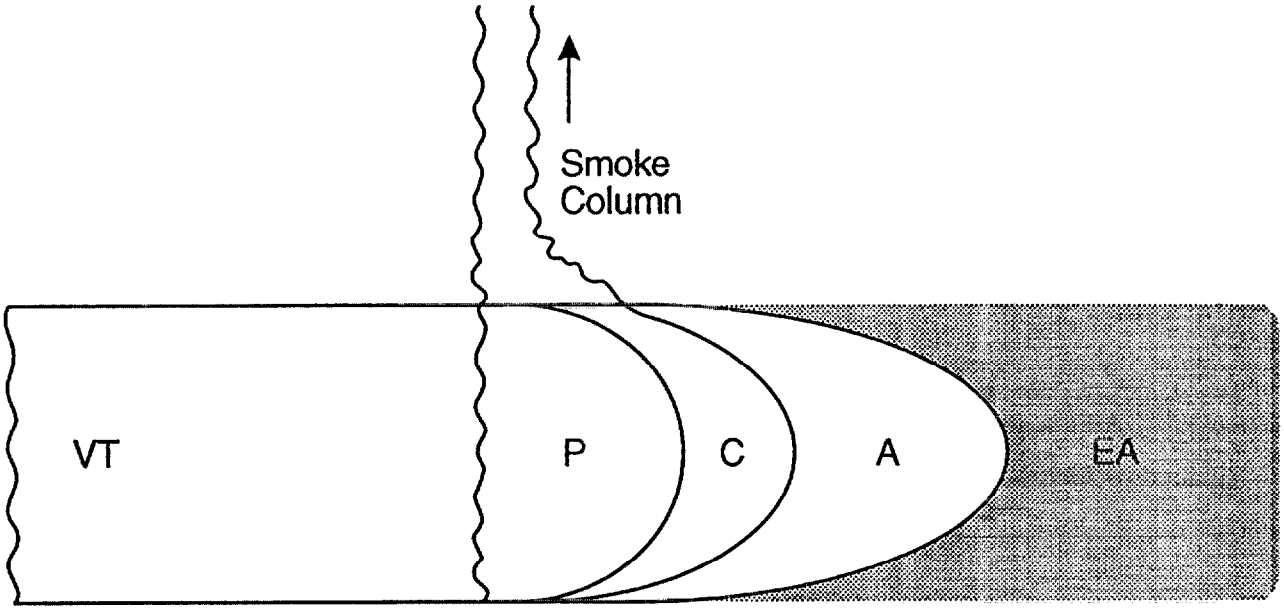

Figure 16. Schematic of a smoldering cigarette. The zone marked VT contains the virgin tobacco. P is the pyrolyzing region; the section marked C is char, A is the residual ash, and EA stands for "evanescent ash," explained in the text.

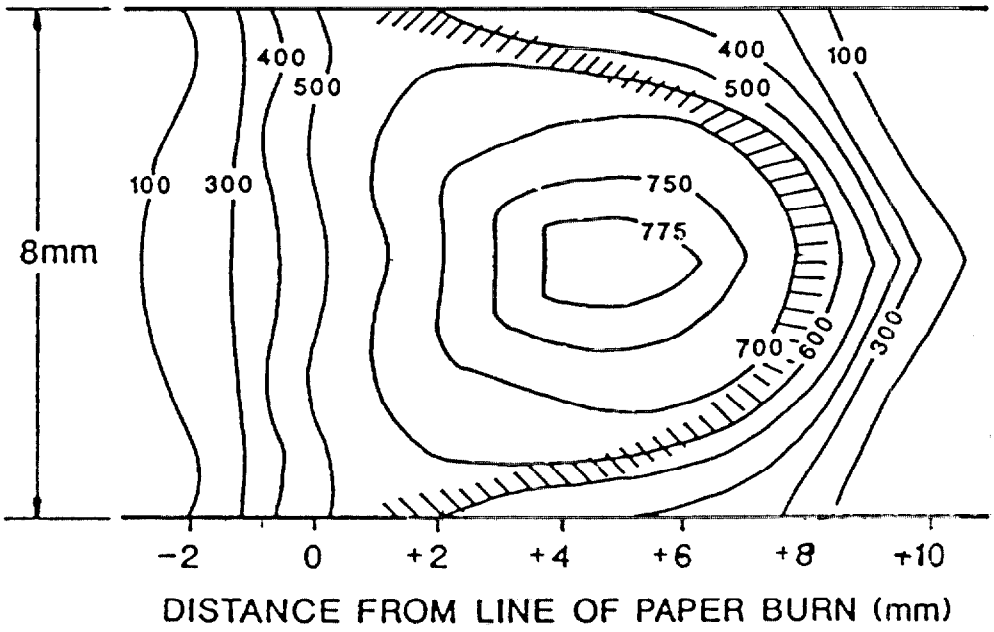

Figure 17. Isotherms in the gaseous part of the cigarette during quiet, steady burning. The shaded region indicates peak reaction rate; i.e., the glowing coal.

Sandusky (1976) shows that if we start with one gram of tobacco, then after pyrolysis about 400 mg of charred residue remains. This char includes 150 mg of inert material, which remains as ash upon combustion. That is, about 70% (600 mg) of the combustible portion (850 mg) of the tobacco evaporates and/or pyrolyses away, leaving about 250 mg of material which can burn completely. To avoid confusion, we will refer to that portion as "char," and the char plus ash (total = 400 mg) as "charred tobacco residue," or CTR, hereafter. We will not go into any more detail here regarding pyrolysis rates.

2. Stoichiometry

We now try to determine a sensible approximation to the stoichiometry of the reactions. This will be useful when the production of CO, H_2O, and CO_2 are modeled. The contents of the tobacco are quite complex, as shown in Sandusky (1976) and elsewhere. The reactions are complex as well. A simplified summary of the reactions is given at the bottom of page V in Sandusky. This is here simplified still further, by assuming that the dehydration and pyrolysis processes leading to char have exothermic as well as endothermic terms which cancel exactly.

When the char burns, the principal products are CO and CO_2, leaving about 150/400 = 37.5% ash, by weight. This residue is somewhat higher than the amount left by the tobacco analyzed by Baker (1975). Sandusky's data is used here, complemented where necessary by Baker's data. Char is assumed to consist of a mixture of carbon and of one other compound which will yield C/H/O ratios comparable to those given by Baker, and for which we know the heat of combustion, H_c. A model molecule is mucic acid, $C_6H_{10}O_8$. This has the molar heat of combustion H_c = 2021 kJ/g mol (Weast, 1976). Its molecular weight is 210; thus h_c = 9620 J/g. The atomic percentages of char (CTR minus ash) are given by Baker as:

O = 25.33%	H = 2.18%
C = 69.40%	N = 3.09%

The "model" char is then

$$\text{char} = xC + yC_6H_{10}O_8,$$

where x and y are such that the above ratios are satisfied. From the carbon and hydrogen fractions, $x \approx 12$ and $y \approx 0.5$ are obtained; nitrogen is ignored. Upon burning the char,

$$12C + 0.5\ C_6H_{10}O_8 + nO_2 \rightarrow (15 - f)\ CO_2 + f\ CO + 2.5\ H_2O$$

In order to determine f, one more relationship is needed. This is obtained by examining the energy produced. We assume complete combustion of the mucic acid,

$$0.5\ C_6H_{10}O_8 + 4.5\ O_2 \rightarrow 3\ CO_2 + 2.5\ H_2O,$$

and incomplete combustion of the carbon:

$$12C + (n - 4.5)O_2 \rightarrow (12 - f)CO_2 + f\ CO$$

The heat of combustion of C (to CO_2) is 393.5 kJ/g mole (32.77 kJ/g), while the heat of combustion of CO is 283.0 kJ/g mol (23.57 kJ/g), so that the heat of partial combustion (C to CO) is the difference, 110.5 kJ/g mol. With these assumptions, the entire char produces

$$G = 12(393.5) - 283.0\,f + 0.5(2021)\ \text{J}$$

The molecular weight of this model char is 249. Thus the heat produced in combustion is

$$h_c = G/249\ \text{J/g}$$

The mean heat of combustion of the tobacco, as measured by Sandusky, is

$$\langle h_c \rangle = 17360 \pm 210\ \text{J/g}.$$

Therefore, $f = 5.0 \pm 0.18$, and $n = 11.75$.

Thus the CO/CO_2 ratio is $f/(15\text{-}f) = 0.5$. This is typical for smoldering, though very large in comparison with the ratio in flaming combustion.

Note that even though there is only 1 mole of $C_6H_{10}O_8$ for every 24 moles of C, its heat of formation contributes 23% to the overall heat of combustion, a quite significant fraction of the energy balance. The overall model reaction, finally, is

$$12C + 0.5\ C_6H_{10}O_8 + 11.75\ O_2 \rightarrow 10CO_2 + 5CO + 2.5\ H_2O \qquad (83)$$

3. Regression (Burning) Rate

This study only considers the quiescent phase of smoldering, *i.e.*, between puffs, since that is the situation when the cigarette lies on the substrate. The paper in commercial cigarettes is chemically treated so that it decomposes and burns at the same velocity as the tobacco during these quiescent periods; this occurs in a region on the order of 1 mm in width. This location is called the "paper burn line," and will serve as the origin of coordinates ($x = 0$) in our further work. It is assumed here that the reactions in the paper do not influence the tobacco reactions, although we realize that there may well be both thermal and oxidative interaction.

Cigarettes vary within a factor of about two in the speed of propagation of the smolder wave. The average cigarette tobacco column is about 7.3 cm long, and it takes 15 ± 5 minutes to be consumed, without drawing or puffing on it. The burning rates have been measured to lie between 40 and 85 mg/min, consistent with the value given in Section III.B.1. The regression velocity is thus

$$V_r = L/\tau = 5.4 \pm 1.8\ \text{mm/min}.$$

The variations depend, at least, on the cigarette radius, the packing density, whether the tobacco leaf has been expanded or not, the moisture content of the tobacco, and the kind of paper, its permeability, and how it has been chemically treated. Note that the moisture content does <u>not</u> affect its peak temperatures (M. Samfield, 1986). Rather, it affects the burning velocity, because it takes time and energy to evaporate the water.

4. Reaction Rates

As will be seen in Section III.D.2, the reaction rates in combustion are well represented by Arrhenius expressions, which can give enormous rates at high temperatures. What limits the reaction rates is primarily the availability of oxygen; that, in turn, depends upon the rate at which the oxygen can be transported into the combustion (Ohlemiller, 1985). Therefore, the rate at which oxygen is allowed to diffuse into the cigarette is the principal determiner of the burning rate, unless the coal is so cooled locally as to cause limitations from the kinetics. The diffusion of oxygen will be discussed further in Section III.B.9.

The mean reaction rate for the cigarette is

$$<RR> \approx 0.85m/V\tau,$$

where 0.85m is the combustible fraction of the tobacco mass, V is the volume of the tobacco column, and τ the total duration of the smolder. We use a nominal mass of m = 1 g. The volume is $V = \pi R^2 L$, where the average L = 7.3 cm and R $\approx$ 0.4 cm; finally, $\tau \approx$ 840 s. Then $<RR> \approx 0.28$ mg/cm^{3}s.

If the reaction rate is described by an Arrhenius expression, then it must be highly peaked in the high-temperature region. Indeed, the simple approximation of an infinitely high reaction rate occurring over a surface which is a paraboloid (or conoid) of revolution might be expected to have some validity. This approach was used by Gugan (1966). Since the actual reaction rate is finite, this "surface" is in fact a thin region. This shell-like region is shown in Figure 17 (taken from Baker (1975)) by the shaded paraboloid. The highest temperatures occur at the centroid of this shell. Thus, suppose an observer were positioned at x = 0, *i.e.*, at the paper burn line. As time progresses and the smolder wave moves to the left, the peak reactions occur in a contracting ring, starting at the periphery and contracting to a point, leaving ash on the outside of the ring.

5. Heat Production Rate

We have seen that the mean mass loss rate is about 60 mg/min for a 870 mg cigarette; hence something like 70 mg/min for a 1 g cigarette. Of this, about 70% is evaporated/pyrolyzed with low energy production or loss, 30% is lost by char oxidation, a highly exothermic reaction. That is, about 20 mg/min are being oxidized this way. With $R_{CO} \approx$ 17 kJ/g, we end up with an energy production rate of about 340 J/min, or about 5.7 W. Note that with the variations among cigarettes described above, this value could easily be 50% greater or smaller:

$$<\dot{Q}> \approx 5.7 \pm 2.8 \text{ W}$$

6. Energy Balance

This heat input is balanced by losses; without going into detail, we can estimate:

a. Enthalpy loss *via* outgassing: $\dot{Q}_e \approx 2.0 \pm 0.4$ W

b. Convective losses from the surface: $\dot{Q}_c \approx 1.7 \pm 0.4$ W

c. Radiative losses from the surface: $\dot{Q}_r \approx 2.1 \pm 0.4$ W

As we see, although the energy losses balance the energy production, the uncertainties in these estimates are very large indeed.

d. Conductive losses: These apply when the cigarette is in contact with a substrate, and are discussed in Section IV. For the "free" cigarette (that is, the cigarette quietly smoldering in wind-free air, distant from any substrate or wall), there are no conductive losses.

7. Distributions Within the Cigarette

Temperature. A representative temperature distribution in a smoldering cigarette is shown by the isotherms in Figure 17. Figure 21, also taken from Baker (1975), shows the measured volume percentage of oxygen. Note that this value is essentially zero in the region of maximum temperature, so that the reaction (oxidation) rate there is low, in spite of the high temperature.

In order to be able to calculate the heat flux delivered to the substrate, the distribution of surface temperature must be known. In particular, most important is the **peak** surface temperature, T_p. Unfortunately, it is not an easy quantity to measure. Indeed, it is not even a well-defined quantity, since (as is seen from Figures 17 and 19) the gas and the solid temperatures are not quite the same.

Moreover, the result depends on the measurement technique. Baker's measurements yielded peak surface temperatures of about 550 °C. Egerton *et al.* (1963) found 616 °C for T_p. Lendvay and Laszlo (1974), using an IR technique, found that $T_p \approx 600$ °C. We will take this to be the mean value. Since peak surface temperatures may well vary by 50 °C among cigarettes, the peak surface temperature is 600 ± 50 °C.

Oxygen. The oxygen concentrations in the freely smoldering (*i.e.*, away from the substrate, in quiescent phase) cigarette are shown in Figure 18. It can be seen that the smoldering is indeed cylindrically symmetric. In fact, in our model it will maintain that symmetry even when interacting with the substrate. Consistent with an oxygen-diffusion-controlled process, the oxygen concentration in the center drops to very low values. The peak reaction rates generally occur in the region where the mole fraction of oxygen, $x(0_2)$, is less than one percent. One can write down some plausible analytic expressions for the radial distribution; but the actual distribution yields some surprises, as can be seen from Figure 18. For example, although one would *a priori* expect the concentration to increase monotonically from the center towards the boundary, examination of the actual dependence along a slice at $z = +6$ mm shows unexpected maxima and minima.

Gas Velocity. Some simple estimates show that the radial outflow velocity of hot gases from the cigarette can be as high as 7 cm/s. Thus inward oxygen diffusion is a counterflow problem. Indeed, this suggests that the principal inflows would be through the ash, away from the paper-burn line, and then axially towards the reaction zone. Note that the buoyancy of the hot gases will in fact affect the gas flow.

Surface Heat Flux. Consider Figure 19, giving the measured temperature of the cigarette surface, parallel to its axis. The net convective flux from this surface to the ambient is

$$\phi_c(x,t) = h[T(x,t) - T_a] \tag{84}$$

Similarly, the net radiative flux is

$$\phi_r(x,t) = \epsilon_C \sigma[T^4(x,t) - T_a^4] \tag{85}$$

where ε_c is the emissivity of the cigarette surface, σ is the Stefan-Boltzmann constant, and T_a is the ambient temperature. These fluxes, when integrated over the cigarette surface, must yield the energy loss rates $\dot{Q}_c$ and $\dot{Q}_r$ given in Section III.B.6.

The heat flux from the escaping hot gases, *i.e.*, the enthalpy loss, can be calculated once we have u_r, the radial convective velocity, as a function of x. Upon integration over the surface, it then yields the total enthalpy loss, $\dot{Q}_e$.

8. Pressure

Upon drawing on a cigarette, a person will generate a (negative) pressure corresponding to several hundred Pa (several centimeters of water, where one atmosphere corresponds to 101 kPa and 10.4 meters of water.) In the quiet state, the pressure difference is positive, but a minute fraction of this value. This pressure difference can be estimated:

The flow through a packed bed follows Darcy's law,

$$\dot{m}'' = f\Delta p \tag{86}$$

But

$$\dot{m}'' = \rho_g u_r, \tag{87}$$

where ρ_g is the gas density at the surface and u_r is the radial velocity. ρ_g is given by the ideal gas law,

$$\rho_g = \rho_a T_a / T_g \tag{88}$$

Hence,

$$\Delta p = \frac{u_r}{f}\frac{\rho_a T_a}{T_g} \tag{89}$$

With $u_{max} \approx 0.07$ m/s, $\rho_a = 1177$ kg/m^3, and $T_g \approx 900$ K $\approx 3T_a$, we have:

$$\Delta p \approx \frac{7\times 1.2\times 10^{-2}}{3f} \quad \textit{Pascals}$$

Sandusky (1976) estimates that for peripheral flow, $f \approx 10^{-3}$ s/cm. Hence:

$$\Delta p \approx 30 \text{ Pascals}$$

One atmosphere is 101 kPa, so this corresponds to 3×10^{-4} atm, or about 3 mm of water equivalent.

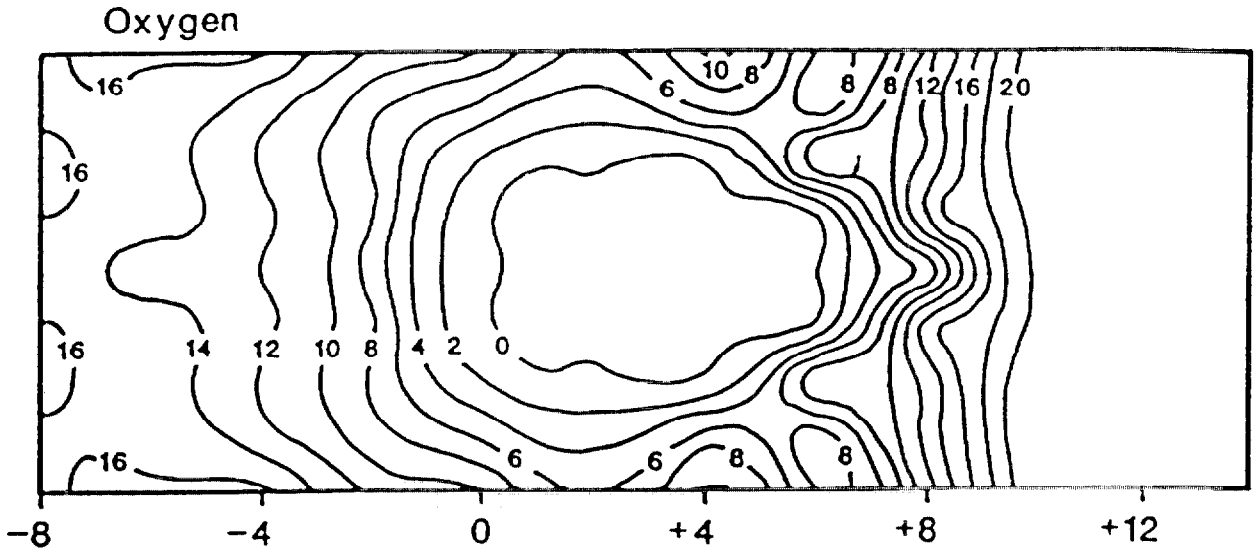

Figure 18. Oxygen concentration in the freely smoldering cigarette during quiet, steady burning.

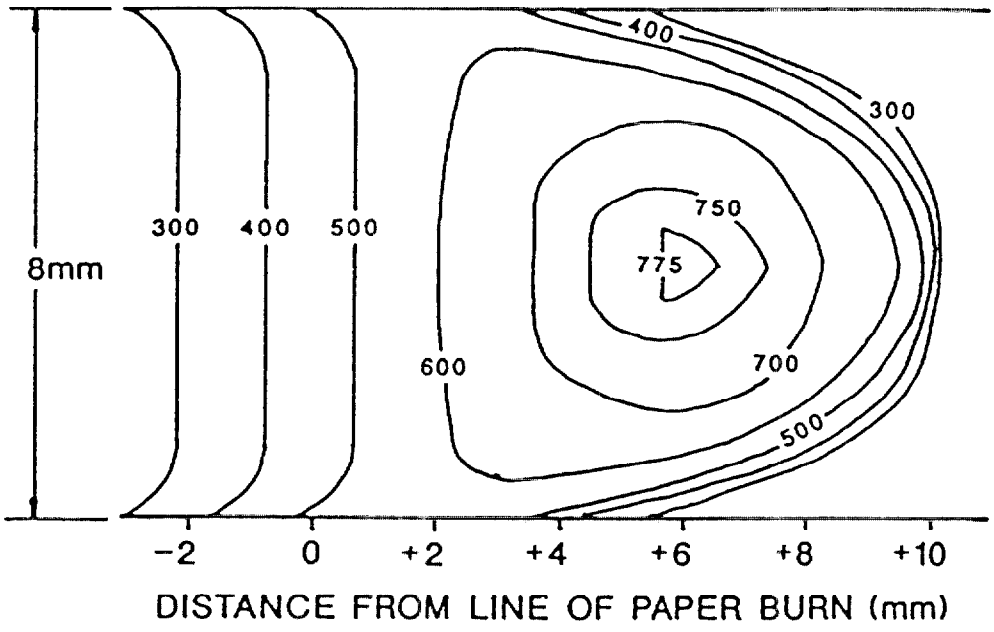

Figure 19. Isotherms in the solid part of the cigarette during quiet, steady burning.

9. Gas Transport

There is a boundary layer surrounding the cigarette, within which the oxygen concentration drops as the surface is approached. Fresh air is supplied by the ambient *via* convection and diffusion, as indicated by the arrows in Figure 20. That the oxygen must transport inward is clear, since the volume of air needed to consume the cigarette is about 1000 times the volume of the solid. Thus, 99.9% of the oxygen needed for combustion of the cigarette must come from the ambient. Some part may be drawn in from (through) the substrate, when the cigarette is in contact with it, but that is estimated to be a small fraction of what is drawn in from the atmosphere Ohlemiller *et al.* (1993, Appendix C), and it has not been modeled here. If there were no substrate, the inward diffusion would be approximately symmetric, the only deviation from symmetry being caused by the upward gas flow due to buoyancy.

Although the cigarette paper is permeable, it largely inhibits the diffusion of oxygen from the air into the tobacco, so long as it is intact. Once it has burned, its resistance to oxygen diffusion is much diminished. Since no measurements of this residual resistance have been published, we assume that it is zero. Therefore, most of the oxygen which is needed to sustain combustion diffuses into the cigarette in front of the paper burn line. [Not **all** of the needed oxygen is drawn in that way, however. If the paper is made non-porous, the cigarette will self-extinguish.]

Similarly, the considerable gradient in CO_2 which is established by combustion means that there is simultaneous outward diffusion of CO_2. Stoichiometrically, each molecule of O_2 reacts with a single carbon atom. This is how the cigarette loses most of its remaining mass upon combustion (recall that 60% of its mass, at a given point, already disappeared during dehydration and pyrolysis). Some of this mass is convected out, and some of it diffuses out, as just described. It is not difficult to show that the convection rate is one to two orders of magnitude greater than the diffusion rate. Note, to begin with, that before there is **any** counterflow diffusion of oxygen, about 60% of the tobacco column mass evaporates/pyrolyses away. This process occurs just adjacent to the combustion region. Thus at least 2/3 of the total outflow is due to convection.

10. Diffusion Coefficients

The diffusion that we are concerned with is that of O_2 in N_2. We will call the diffusivity of O_2 in N_2, D_o. For porous media, the effective diffusivity depends on the porosity, or the void space. It is shown in Szekely *et al.* (1976) that

$$D_{eff} / D_o = 0.677\, \Phi^{1.18} \tag{90}$$

for $\Phi < 0.7$. Although the total void fraction is $\Phi = 0.85$ (Muramatsu, 1981), we use this relationship nevertheless. We thus obtain the effective diffusion coefficient

$$D_{eff} \approx 0.56\, D_o = 0.112\ cm^2/s$$

at ambient temperature. This is precisely the value used by Muramatsu (1981). The diffusion coefficient is assumed to be the same for all the gases.

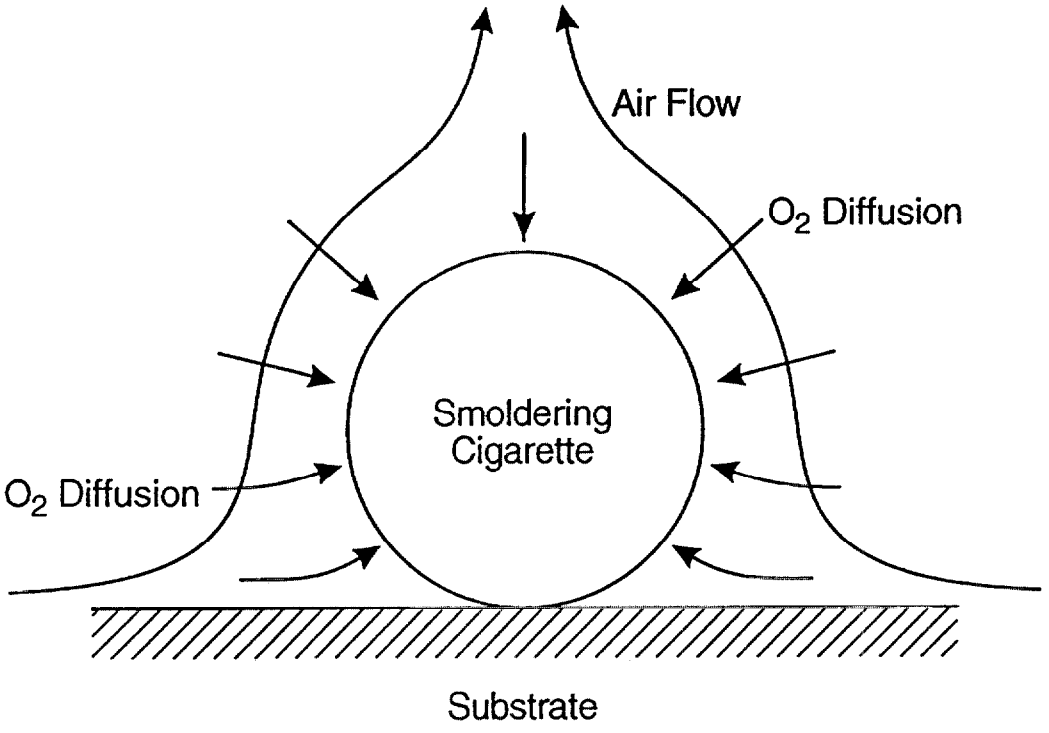

Figure 20. Schematic of how air enters the smoldering cigarette when it is resting on a surface.

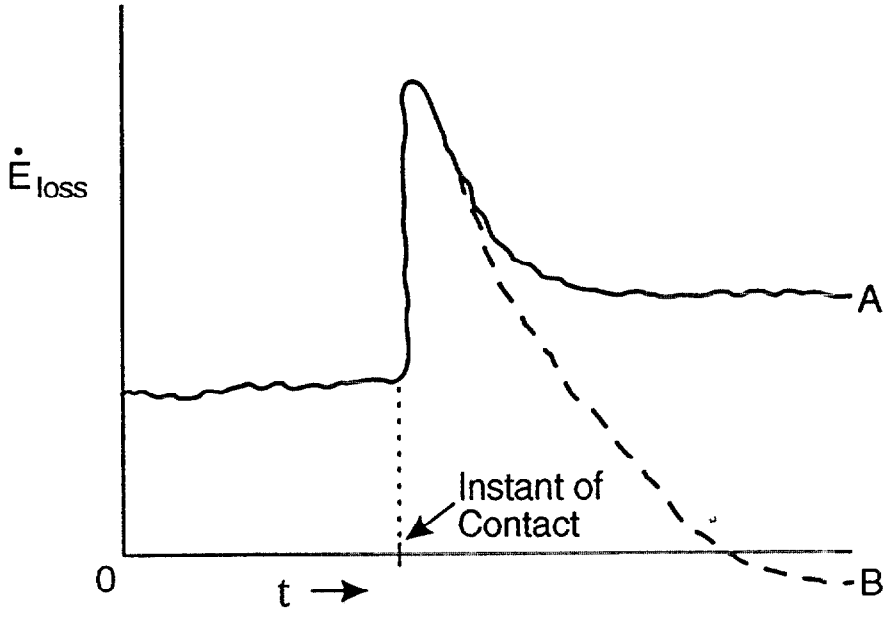

Figure 21. Schematic of the energy losses of a smoldering cigarette as a function of time, when it is dropped onto a surface. Curve A corresponds to a dense, inert substrate. Cuve B corresponds to a substrate which undergoes exothermic reactions.

From equation (16.3-1) of Bird *et al.* (1960), we find that for O_2 in N_2, the temperature dependence is

$$D_o(T) = 0.199\left(\frac{T}{293.16}\right)^{1.823} \quad \text{cm}^2/\text{s} \tag{91}$$

We shall use the same coefficient, but the theoretical temperature dependence

$$D_e = D_o(T/273)^{7/4} \tag{92}$$

rather than the empirical relation above.

11. Conduction Losses

These apply when the cigarette is in contact with a substrate, the situation of concern in actual fire initiation. According to the estimates made in Gann *et al.* (1988), the **initial** power loss to the substrate is about 2.1 $\pm$ 0.35 W, going down to about one-third of this in the steady state.

C. PREVIOUS MODELING EFFORTS

A number of attempts have been made to model the isolated smoldering cigarette or similar object. All of these attempts make some simplifying assumptions in order to make the problem tractable.

An early, related model is due to Moussa *et al.* (1977). They experimented with, and then modelled, the smoldering and extinction of a cellulose cylinder without any paper wrapping. They assumed the smoldering to be steady-state, and they treated the problem as one-dimensional (*i.e.*, no radial gradients). They found, experimentally,

- the smoldering velocity to be closely related to the maximum temperature in the cylinder;
- reasonable agreement between theory and experiment for the extinguishment limit;
- the rate-limiting step in the combustion to be diffusion of oxygen to the char, which is in good accord with experiment.

They also calculated values for v, the propagation velocity of the smolder wave. However, that calculation depends on an uncertain parameter, and the overall accuracy of the model is questionable.

A much more realistic and detailed model of a cigarette was produced by Sandusky (1976) and by Summerfield *et al.* (1978). It is also a one-dimensional model, but it considers the steady-draw case, rather than the free-burn condition. The model is heterogeneous; that is, it explicitly takes into account the fact that the tobacco comes in shreds. It considers a two-step process: pyrolysis to a char, followed by the oxidation of the char. It ignores water evaporation. The char-oxidation reaction is assumed to be a linear function of the oxygen concentration. The combustion model is time-dependent rather than steady-state, and considers the cover paper indirectly, via a varying surface permeability to oxygen. It uses a sophisticated treatment of heat transfer inside the cigarette, including heat transfer by radiation as well as by solid phase conduction.

The model consists of ten simultaneous, coupled partial differential equations (PDEs), and the starting condition assumes the presence of fixed amounts of ash, char, and tobacco. The calculation predicts the burning velocity fairly well, as a function of draw rate. The dependence on oxygen mole fraction in the atmosphere is less well predicted, although this is not important for the current purpose. The calculated gas temperature profile is fairly good: the peak is about right, but the width of the distribution is too narrow. Since it is a steady-draw model, diffusion and natural convection within the cigarette are considered as being of relatively minor importance.

The most elaborate model is that due to Muramatsu *et al.* (1979, 1981); it was developed in two stages. In the 1979 reference, they developed a one-dimensional, steady-state model for the pyrolysis of the cigarette. They focused on the evaporation-pyrolysis zone in a naturally smoldering cigarette. The model considers:

- pyrolysis of tobacco obeying Arrhenius kinetics,
- evaporation of water from tobacco following a mass-transfer and rate-determined process,
- weight loss of tobacco due to pyrolysis and evaporation,
- internal heat transfer characterized by an effective thermal conductivity which includes approximate radiation heat transfer,
- heat loss attributable to free convection and radiation from the outer surface of the cigarette and to endothermicity of the evaporation process, and
- smoldering speed.

These processes are expressed by a set of simultaneous ordinary differential equations that are solved numerically by the Runge-Kutta-Gill method. The equations are ODE's rather than PDE's, since they are independent of t and depend only on x, the position along the axis. The propagation velocity, v, is imposed. They do not include the convection or diffusion of gases other than water vapor. They take the existence of the paper wrapping into account only through its effect on the loss of water vapor.

These approximations work well. The model yields good agreement between theory and experiment for the temperature and density along the axis in the pyrolysis-evaporation region. Thus, the agreement for $T(x)$ and $\rho(x)$ is good for $x < 0$, *i.e.*, before the char-oxidation region, which is not considered in this part of their model. [As in Section III.B, we use $x = 0$ as the boundary between the pyrolysis region and the char-oxidation region, at the surface.] For $x > 0$, the calculated temperature profiles deviate substantially from measured ones, as might be expected. The dependence of the profiles on the imposed velocity shows only semi-quantitative agreement.

In the 1981 Muramatsu work, a char-oxidation model was added to describe the processes occurring in the region $x > 0$. The model is quite detailed; it takes two char oxidation reactions into account and is two-dimensional (cylindrically symmetric). Unlike the Sandusky model, it is a homogeneous model, *i.e.*, it does not take directly into account the fact that there are solid particles and a gaseous medium. Energy loss is through radiation and convection at the outside surface of the cigarette. Again unlike the Sandusky model, it assumes that there is no temperature difference between the solid and gaseous phases. This is not a bad approximation for natural smolder, and simplifies the problem considerably. Heat transport by thermal radiation inside the cigarette is taken into account in a somewhat different way than is done

in Summerfield *et al.* The thermal conductivity at any point is assumed to be isotropic. Similarly, the temperature-dependence of the gaseous diffusivity is taken into account explicitly. Finally, the pyrolysis/evaporation model and the char oxidation model are tied together through an energy-flow matching condition at the pyrolysis/char-oxidation boundary to obtain the appropriate smolder velocity.

The results of calculations made by Muramatsu for six representative cigarettes agree well with experimental data:

- The peak temperatures, when expressed in °C, are only 2.7% to 5.7% higher than the experimental data. [Since the temperature calculations are made with $T_a \approx 20$ °C as the datum, it is appropriate to use degrees Celsius for comparisons.]

- The smolder velocities are 14% high, on the average, varying between 4% low and 26% high.

- The calculated variations of smolder rate (V) and peak temperature (T_m) with R (the cigarette radius), the packing density, ρ_p, and the moisture content in the tobacco shreds are indistinguishable from the experimentally observed variations. The dependence of V and T_m on ambient oxygen partial pressure is not well-predicted; this is not an important consideration in our study.

- The calculated distributions of temperature and oxygen concentration in the char oxidation region are in agreement with measurement, except for a scale factor: the predicted distribution is narrower than observed. Because of this last point, Muramatsu *et al.*'s model cannot be used directly to obtain the flux emitted to the substrate: the too-narrow temperature distribution would substantially underpredict the energy output of the cigarette to the substrate. However, the model is excellent for some purposes; in particular, to estimate cigarette smolder velocities.

Although the model is very good, it may be appropriate to list some of its limitations:

- Prior to decomposition, the paper wrapping is assumed to be impervious to oxygen. According to experiment, this should result in the cigarette going out.

- Perhaps in order to be consistent with the above assumption, radial convection of gases is not included.

- Their calculation uses an iterative procedure to converge to a solution. If the calculation has not converged after 1000 iterations, the unconverged result is nevertheless accepted as correct.

Mitler (in Gann *et al.*, 1988) and Mitler and Davis (1987) developed a detailed, homogeneous model of a freely smoldering cigarette, called CIG25. Unlike Muramatsu's models, it is time-dependent rather than steady-state and two- rather than one-dimensional. Unlike Sandusky's model, diffusion and natural convection within the cigarette are included, since there is no steady-draw convection to overwhelm these effects. We may make some further comparisons; CIG25 differs from the model introduced by Sandusky *et al.* in a number of ways:

- Sandusky's model is heterogeneous, with tobacco shreds embedded in a gas. Therefore the local "ambient" for oxygen varies, and the rate at which oxygen reaches the shred surface is given by

$$k_m(y_o - y_s) \tag{93}$$

where y_o is the local ambient mass fraction of oxygen and y_s is the value at the shred surface.

CIG25 is homogeneous, with the cigarette core being a mixture of "solid" and "gas." The oxygen available to react with the solid is the local value, obtained by solving the diffusion equation for y, the oxygen mass fraction.

- The Sandusky *et al.* model is a steady-draw model with substantial axial convection and no natural smolder; CIG25 considers natural smolder **only**, and neglects axial convection in comparison to radial convection.

- The Sandusky model is a one-dimensional model which averages over the cross-section. CIG25 is two-dimensional, having radial gradients.

- CIG25 takes only <u>one</u> reaction into account, effectively considering a char cigarette, rather than a real tobacco cigarette.

Of course the models have a number of similarities; for example, they both neglect the production, transport, and effect(s) of water.

Mitler (1988) also described a "semi-empirical" model. This simple version consists of a number of correlations, partly based on results of making parametric runs with Muramatsu's model and corrected by experimental data where possible.

D. MODELING THE CIGARETTE

1. Assumptions

Based on the successes of the prior models, this Section lists the assumptions and equations valuable to a good, yet tractable model of a cigarette on a substrate. CIGARET uses a subset of them and is described in Section III.D.3. The following are facets to be included and their physical forms:

1. The cigarette model is two-dimensional, with axial and radial coordinates. It is also time-dependent, yielding V directly, whether or not it is constant. If a steady state were assumed, then the equations would simplify; however, it would then be necessary to choose the smolder velocity correctly (*i.e.*, as an eigenvalue), as Muramatsu did. Moreover, if the equations are taken to be time-dependent, the heat and mass transfer equations are parabolic partial differential equations (PDE's) which are easier to solve, in some ways. Finally, the convergence for the steady state equations is very slow. Indeed, Muramatsu found that one thousand iterations would not suffice, at times.

2. The cigarette is modeled with one pyrolysis reaction and one char-oxidation reaction.

3. The (internal) gas flow velocities depend on the pressure gradients; since the axial gradients, of order $\Delta p/L$, are generally much smaller than the radial gradients, of order $\Delta p/R$, axial convection is neglected, as being much smaller than radial convection.

4. The water (pre-existing or produced during combustion) in the tobacco column is also ignored.

5. The tobacco column is treated as a homogeneous, uniform mixture of gas and solid; there are no tobacco shreds.

6. The gas and solid phases are at the same temperature, locally.

7. Species or temperature gradients within the tobacco shreds will be neglected, consistent with assumption #5.

8. Radiation transfer within the cigarette is treated as an effective thermal conductivity.

9. The thermal conductivity is the same function of temperature throughout the cigarette, *i.e.*, whether in ash, char or tobacco.

10. The paper behavior appears only in the boundary conditions.

11. Consistent with assumption #10, any (axial or radial) gradients in the paper are ignored; an effective mass transfer coefficient is used to model diffusion through the paper.

12. The gases generated or heated by combustion move radially outward to the side boundary (aside from diffusion). Thus there is a radial flow calculated strictly by mass conservation. The gas pressure within the cigarette is assumed to be only negligibly different from atmospheric, and therefore no momentum equations are written.

13. The gas phase is quasi-steady; that is, $\partial \rho_g / \partial t \approx 0$.

14. No particulate aerosols are produced.

15. The cigarette combustion zone retains its cylindrical symmetry when lying on a substrate. This is observed to be approximately correct for some cigarettes on some fabric/foam substrates, especially after the cigarette "recovers" from the transient cooling effects of the substrate.

16. Prior to its ignition, the substrate's presence has two effects on the cigarette, both of which can be assumed to apply symmetrically (on the average) to the entire cigarette periphery:

    (a) The oxygen supply to the cigarette is reduced by some factor. The degree of reduction will depend on the permeability of the substrate.

    (b) The thermal effects (*e.g.*, as a heat sink) can be calculated in a decoupled manner (this assumption is weak, and may eventually have to be dropped).

It should here be made explicit that this model is for an isolated (that is, not in contact with any surface), quietly smoldering cigarette. Such a model will predict, among other things,

- the external heat flux from it, and the extent of the heating zone,
- the velocity of smolder propagation, and
- how these depend on: the radius of the cigarette (R), the tightness of packing (via the void fraction ϕ), the type of tobacco (*via* its thermophysical and kinetic parameters: heat of gasification H_v, heat of combustion H_c, activation energies and pre-exponential factors, density ρ, thermal conductivity k, specific heat C_p, etc), and the wrapping paper, *via* its permeability and its ignition, or decomposition, temperature. A better model would explicitly include paper thickness, chemical composition, porosity, and kinetic parameters, as well.

2. Governing Equations

The equations which describe the mass and energy transport in a smoldering cigarette will now be presented. Any simplifying assumptions beyond the 16 above will be indicated as each equation is discussed.

It is necessary to clarify some of the terms appearing in the equations. In the decomposition of the tobacco, one gram of tobacco, upon pyrolysis, produces n_c grams of char. The other 1-n_c grams are gaseous products. Each gram of char reacts with n_{O2} grams of oxygen to produce some heat, n_A grams of ash, and 1 - n_A + n_{O2} grams of gaseous products of combustion. Since the combustion process mostly proceeds at very low oxygen concentrations, it can be expected to be incomplete, and n_{O2} is smaller than the stoichiometric value. In the following equations, x is the axial coordinate.

Mass Conservation.

$$\frac{\partial \rho_s}{\partial t} = -[(1-n_C)R_p + (1-n_A)R_{CO}] \,. \tag{94}$$

where ρ_s is the mass density of the solid, R_p is the pyrolysis rate (in gm/cm^{3}s) and R_{co} the char oxidation rate. Axial convection is dropped, according to assumption #2, and the equation of continuity in cylindrical coordinates becomes

$$\frac{\partial}{\partial t}[\rho_s(1-\phi) + \rho_g\phi] + \frac{1}{r}\frac{\partial}{\partial r}(\phi r \rho_g u_r) = 0 \tag{95}$$

where r is the radial coordinate, ρ_g is the mass density of gases, ϕ is the void fraction in the cigarette (*i.e.*, the volume fraction of gas, rather than of tobacco shreds), and u_r is the radial velocity of the gas. Since the shreds are assumed not to shrink, ϕ remains constant. Assumption #11 implies

$$\frac{\partial}{\partial t}(\phi\rho_g) = \phi\frac{\partial \rho_g}{\partial t} \approx 0 \tag{96}$$

and using equation (95), the gas equation results:

$$\frac{\phi}{r}\frac{\partial}{\partial r}(r\rho_g u_r) = (1 - \phi)[(1 - n_C)R_p + (1 - n_A)R_{CO}] \tag{97}$$

Momentum. The procedure used in CIGARET is to assume no pressure difference so that the ideal gas law is satisfied. Mass conservation then gives the velocities directly, *via* the gas equation, Equation (97). The reason is that any attempt to calculate the convective outflows and velocities from a calculated pressure difference would require that we know the coefficient in Darcy's law (Section III.B.9) very well, *and* that we accurately calculate very small differences of large numbers. That would be extremely demanding of the computation and possibly prohibitive.

Species. V is the total volume of the cigarette; the total volume occupied by the solids in the cigarette is

$$V_s = (1 - \phi)V$$

We define the mean densities

$$\rho_i \equiv m_i/V_s \qquad i = A, C, T \tag{98}$$

where A, C, and T stand for ash, char, and tobacco, respectively. In this equation, m_A = total mass of ash, etc. Then the cumulative density of the solid parts of the cigarette is

$$\rho_S = \rho_A + \rho_C + \rho_T \tag{99}$$

Each of these densities varies with time.

The equations for the changes in tobacco and char densities are

$$\frac{\partial \rho_T}{\partial t} = -R_p \tag{100}$$

and

$$\frac{\partial \rho_C}{\partial t} = n_C R_p - R_{co} \tag{101}$$

The ash is inert and simply accumulates, so that an equation for ρ_A is not required.

Oxygen. We must know the oxygen concerntration everywhere in order to calculate the char-oxidation rate. The other gases are inert or nearly so. Moreover, the gases and solids are assumed to have the same temperature, so there is no energy exchange, and we do not need to consider the CO_2 diffusing out. Therefore, of the gaseous species equations, it is only necessary to include that for oxygen. Rather than dealing with the oxygen density ρ_{02}, the equations are best written in terms of y, the oxygen mass fraction:

$$y \equiv \rho_{O_2}/\rho_g \tag{102}$$

The equation is

$$\rho_g \frac{\partial y}{\partial t} + \rho_g u_r \frac{\partial y}{\partial r} = \frac{\partial}{\partial x}\left(\rho_g D_e \frac{\partial y}{\partial x}\right) + \frac{1}{r}\frac{\partial}{\partial r}\left(r \rho_g D_e \frac{\partial y}{\partial r}\right) - \left(\frac{1-\phi}{\phi}\right)\{y(1-n_C)R_p + [y(1-n_A) + n_{O_2}]R_{CO}\} \tag{103}$$

where D_e is the oxygen diffusion coefficient, and the axial convection term has been dropped.

Energy. Assuming that the gas is quasi-stationary, as in assumption #12 above, and that the specific heats of all gases are the same and independent of temperature, then the energy conservation equation can be written in terms of the temperature. It is:

$$(1-\phi)\rho_s C_s \frac{\partial T}{\partial t} + \phi \rho_g u_r C_g \frac{\partial T}{\partial r} = \frac{\partial}{\partial x}\left(k \frac{\partial T}{\partial x}\right) + \frac{1}{r}\frac{\partial}{\partial r}\left(rk \frac{\partial T}{\partial r}\right) + (1-\phi)(Q_{CO} R_{CO} - Q_p R_p) \tag{104}$$

where
C_s = specific heat of the solid
C_g = specific heat of the gases
k = thermal conductivity of the cigarette (see assumption #8)
Q_{co} = energy released from char oxidation (lower heat of combustion)
Q_p = energy absorbed in (endothermic) pyrolysis

The internal heat transfer has a radiative and a conductive component, as described earlier. The expression used here is the same as that used in Muramatsu (1981) and is due to Kunii (1961); for porous materials,

$$k(T) = (1 - \Phi^{2/3})k_s + \Phi^{1/3}\left(k_g + \frac{2}{3}h_r D_p\right) \tag{105}$$

where h_r is a heat transfer coefficient for radiation:

$$h_r = \epsilon_T 4 \sigma T^3 \tag{106}$$

D_p is the mean pore diameter, Φ is the total void fraction (including the void space in the shreds, and is therefore larger than ϕ), ε_T is the emissivity of the shreds, k_g is the thermal conductivity of the gas, and k_s that of the solid shred (and depends on the shred's mass density).

Since the gas pressure in the quiescent cigarette is very nearly the ambient air pressure, and since there is not a great difference between the molecular weight of the product gases and air, the ideal gas law permits one to write the gas density in the form

$$\rho_g = \rho_{go} T_o / T \tag{107}$$

where T is the absolute temperature.

Reactions. Finally, expressions for the tobacco and char reaction rates are needed. It is assumed that each is given by an Arrhenius relation:

$$R_p = \rho_T^m Z_p \exp(-E_p/RT) \tag{108}$$

where the exponent m is to be determined experimentally, as is the "frequency factor" (or "pre-exponential factor") Z_p. E_p is the activation energy for the pyrolytic reaction and R is the universal gas constant. The tobacco density ρ_T may be expressed as

$$\rho_T = \rho_S y_T \tag{109}$$

where y_T is the tobacco mass fraction.

Similarly, the char-oxidation reaction rate is taken to be

$$R_{CO} = \rho_C^n \rho_{O_2}^p Z_{CO} \exp(-E_{CO}/RT) \tag{110}$$

where (again) the exponents n and p are to be determined experimentally, and the densities are written in terms of the respective mass fractions:

$$\rho_c = \rho_s y_c \qquad \text{and} \qquad \rho_{O2} = \rho_g y \tag{111}$$

Initial Conditions. Before ignition of the cigarette, the initial conditions are

$$\rho_S(x,r,0) = \rho_{so} = \rho_{To} \tag{112a}$$
$$\rho_C(x,r,0) = \rho_A(x,r,0) = 0 \tag{112b}$$
$$T(x,r,0) = T_o \tag{112c}$$
$$y(x,r,0) = y_a \; (= y_{ambient} = 0.232) \tag{112d}$$

For the calculations, however, it was assumed that a match had been applied to the x = 0 end of the cigarette, producing some reactions. These used up only a small fraction of the tobacco, but most of the oxygen that had been *in situ*. The initial temperature distribution was assumed to be very high (1000 K) in the first millimeter of the tip, then to decrease linearly to ambient temperature in the next millimeter.

The oxygen mass fraction behaves in complementary fashion, as follows. For the following calculation, we may ignore the stoichiometry developed earlier and simply assume that the combustion of char proceeds according to

$$C + [(1+a)/2]O_2 \rightarrow aCO_2 + (1-a)CO$$

Then 16(1+a)/12 grams of oxygen are needed to burn one gram of carbon (char). As combustion lowers the local mass fraction of oxygen from y_a to y, it will lower the relative density of char (and hence tobacco) from 1 to x, where

$$x = 1 - [0.75/(1+a)n_c](\rho_g/\rho_T)(y_a - y)$$

This permits us to enter the initial density of tobacco so that it is consistent with the assumed distribution of $y(O_2) = y$. ρ_o is the actual mean tobacco density in the virgin cigarette.

Boundary Conditions. On the axis,

$$\left(\frac{\partial y}{\partial r}\right)_{r=0} = \left(\frac{\partial T}{\partial r}\right)_{r=0} = 0 \qquad \textit{for all } x, t \tag{113}$$

At the lit end of the cigarette, the temperature boundary condition is:

$$k\left(\frac{\partial T}{\partial x}\right)_{x=0} = \epsilon_A \sigma (T^4 - T_a^4) + h_e (T - T_a) \tag{114}$$

for all r and t. $T = T(0,r,t)$ and $T_a = T_{ambient}$.

Here, too, h_e = convective heat transfer coefficient (at the end), σ is the Stefan-Boltzmann constant, and ϵ_A = emissivity of the cigarette at the x = 0 end. We are assuming a grey body. The value to be used here should be that of the tobacco ash. It is assumed that the ash never falls off the cigarette, not realistic for active smoking, but appropriate for the case when the cigarette rests on a substrate. Moreover, if it were not made, the geometry would be continually changing, and the boundary conditions would become exceedingly complicated.

There is usually a filter at the other (x = L) end. It has been observed that the presence of a filter increases ignition propensity (Gann *et al.* 1988). This is probably due its limiting axial flow of air through the tobacco column. This model presumes no such flow. Thus, for the temperature boundary condition at the other end,

$$-k\left(\frac{\partial T}{\partial x}\right)_{x=L} = \epsilon_T \sigma (T^4 - T_a^4) + h_e (T - T_a) \tag{115}$$

for all r and t (where now $T = T(L,r,t)$).

Next, the cigarette's side surface must be considered. It is covered by paper. This paper wrapper in principle should also be included with its own set of equations, which include its reaction kinetics. However, the amount of heat released when it burns is negligible in comparison to that released by the tobacco. If a unique paper decomposition or ignition temperature can also be specified, then the paper's kinetic equations can be replaced by two appropriate boundary conditions, which simplifies the problem considerably.

If there were no paper, then the temperature boundary condition at the sides would be

$$-k(x,R)\left(\frac{\partial T}{\partial r}\right)_{r=R} = \epsilon_c(x) \sigma (T^4 - T_a^4) + h(T - T_a) \tag{116}$$

The emissivity of the cylinder surface is different for ash, char, or virgin material (except at the tip, the relevant material is paper, rather than tobacco, as is pointed out below); thus the emissivity is a function of x. Also, the thermal conductivity at the surface will in general depend on whether it is ash, char, or virgin material. The assumption which is made here is that k is the same for all three (assumption #9).

Similarly, although the heat transfer coefficient at the sides, h, will be different from what is at the ends, we simplify by assuming that

$$h_e = h$$

Moreover, since the ends generally emit much less heat than do the sides, it is not so important that we use the exactly correct values there. The emissivity ε_c has one value for the virgin region, another for the char region, and a third for the ash region. Note that these refer to *paper* char and ash, and may occur at different temperatures, and therefore different locations, than for the just-underlying *tobacco* char and ash. Because of these differing emissivities, ε_c will vary along the surface. Although $\varepsilon_c(x)$ may be a continuous function, the simplest approximation that can be made is that the paper pyrolyses, ignites, and disappears at some paper ignition temperature T_{ip}, so that there are just two values for ε_c - that for the virgin paper and that of ash. These meet at the paper burn "line." Experiments (Sandusky, 1976) have shown that $T_{ip} \approx 450 \pm 100$ °C.

The peak surface temperature occurs towards the "tip" end of the cigarette (*i.e.*, at $x < 0$), and therefore it is most important that ε_A be accurately chosen.

Finally, the oxygen boundary conditions must be considered. It is assumed, for the sake of simplicity, that the filter prevents any oxygen diffusion at the cold end ($x = L$):

$$D\left(\frac{\partial y}{\partial x}\right)_{x=L} = 0 \tag{117}$$

where D is the diffusion coefficient for oxygen within the cigarette. At the other end, the conditions must be

$$D\left(\frac{\partial y}{\partial x}\right)_{x=0} = \gamma_b (y_a - y_e) \tag{118}$$

where $y_e = y(0,r,t)$ is the oxygen mass fraction at the "hot" end of the cigarette and y_a is the ambient fraction, defined in equation (112d). D is a function of temperature; for the sake of simplicity, it is assumed that it is the same function for ash as it is for virgin tobacco and for char. γ is the mass transfer coefficient, sometimes referred to as k_g or k_m; see, for example, equation (93). Muramatsu (1981) gives it as

$$\gamma_b = 6.38 \times 10^{-3} \left[\frac{T^{2.75}(T - T_a)(T + 123.6)}{R T_a}\right]^{1/4} \quad \text{cm/s} \tag{119}$$

for the effect of the boundary layer, where T is the mean value between T_c (the local cigarette surface temperature) and T_a (the ambient temperature), and all temperatures are in Kelvins. This holds for the **free** cigarette, where there is no blockage by a substrate

For the side surface, the counterflow convection must be taken into account:

$$D\left(\frac{\partial y}{\partial r}\right)_{r=R} - u_r y_s = \begin{cases} \gamma (y_a - y_s) & x \geq x_p \\ \gamma_b (y_a - y_s) & x < x_p \end{cases} \tag{120}$$

where $x_p = x_p(t)$ is the position of the paper burn line at time t, u_r is the (outward) radial velocity at the surface, and y_s is the oxygen mass fraction at the surface.

The paper resistance to oxygen diffusion can be expressed as

$$\gamma_p = D_p/\delta \tag{121}$$

where D_p is the diffusion coefficient in the paper and δ is the mean paper thickness. The total resistance of both paper and boundary layer is then

$$\gamma = (\gamma_b^{-1} + \gamma_p^{-1})^{-1} \tag{122}$$

According to equation (120), the remains of the paper wrapper, where the paper has burned, present no barrier at all, and the radial oxygen diffusion at the boundary depends only on the properties of the boundary layer.

It is instructive to make estimates for the magnitudes of these terms. From equation (106), we see that at the peak surface temperature, 600 °C, $D_e \approx 0.856$ cm^2/s. For the gradient, we see that $x(O_2) \approx 0$ to about halfway out along the radius, so that we can take

$$\frac{\partial y}{\partial r} \sim \frac{y_s - 0}{R/2} \tag{123}$$

For γ, we use $\gamma \approx 0.8$ cm/s (from Table 5-B-1, Gann *et al.*, (1988)). Then equation (120) relates u_r and y_s. From Figure 18 (Figure 5-3b in the same reference), $[O_2]_s = 8 \pm 2\%$ in the most active region. Therefore, $y_s \approx 0.09 \pm 0.02$. Hence,

$$u_r \approx \frac{2D}{R} - \gamma\left(\frac{y_a}{y_s} - 1\right) \approx \frac{0.856}{0.2} - 0.8\left(\frac{0.232}{.09 \pm .02} - 1\right) = 2.9 \pm 0.5 \quad \text{cm/s}$$

If the gradient is indeed given by equation (123), then in order to be able to satisfy equation (120), we must have

$$u_r < 2D/R. \tag{124}$$

That is, too large a radial convective flow will prevent any oxygen from being able to enter the cigarette through the sides. This quantitatively confirms our physical intuition.

3. Choices for CIG25

The model CIG25 used a subset of the above equations which was believed to capture the most important processes. The key simplifications were:

- Since the pyrolysis is only weakly endothermic, it was dropped -- that is, it was assumed that $R_p = 0$ in equations (97), (101), (103), and (104).
- Probably more limiting, it was assumed for simplicity in some parts of the program that ρ_c and ρ_g are constant and uniform. In other parts of the program, the ideal gas law was properly used; hence, the relationships were inconsistent.
- There was no boundary condition for convective flow. This was not a serious issue, although the intact paper forms a barrier against convection. However, since there is no pyrolysis in this model, the only place where gas flow can originate is where high

reaction rates occur, producing high temperatures and expanding gases. All this takes place largely in front of the paper burn line, and therefore one would not expect significant flow behind that line. Therefore there was no need for such a boundary condition.

- The radiative losses from the surface were linearized (see equation (131)).

Because this was only a "partial" model, we would expect the results obtained with the correct values of input parameters to be somewhat unrealistic. The input parameters therefore have to be modified, in order to compensate for this.

E. NUMERICS

1. Discretization of the Equations

For the numerical calculations, the cigarette is divided into 10 or 20 cylindrical shells, *i.e.*, $\Delta r = 0.4$ or 0.2 mm, and into slices of the same thickness, $\Delta x = \Delta r$. This last equality makes the expressions a little simpler and more compact.

Originally, the equations were discretized using central differences for the spatial derivatives. This gives simple expressions which are accurate to second order in Δx. However, it is easy to show (*e.g.*, Peyret and Taylor (1983), Chapter 2) that this approximation introduces an artificial (*i.e.*, numerical) diffusion term with a negative sign. Hence, if the actual diffusion term is not large enough, numerical oscillations will begin, and instability ensue.

The stability criteria for the homogeneous convection-diffusion equation

$$\frac{\partial f}{\partial t} + A\frac{\partial f}{\partial x} + B\frac{\partial f}{\partial y} - D\nabla^2 f = 0 \tag{125}$$

are

$$\Delta t \leq \frac{4D}{|A|^2 + |B|^2} \tag{126}$$

and

$$\Delta t \leq \frac{\Delta x^2}{4D}, \tag{127}$$

assuming that $\Delta y = \Delta x$. Equation (126) is the Courant criterion.

Care was taken to satisfy the constraints on Δt and on the magnitude of the mass diffusion coefficient. Nevertheless, severe oscillations arose within a few hundred time steps. This was traced to the inhomogeneous source terms. Thus, when the convective-diffusive equation we are solving has a source term, that invalidates the criteria for Δt found above. The source terms are of Arrhenius type, and produce considerable stiffness in the equations. It would have been necessary to constrain Δt to a microsecond or so in order to avoid these oscillations. These problems could have been overcome by using implicit solution schemes and/or operator-splitting methods (Wichman, 1991). Another approach which is often used is to quasi-linearize the equations. This, however, would have reduced the accuracy

of the solutions. Thus, it was decided to use the same numerical technique as is used in CIG25. It is described in Section III.E.2.

If one takes $\Delta x = 0.2$ mm, then with the present DIMENSION statements, that only allows for cigarettes of 30 mm length (ordinary cigarettes average about 73 mm). However, it is likely that a quasi-steady state or ignition would develop long before 30 mm of cigarette was consumed.

2. Method of Solution

Ames (1969) shows that an equation of the form

$$\frac{\partial^2 u}{\partial x^2} + f(x,t,u)\frac{\partial u}{\partial x} + g(x,t,u) = p(x,t,u)\frac{\partial u}{\partial t} \tag{128}$$

can be put into the Crank-Nicolson form as follows:

$$\frac{1}{2h^2}\delta_x^2[u_i^{j+1} + u_i^j] + \frac{1}{4h}f[ih,(j+1/2)k,(u_i^{j+1} + u_i^j)/2]\delta_x(u_i^{j+1} + u_i^j) +$$

$$g[ih,(j+1/2)k,(u_i^{j+1} + u_i^j)/2] = p[ih,(j+1/2)k,(u_i^{j+1} + u_i^j)/2]\frac{(u_i^{j+1} - u_i^j)}{k} \tag{129}$$

where δ_x is the central-difference operator, h ≡ Δx, and k ≡ Δt. The equations above are precisely of this form. The method used to converge to a solution at each time step, is to iterate according to an under-relaxed Gauss-Seidel scheme. See Mitler (1988) for more details.

F. Improvements in CIGARET Over CIG25

There are five categories of improvements in CIGARET:

- The physics has been improved.
- The input is much more user-friendly. It also accepts input from SUBSTRAT.
- The output is in a form which can be used directly by SUBSTRAT.
- The program has been redesigned to be quasi-interactive with SUBSTRAT and can calculate the effects a substrate has on the smoldering.
- The documentation is improved.

These are described in the next three subsections. There is one more improvement which does not fit into any of the above five categories: The power of personal computers has increased substantially in the past six years, so that it is now feasible to run the program on a 486-level computer. Therefore the

program has been modified to run on a PC, rather than on a CYBER, as was the case for the antecedent program, CIG25.

1. Physics

The improvements in physics are four:

1. The gas density is now given by the ideal gas law, rather than taking it to be constant in the oxygen and the gas velocity equations, as was done earlier. See equations (97) and (103). In CIG25 the approximation was made that the product $\rho_g D_e$ could be taken from inside the derivatives in the first two terms on the right-hand side of equation (103). This eliminated the effects of gradients in the equations, and also allowed ρ_g to be factored out from all terms in that equation but the last. That is, in the identity

$$\frac{1}{\rho_g}\nabla\cdot(\rho_g D\nabla y) = D\nabla^2 y + T\nabla y\cdot\nabla\left(\frac{D(T)}{T}\right) \tag{130}$$

the second term on the right-hand side (where the ideal gas law was used to eliminate ρ_g), was dropped. This term has now been inserted into the program. Note that here we have taken into account not only the gradients in the gas density, but those of the diffusion coefficient as well.

2. Likewise, the char density now behaves correctly in the velocity subroutine, rather than assuming ρ_c also to be constant. In equation (97), the reaction rate R_{CO} depends on the char density (which falls with time). In CIG25, the density was taken to be constant, in this equation. Similarly, so was the gas density, ρ_g. Both of those densities now vary with time and position, properly.

3. The view factors for radiation exchanges have been calculated (see Section IV) and incorporated into CIGARET.

4. The radiation losses from the surface of the cigarette are now correctly calculated. That is, they are as given by equations (114), (116), and (148), rather than using the linearized form

$$\phi_{loss} = h'(T_c - T_a) \tag{131}$$

where h' is an effective heat transfer coefficient, which only approximates the effect of radiation loss.

2. Input and Output

The input section has been redesigned for much greater ease of comprehension and use. For example, the program now requests dimensional physical quantities, rather than the ratios used in the program and called for in the input section of CIG25. The program has also been redesigned so that it can indirectly interact with SUBSTRAT. See the USERS' GUIDE (Section II.H), for further discussion of these points.

The output files have been changed to accomplish the following:

- There is a complete "dump" at the end of each output time (file CIGOUT2), *the previous dump being eliminated*. This permits one to resume a calculation which has been interrupted for whatever reason. It also keeps the file from being too large.

- A small subset of CIGOUT2, the axial and the surface temperature distributions, is saved at each time step, and added to the other output file, CIGOUT1. SUBSTRAT uses only the surface distribution part.

It is appropriate at this point to indicate the modifications which have been made to TMPSUB2 to produce SUBSTRAT:

- SUBSTRAT uses the cigarette surface temperature distribution computed by CIGARET and passed to SUBSTRAT via the file CIGOUT1, to create the incident flux distribution. TMPSUB2 created a prescribed flux distribution used by the program, using a simple formula whose coefficients were obtained from its input file (magnitude of peak flux, σ_x, σ_y, prescribed velocity v). See equation (G2), Appendix G.

- SUBSTRAT now produces the file CIGIN1, to be used by CIGARET.

- What was previously called "initial x-position of (the flux) peak" (on the substrate) is now the x = 0 end of the cigarette.

3. Documentation

Besides the present report, the internal documentation in CIGARET has been somewhat expanded over what was in CIG25, so as to make it easier to follow the program. Also, the NOMENCLATURE section includes many of the symbols used in the program, which again facilitates understanding it, for anyone who wishes to do so.

G. RESULTS

1. Sensitivity of Calculation

The temperature dependence of the reaction rate given by equations (108) and (110) is very strong. Thus, assume the peaked spatial dependence

$$T(x) \approx T_a + \Delta T \exp\left[-(x - x_o)^2/\sigma^2\right] \tag{132}$$

for T, where $\Delta T \equiv T_{max} - T_a$. (See equations (C9) and (F2)). Then it is not difficult to show that the width of the resulting reaction rate distribution is approximately $\sigma\sqrt{\delta}$, where

$$\delta \equiv \frac{T_m}{T_m - T_a} \frac{T_m}{T_A + T_m}, \tag{133}$$

$T_m = T_{max}$, and $T_A \equiv E_A/R$ is the activation temperature. T_A is of the order $T_A \sim 22{,}000$ K, while $T_m \approx 1000$ K. Hence $\delta << 1$, and the reaction rate distribution R(x) is quite narrow. Hence the gradient is high:

$$\frac{\partial R}{\partial x} \approx \frac{0.63 R_m}{\sigma\sqrt{\delta}}, \tag{134}$$

where R_m is the peak reaction rate. Integration of the reaction over a volume shows that we must also have

$$R_m \sim \frac{const}{\sigma^2 \delta}. \tag{135}$$

Hence

$$\frac{\partial R}{\partial x} \propto (\sigma\sqrt{\delta})^{-3}, \tag{136}$$

and the gradient thus rises rapidly with T_A. Thus the grid size must be adequately small in order for the numerics to adequately cope with this. In fact, with a grid size $\Delta x = 0.2$ mm, the program could not converge with $T_A = 22{,}660$ K, the measured value. The "brute force" approach would be to halve the grid size to 100 microns. Not only would that quadruple the computational time to impractical levels, it could not even be done with DOS-based PC's, because of inadequate memory space. It was therefore necessary to use a lower, "model" value for T_A. To compensate, we also lowered the pre-exponential factor such that the rate constant was approximatly correct in the temperature range of interest. The program converges with $T_A = 15{,}000$ K.

2. Velocity of Smolder Wave

Three 30-second runs were made with the input data shown in the sample input data, Section III.H.4, to obtain 90 seconds of free smolder by this hypothetical cigarette. Some of the results are shown in Figure 22. The upper and lower curves in that figure show the positions of the intersections of the 600 K isotherms with the surface, as a function of time. Note that these isotherms enclose the reaction zone. Since the distance between them is still growing at t = 90 s, it is clear that a steady state has not yet been reached.

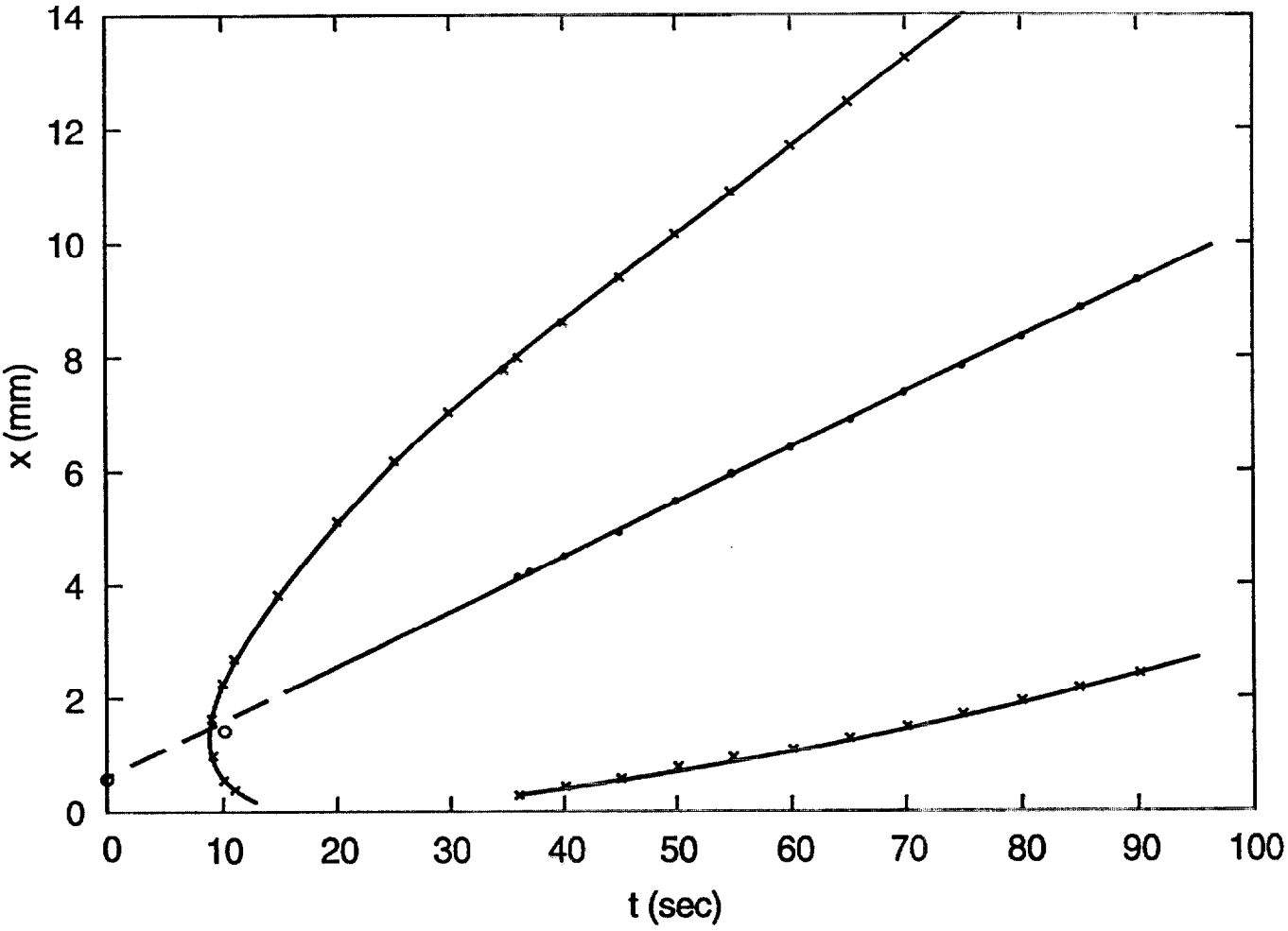

Figure 22. Result of a sample run with CIGARET. The upper and lower curves show the positions of the intersections of the 600 K isotherms with the surface, as a function of time. The central line is the locus of the midpoints between the curves.

Assuming that the isotherms are approximately symmetrical fore-and-aft, we have taken the midpoints of the intersections of the 600 K isotherms at the surface to represent x_o, "the" position of the smolder wave front. The fore-and-aft symmetry is not, in fact, perfect: the same procedure used for several different isotherms at t = 60 s yields the values shown in Table 6.

Table 6. Position of Cigarette Smolder Front at 60 Seconds as a Function of the Choice of Isotherm

Isotherm (K)	x_0 (mm)
600	6.4
700	6.6
800	6.7

Thus, as can be seen, although the "centroid" positions depend on which isotherm is chosen, the differences are quite small, so that the 600 K isotherm is representative of the front.

The central curve shown in the figure is the mean value of the isotherms, which we may refer to as $<x>_{600}$. The points have been joined by a straight line, in fact, indicating that the smolder wave (regression) velocity calculated this way is remarkably constant in the period shown, even though a steady state has not (yet) been achieved. The slope of this line is V_{600} = 5.36 mm/min, a reasonable velocity.

The peak temperature in this calculation is not always on the axis. Although it is not plotted, the position of the peak temperature is <u>not</u> a good indicator of the regression rate during these first 90 seconds. At times it does not make any forward progress at all, for example. As the smolder continues, steady state would presumably be approached; when that eventually happens, of course the peak temperature will then move at the same velocity.

3. Temperature Profiles

The temperature profiles at t = 60 s, from the run described above, are shown in Figure 23 as a function of x, the distance from the cigarette tip. The upper curve is that on the axis; the lower one, the surface temperature. Note that the axial temperature peak is at x = 3.2 mm, well forward of the surface peak, at x = 5 mm. The interior peak evidently corresponds to the cone tip, and therefore it is quite reasonable that the peak should be in front of the surface peak. Note, further, that the paper burn line must be at 450 °C = 723 K, and that that occurs at x = 10.8 mm; hence the cone length is 10.8 - 3.2 = 7.6 mm, a not unreasonable length.

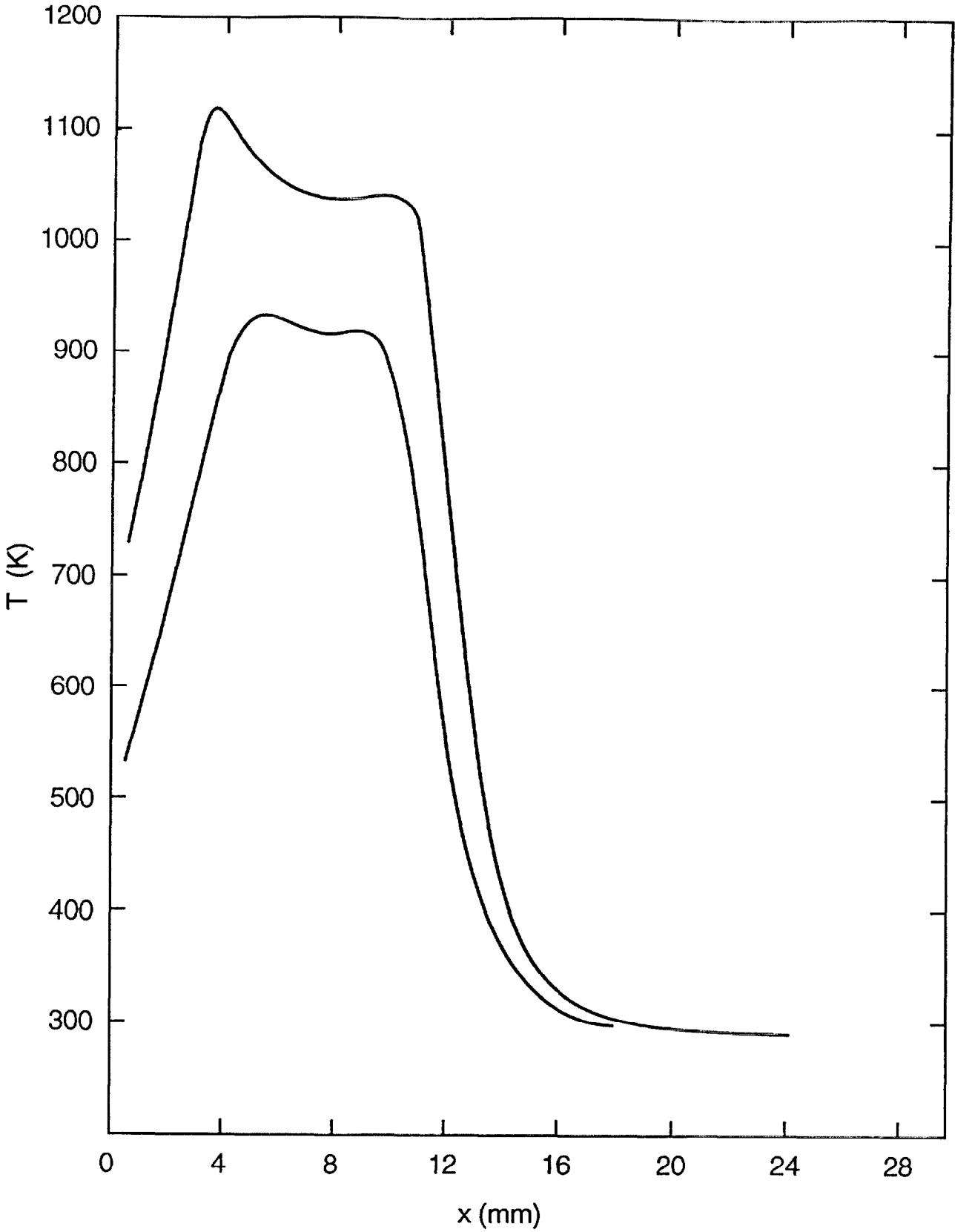

Figure 23. Longitudinal temperature distributions, along the axis and along the surface, at t = 60 s, for a sample run with CIGARET.

H. USERS' GUIDE

1. Running CIGARET

CIGARET and two helper programs together with the SUBSTRAT program are available on a diskette for IBM PC-compatible computers. The distribution diskette includes both executable and source code for CIGARET and SUBSTRAT, executable code for the helper programs, and sample input files. The CIGDATA program is used to prepare data files for CIGARET. CIGDATA must be run on an IBM PC-compatible computer with VGA graphics. CIGARET requires a 486 class PC (no graphics needed) in order to achieve satisfactory performance. On a 486/33 computer, 1 second of simulation time requires about 6 minutes of clock time, a factor of over 300, for $\Delta x = 0.2$ mm (3172 nodes). Running the program on a Silicon Graphics workstation, which is about 20 times faster than a 486/33 computer, is much more satisfactory.

The CIGARET source code (file CIGARET.FOR) can be compiled using any ANSI FORTRAN compiler. All CIGARET input and output files are ASCII files. Therefore, CIGARET can be recompiled and run on a different computer, while still using CIGDATA and SUBSTRAT on a PC and transferring files between the computers. A different computer may allow CIGARET to execute faster.

The user should be sure to inspect the README file on the distribution diskette. One way to read this file is to place the diskette in drive A: (or drive B:) and type

MORE < A:README or **MORE < B:README**

A permanent copy may be made with

PRINT < A:README

The README file contains a list of all files on the diskette, instructions for installing the necessary files on your hard disk, and information on any changes or additions to the program.

There should be at least 1 MB available on your hard disk. It is best to create a single subdirectory for the executable programs and related data files. This will allow you to easily delete all the files related to this program when you are finished with it. In general, *keep all files in the current working directory.*

Install the CIGARET program following the instructions in the README file. For example, from the directory on the hard disk where you want CIGARET installed and with the diskette in A:, type

A:INSTALL A:

2. Input and Output Files

All input for CIGARET must be placed in a data file, whose contents are described in Section III.H.4. This file is read as the "standard input stream," so CIGARET executes on MS-DOS and UNIX computers by redirecting the input file. For example, begin a run by typing

CIGARET < CIG1.DAT

where "CIG1.DAT" is the name of your input data file. [There is a sample input file available on the distribution diskette, TEST2.DAT]. As CIGARET completes each time step during the simulation, it displays the time (in seconds), the iteration number (K) within the current time step, and the time step number (IT). This allows you to monitor the progress of the simulation. At first, it takes over 100 iterations per time step to converge; as time goes on, fewer and fewer iterations are required, until as few as two or three suffice.

Two files are written by CIGARET:

CIGOUT1 provides cigarette surface temperature data for the SUBSTRAT program which are used to determine the incident heat flux on the substrate.

CIGOUT2 contains a dump of the cigarette field variables, which allows the program to be restarted at any future time (see Section III.H.3).

3. Restarting a Run

CIGARET can be aborted in the usual way by pressing CTRL and C at the same time. The dump file CIGOUT2 will be produced.

A terminated run (either aborted or terminated in some other way) can be restarted by using the dump file CIGOUT2. First, change its name to CIGIN2. Then, the input file (CIG1.DAT, in our example) must be edited by changing the last data value in the file from 0 to 1; this alerts the program to use CIGIN2 to initialize the variables. Then type "CIGARET < CIG1.DAT" as before, and the execution begins.

If a run is expected to be prohibitively long, it can be run in several steps. However, since a new copy of CIGOUT1 is produced every time CIGARET is run, it is necessary to save and then merge these files into a single CIGOUT1 file. This is best done by renaming each file as it is created. For example, type

RENAME CIGOUT1 CIGOUT.1,

RENAME CIGOUT1 CIGOUT.2, etc.

Finally, combine the files by using the CMERGE program:

CMERGE CIGOUT.1 CIGOUT.2 ... CIGOUT.N

The above command merges the specified files to create a new CIGOUT1.

4. Contents of the Data File

Line	Variables		Brief description
1	NR NZ RAD	NR	number of cells in radial direction
		NZ	number of cells in axial direction
		RAD	radius of cigarette [cm] (normalization: R)
2	PH PH1 DP	PH	void fraction
		PH1	total void fraction
		DP	diameter of pores [cm]
3	D1 D2 D3	D1	tobacco density / gas density
		D2	char density / tobacco density
		AN	ash density / tobacco density
4	SPHGS A FK	SPHGS	Cp(air) / Cp(tobacco)
		A	1/[density(solid)*Cp(sol)*R^2] [cmK/J]
		FK	thermal conductivity of tobacco [W/cmK]
5	D CN GK	D	oxygen diffusion coefficient / R^2 [s^{-1}]
		CN	mass of oxygen / mass of char consumed
		GK	thermal conductivity of gas [W/cmK]
6	B C E	B	pre-exponential factor * density [1/s]
		C	heat of combustion / Cp(tobacco)
		E	activation temperature [K]
7	TA TP EC	TA	ambient/initial temperature [K]
		TP	paper ignition temperature [K]
		EC	cigarette surface emissivity, ε_A
8	YA GAR GARP	YA	ambient oxygen mass fraction
		GAR	mass transfer coefficient for air,/R: γ_g/R [1/s]
		GARP	combined coefficient (air+paper): $R^{-1}(\gamma_p^{-1} + \gamma_g^{-1})^{-1}$
9	ISP INP IEB	ISP	number of time steps
		INP	number of time steps between data outputs
		IEB	number of time steps between energy balance checks
10	TS1 TS2 ERR	TS1	time step for first 50 steps [s]
		TS2	time step for later iterations [s]
		ERR	Gauss-Seidel convergence criterion
11	IDATA	IDATA	1 = read CIGIN2 to restart CIGARET

Sample Data File
(Note: the number of spaces between inputs on a line is arbitrary.)

```
21   151   0.40
0.65   0.85   0.0575
627.   0.341   0.13
0.777   6.5   3.16E-3
0.7   1.6428   4.514E-4
1.1085E9   13461.5   1.50E4
293.15   723.15   0.73
0.232   8.225   2.725
10000   200   80000
0.005   0.005   0.001
0
```

5. Producing a Data File

The CIGARET input data file can be created with any ASCII line editor. CIGDATA creates these data files interactively and thus uses certain commands which restrict its operation to IBM PC-compatible computers. It includes some checking of the input data. CIGDATA is especially useful for creating a data file which is only slightly different from another data file. This is useful in performing the parametric studies for which CIGARET was designed.

There are two special files in CIGARET to help the user with CIGDATA:

> The help file, CIGDATA.HLP, contains the text of the interactive help messages. Help is activated by pressing the F1 function key. If the help file is not available in the current working directory, no interactive help will be available.
>
> The configuration file, CIGDATA.CFG, sets the colors of the display. The file included on the distribution diskette assumes that a standard VGA monitor is being used. If the configuration file is not in the current working directory, a set of default colors will be used. A new configuration file can be made by using the MAKECFGT program. See the README file for instructions.

The operation of CIGDATA is explained on the following pages, which show the messages and input screens which will appear as the program is run. After reading through these pages, try using CIGDATA with one of the sample data files. Begin the program by typing **CIGDATA**. Abort the program by pressing CTRL and C simultaneously.

Data input screens from CIGDATA:

Screen 1: (primary menu)

```
=======================================================
CIGARET data preparation:

   #   File information

   #   Geometry data

   #   Tobacco data

   #   Pyrolysis data

   #   Gas data

   #   Boundary data

   #   Simulation control

   #   Exit data preparation

Use cursor keys to move between menu selections.
Press ENTER to activate the menu selection at the X.
Press ESC to return from a selection.  Press F1 for help.
```

Screen 2:

```
=======================================================

File data:                          press ESC when done;  press F1 for help.

    Name of old data file: ▓▓▓▓▓▓▓▓▓▓▓▓
    Name of new data file: ▓▓▓▓▓▓▓▓▓▓▓▓
```

Screen 3:

```
=======================================================

Geometry data:                      press ESC when done;  press F1 for help.

          Radius of cigarette: ▓▓▓▓▓▓▓▓▓▓▓▓ [mm]
 Number of cells in radial direction: ▓▓▓▓▓
  Number of cells in axial direction: ▓▓▓▓▓
```

Screen 4:

```
Tobacco data:                          press ESC when done;  press F1 for help.
       Density of tobacco: [          ] [kg/m^3]
     Thermal conductivity: [          ] [W/m K]
            Specific heat: [          ] [kJ/kg K]
             Void fraction: [          ]
       Total void fraction: [          ]
          Diameter of pores: [          ] [mm]
```

Screen 5:

```
Reaction data:                         press ESC when done;  press F1 for help.
   Pre-exponential factor: [          ] [m^3/kg s]
   Activation temperature: [          ] [K]
          Heat of reaction: [          ] [kJ/kg]
  Oxygen mass / char mass: [          ]
           Density of char: [          ] [kg/m^3]
            Density of ash: [          ] [kg/m^3]
```

See the explanatory note on the next page re "Activation temperature."

Screen 6:

```
Gas data:                              press ESC when done;  press F1 for help.
  Thermal conductivity of the gas: [          ] [W/m K]
          Specific heat of the gas: [          ] [kJ/kg K]
     Oxygen diffusion coefficient: [          ] [m^2/s]
```

Screen 7:

```
======================================================

Boundary data:                    press ESC when done;  press F1 for help.

     Initial/ambient temperature: [redacted] [°C]

      Paper ignition temperature: [redacted] [°C]

            Cigarette emissivity: [redacted]

    Ambient oxygen mass fraction: [redacted]

Mass transfer coefficient through boundary layer: [redacted] [m/s]

  Mass transfer coefficient through virgin paper: [redacted] [m/s]
```

Screen 8:

```
======================================================

Simulation control:               press ESC when done;  press F1 for help.

            Total number of time steps: [redacted]

          Steps between outputs to substrate: [redacted]

          Time step for first 50 steps: [redacted]

        Time step for later iterations: [redacted]

     Gauss-Seidel convergence criterion: [redacted]

    ([redacted]) begin simulation with default start-up conditions
    ([redacted]) read CIGIN2 to resume a simulation
```

Activation Temperature: As in TMPSUB2 (and therefore in SUBSTRAT), we use the activation **temperature** of the reaction, defined as:

$$T_A \equiv E_A/R$$

(where E_A is the activation energy and R is the universal gas constant), as the input parameter, rather than E_A itself.

I. SUMMARY OF SECTION III

The dynamics of a freely smoldering cigarette have been discussed. Similarly, what happens when it is resting on a substrate has been considered. Some of the mathematical models designed to simulate a smoldering cigarette have been outlined. Then the equations that must be satisfied by a cylindrically symmetric, homogeneous model of a cigarette quietly (freely) smoldering in air have been set down, within some specified simplifying assumptions (Section III.D.1). The effects of the paper wrapping, which pyrolyses away, are included.

The present program, CIGARET, is the outgrowth of an earlier model, CIG25, which employed some simplifications to the equation; principally, the neglect of pyrolysis (which has relatively little consequence in terms of the energy balance). CIGARET is a much-improved program in a number of ways which are described in detail in Section III.F. The numerical method used for solving the equations is described, and some of the problems discussed, in Section III.E. A primer on the use of CIGARET is given in Section III.H.

Some of the results obtained from using CIGARET are given in Section III.G. One remarkable result is that after ignition, the velocity of the resulting smolder wave quickly becomes constant, long before a steady state is achieved. The region in which char oxidation is proceeding rapidly (the glowing region) is correctly calculated to be conoid-shaped, and of the correct length.

IV. SIMULATING A BURNING CIGARETTE ON AN IGNITABLE SUBSTRATE

A. Introduction

The process which we are simulating is the heating and possible ignition of a substrate by a cigarette. In order to do that, the models SUBSTRAT and CIGARET developed in Sections II and III must be used in conjuction with each other. In this Section, the effects which take place when the lit cigarette and the substrate are in intimate contact are discussed. Next, it is shown in Section IV.C how the two programs are to be used in tandem in order to simulate the interaction. Finally, the effects are then calculated in detail. It is not essential that the reader read these last subsections in order to be able to use the program intelligently.

B. Qualitative Description

Consider the effects of a cigarette on a horizontal substrate that might affect the ignition of the substrate:

- The principal effect is the heating of the substrate by the hot cigarette coal.
- If any oxidative reaction takes place in the substrate, the cigarette competes with the substrate for oxygen.
- Some of the water vapor and tar emitted by the cigarette may recondense on the surface of the substrate and change its thermal characteristics.
- The cigarette affects the boundary conditions on the substrate: it interferes with convective cooling over the entire length of the cigarette.

Conversely, the horizontal substrate will influence how the cigarette smolders and thereby affect the likelihood that the cigarette will ignite it:

- The cold substrate initially provides a substantial conductive heat sink to the cigarette.
- If the substrate eventually undergoes exothermic reactions, it will heat the cigarette, instead.
- The substrate obstructs access of oxygen to the cigarette.
- If the substrate begins to react with oxygen, then the oxygen depletion for the cigarette would become still more severe.

These effects fall into two categories: gas transport effects and thermal effects. Consider the former first. There is a boundary layer surrounding the cigarette, within which the oxygen concentration drops as the surface is approached. Oxygen is supplied to the combustion site by the ambient *via* diffusion, as indicated by the arrows in Figure 23. The proximity of the substrate reduces the availability of oxygen to the cigarette from below. This will tend to inhibit the smoldering rate. This effect can be simulated by assuming that $y_a < 0.232$; CIGARET is given the information through the input file. See Section IV.D.4.

Thermally, the colder substrate cools the cigarette near the line of contact with the substrate, further inhibiting smoldering. This sink is not constant: as time progresses, the substrate heats up, and its cooling effect becomes progressively weaker. Radiative losses from the cigarette are decreased both because the cigarette is cooler and because one of the "targets" for this heat is warming and re-radiating back to the cigarette. If the heat loss from the cigarette is sufficiently high, the cigarette goes out. This effect is schematically indicated as curve A in Figure 21. If the substrate is not inert and exothermic reactions take place, cooling may be replaced by heating; this is sketched as curve B in the figure. This effect is also given in the input file for the cigarette, through the surface boundary conditions, as discussed in Section IV.D.

When both the cigarette and the substrate are reacting with oxygen, they are concurrently (a) generating heat, which accelerates their heat production, and (b) competing for oxygen, which retards their heat production. The modeling of effect (a) has been extensively described in Sections II and III; the modeling of (b) is not treated in this study.

C. Use of the Two Programs

It is important to understand how CIGARET and SUBSTRAT are used to obtain the interaction between the smoldering cigarette and the substrate with which it is in contact. The cigarette-substrate interaction is obtained through the boundary conditions which apply to each of the two models.

A full simulation requires an iterative use of CIGARET with SUBSTRAT (Section IV). Before starting, one should be sure there is no file named CIGIN1. First, run CIGARET (see Section III.H), generating CIGOUT1. The latter is now read by SUBSTRAT by typing

SUBSTRAT < INPUTFILE

(see Appendix B). [This was done before for TMPSUB2, as well.]

SUBSTRAT now produces a new input file, CIGIN1, for the CIGARET program. This file contains substrate surface temperature data which become part of the boundary conditions for the cigarette. Then run CIGARET, which will read CIGIN1 and create a new CIGOUT1. This simulation now includes an estimate of the influence of the substrate on the cigarette. Then run SUBSTRAT again, and so forth until convergence is obtained. *The input data files produced by the user for CIGARET and for SUBSTRAT (as distinct from the files produced by the programs themselves) must remain the same during these iterations.*

Since the principal effect of the cigarette is to heat the substrate, how to find the heat flux from the cigarette to the substrate will now be considered in detail. Then, the reciprocal effects of the substrate on the cigarette are discussed.

D. DETAILED CALCULATIONS OF INTERACTIONS

1. Conduction Flux to Substrate

We begin by calculating the heating flux delivered to the substrate by the cigarette. The substrate starts out at the ambient temperature and is in fair thermal contact with the cigarette. As shown in Figure 24, the measured flux is the initial (and momentary) flux from the cigarette to the cold substrate at the very small area of contact between them, along the LC (line of contact). The peak measured flux shown is about 5.6 W/cm^2. Since the measured coal surface temperature there was about 550 °C, the (net) blackbody radiation to the ambient is 2.56 W/cm^2. Muramatsu measured $\varepsilon_A = 0.73$; hence the actual radiation loss (assuming a grey body) is $\phi_{rad} = 1.9$ W/cm^2. This leaves 5.6 - 1.9 $\approx$ 3.7 W/cm^2 loss rate via conduction. With a surface temperature of 550 °C and an ambient temperature of 20 or 25 °C, one infers that the effective heat transfer coefficient is 71 W/m^{2}K, about seven times what it is in air. This large flux (5.6 W/cm^2) heats the substrate rapidly, so that the net flux, given by the first part of equation (137), falls rapidly to lower values.

The flux distribution $\phi(x)$ shown in Figure 24 is that along a narrow region (1.5 mm wide) about the line of contact; that is, it is $\phi(x,0)$. In order to find the heating of the substrate, we must also know the transverse and time dependences of the flux: $\phi = \phi(x,y,t)$.

It has been assumed that the initial substrate surface temperature is the ambient temperature, *i.e.*, $T_s(x,0) = T_a$. The heating flux from the cigarette to the substrate along the CL, $\phi_c(x,0,t)$, is given by experiment, as in Figure 24; the flux from the (resulting) hot substrate, $\phi_s(x,t)$, is calculated by the substrate program.

Moving away from the line of contact, the temperatures rapidly approach ambient. Therefore, the convective heat transfer effects of the cigarette diminish and the heat transfer coefficient asymptotically falls to its ambient value. A reasonable approximation to how the net convective flux to the substrate must vary with y is

$$\begin{aligned} \phi_{net,c}(x,y) &= h_c[T_c(x) - T_s(x,y)]\,\Omega_c(y) \\ &\quad + h_o[T_a - T_s(x,y)][1 - \Omega_c(y)] \end{aligned} \tag{137}$$

where h_c is the heat transfer coefficient for convective heat loss from the cigarette to the substrate at the point at the line of contact corresponding to the peak flux (about 71 W/m^{2}K). h_o is the heat transfer coefficient for convective heat loss from the surface to the ambient (about 10 W/m^{2}K), and $\Omega_c(y)$ is a fraction indicating the convective influence of the cigarette at the distance y. Note that the net convective flux "into" the surface can become negative. If the cigarette extinguishes, for example, the fluxes from the cigarette disappear, and $T_c - T_s$ is asymptotically replaced by $T_a - T_s$.

We can break this flux into two parts, one of which is independent of the substrate temperature, and the other of the cigarette temperature. Thus, the cigarette "emits" the convective flux

$$\phi_{cig,c} = h_c(T_c - T_a)\Omega_c \tag{138}$$

to the substrate at (x,y), and the substrate at that point loses energy (convectively) at the rate

$$\phi_{sub,c} = [h_o + (h_c - h_o)\Omega_c](T_s - T_a) \tag{139}$$

where the arguments x and y have been suppressed for the sake of brevity.

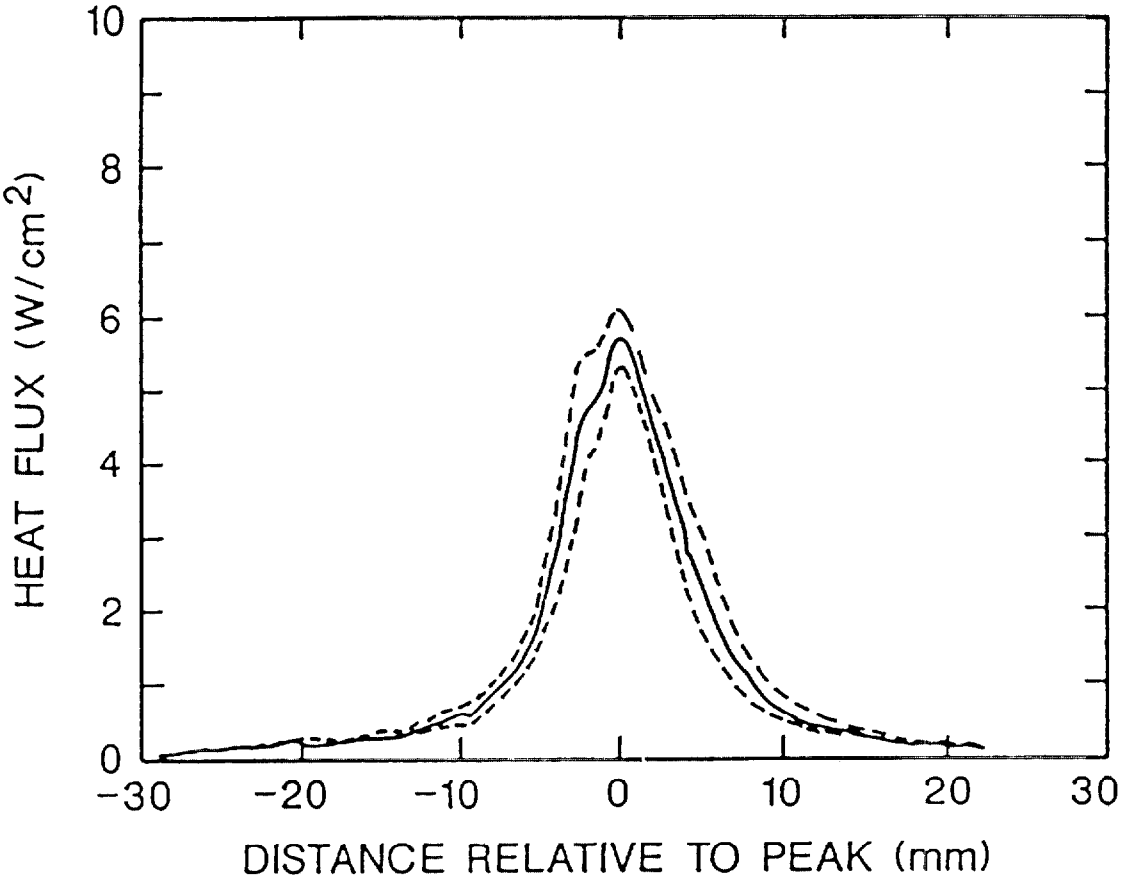

Figure 24. Flux emitted by a cigarette toward the substrate, along the contact line. The dashed curves indicate the probable errors (variance).

It is shown in Appendix G that $\Omega_c(y)$ can be approximated by a Gaussian. It follows that the effective heat transfer coefficient in equation (139) becomes

$$h_s(y) \approx h_o + \Delta h\, e^{-y^2/\sigma_y^2} \tag{140}$$

where

h_o = background $\approx$ 10 W/m^{2}K and $\Delta h = h_c - h_o \approx 61$ W/m^{2}K.

What is to be used for σ_y in equation (140) is discussed in Section IV.D.2, just below.

2. Radiative Flux to the Substrate

The radiation exchange experienced by the substrate at point (x,y) is

$$\phi_{net,r} = \epsilon_r \Omega \sigma (T_c^4 - T_s^4) - (1 - \Omega)\epsilon_s \sigma (T_s^4 - T_a^4), \tag{141}$$

where the x,y arguments have again been left out for clarity, and where

$$\epsilon_r \equiv \frac{\epsilon_c \epsilon_s}{1 - a} \tag{142}$$

is the effective emission coefficient. The radiation flux is treated in the same way as the convective flux; that is, this is split into an effective radiation flux from cigarette to substrate,

$$\phi_{cig,r} = \epsilon_r \Omega \sigma \left(T_c^4 - T_a^4\right), \tag{143}$$

while the substrate radiates away at the rate

$$\phi_{sub,r} = \left[\epsilon_r \Omega + \epsilon_s (1 - \Omega)\right] \sigma \left(T_s^4 - T_a^4\right) \tag{144}$$

In Appendix 5-D of Gann *et al.* (1988), it was shown that the variance of the Gaussian approximation to the convective distribution is about 0.57R. In Appendix H of the current work, it is found that Ω is reasonably well-approximated by a Gaussian also, of variance s. In Appendix G, it is shown that the joint convective-plus-radiative flux distribution is also approximated by a single Gaussian. We therefore use the approximation

$$\Omega_c(y) \approx \Omega(y) \approx \exp\left(-y^2/\sigma_y^2\right) \tag{145}$$

(See equation (H13)). Since we found above that $\sigma_y \approx 3.2$ mm for R = 4mm, we may assume, in general, that the net variance is 0.8R:

$$\sigma_y = 0.8R \tag{146}$$

(Also see equation (H14)).

3. Complete Flux

The cigarette, substrate, and net fluxes are the sums of the convective and radiative contributions. Adding together the terms from the two previous subsections, we can, for the general case, write this in the form

$$\phi_{net} = \phi_{cig} - \phi_{sub} \tag{147}$$

Here the flux at (x,y) from the cigarette is

$$\phi_{cig}(x,y) = h_c \Omega_c (T_c - T_a) + \epsilon_r \Omega \sigma \left(T_c^4 - T_a^4\right) \tag{148}$$

while the loss from the substrate to the ambient surroundings at (x,y) is

$$\phi_{sub}(x,y) = h_s (T_s - T_a) + [\epsilon_r \Omega + \epsilon_s (1 - \Omega)] \sigma \left(T_s^4 - T_a^4\right) \tag{149}$$

where the x-dependencies of T_c and T_s are not shown explicitly in the terms on the right, for the sake of brevity. These model fluxes hold for $0 \leq x \leq L$. ϕ_{cig} is the model flux from the cigarette; ϕ_{sub} is the model flux loss from the substrate.

We note that this separation does not quite succeed in giving a flux ϕ_{cig} which depends only on cigarette/air properties and another which depends only on substrate/air properties. However, ϕ_{cig} does not depend (as it must not) on $T_s(x,y,t)$, and ϕ_{sub} does not depend on $T_c(x,y,t)$. The separation into ϕ_{cig} and ϕ_{sub} is thus good enough that one can run the CIGARET and SUBSTRAT programs independently. One obtains the effects of the cigarette on the substrate from using, as input to SUBSTRAT, the flux ϕ_{cig} which is independent of T_s. On the other hand, by using ϕ_{sub}, one gets the surface losses of the substrate without having to know $T_c(x)$. Of course the substrate "knows" about the cigarette through the latter's flux, ϕ_{cig}, which is entered as an input to CIGARET. The substrate temperature equally influences the cigarette, but by a slightly different mode; that is discussed in the next Section.

4. Effects of the Substrate on the Cigarette

We next consider the inverse problem. The energy losses of the cigarette will be affected by the presence of the surface. Those effects are estimated in this Section. Moreover, since CIGARET is a model of a *freely* smoldering cigarette, the only way we can determine the effect of the substrate on it is to express the cigarette loss rate so that it appears to be simply losing energy to the air. This can be done by using an effective heat transfer coefficient and an effective surface emissivity, such that the presence of the substrate is correctly, if "covertly," taken into account. This is in fact possible to do, as is shown below.

Thermal Effects: Convection. It is shown in Appendix F that the convective loss of the cigarette can be expressed as:

$$\phi_{c,con} \approx h^* (T_c - T_a), \tag{150}$$

where

$$h^* \approx 21.22 - 10.47\left(\frac{T_s - T_a}{T_c - T_a}\right) - 9.02\left(\frac{T_c - T_{c,min}}{T_c - T_a}\right) \qquad \text{W/m}^2\text{K} \qquad \text{(F10)}$$

In deriving this, it was assumed that there is no longitudinal dependence of temperature for either the cigarette or the surface. We now relax this assumption, and recognize that there are longitudinal variations for both T_c and T_s. To be consistent with the approach outlined below equation (H11), we assume equation (F10) to be valid at every x, independent of adjacent regions. That immediately gives the x-dependence of h* to some approximation. This will likely be a weak dependence. Consider the middle term in equation (F10). Along a constant-y line (*e.g.*, $y = y_o$), the smaller $T_c(x)$ is, the smaller will be $T_s(x,y_o)$, since that substrate surface temperature was produced by T_c. That suggests that the ratio $(T_s - T_a)/(T_c - T_a)$ in equation (F10) will not vary strongly with x.

In order to use equation (F10), we must know $T_{c,min}$. This temperature is defined in Appendix F; it is the lowest temperature around the cigarette circumference, and lies at the contact line. This varies with time, as well as with x; hence $h^* = h^*(x,t)$. Also τ, as defined by equation (F8), is a function of t. The resulting $T_{c,min}(t)$ is found in Appendix I. The result is that the temperature difference between the top and the bottom of the cigarette is δT_{max}, given by

$$\delta T_{max} \approx 0.62\, r\, \bar{T} \qquad \text{(I5)}$$

where

$$\bar{T} = \frac{T_a + T_c}{1 + r} \qquad \text{(I1)}$$

and where r is the ratio of the thermal inertias of the materials:

$$r \equiv \sqrt{\frac{(k\rho c)_s}{(k\rho c)_c}} \qquad \text{(I2)}$$

We assume that this minimum temperature is reached in two seconds. It is indicated in Appendices F and I that this is the drop at the flux peak. The drop will be smaller away from the peak, and we may expect something like

$$\delta T_{max}(x,t) \approx \delta T_{max}(x_o,t)\left[\frac{T_c(x,t) - T_a}{T_c(x_o,t) - T_a}\right] \qquad \text{(151)}$$

to hold.

It has been observed that it takes quite a long time for the cigarette to "recuperate" from this drop in (lower) surface temperature, assuming it does not, in fact, extinguish. Again for the sake of simplicity, we will take the recovery period to be 2 minutes.

Suppose the cigarette is dropped onto the substrate at time t_o. Then collecting all these observations, we obtain the estimate

$$\tau(x,t) = \begin{cases} \delta T_{max}(x,t)\,(t-t_o)/2 & t_o \le t \le t_o+2 \\ \delta T_{max}(x,t_o+2)\left(\dfrac{122+t_o-t}{120}\right) & t_o+2 < t < t_o+122 \\ 0 & t > t_o+122 \end{cases} \tag{152}$$

where

$$\tau(x,t) \equiv T_c(\theta=\pi/2,x,t) - T_c(\theta=0,x,t) \tag{F8}$$

With these specifications, equation (F10) can be implemented.

Thermal Effects: Radiation. We next determine how the **radiation losses** of the cigarette are modified by the presence of the substrate. The radiation loss for the free cigarette at any point on its surface is given by equation (143), with ε_r replaced by ε_c. For the cigarette on the substrate, along the contact line, it is given by equation (H16). Notwithstanding the arguments made earlier about the difficulties in calculating the relevant radiation view factors, this was done, making some substantial simplifications.

We assume that the radiation flux emanating from the substrate is

$$\phi_s(y) \cong \phi_a + \Delta\phi \exp(-y^2/p^2) \tag{153}$$

where

$$\Delta\phi \equiv \epsilon_s \sigma T_s^4(y=0) - \phi_a \tag{154}$$

and

$$\phi_a \equiv \sigma T_a^4 \tag{155}$$

The x-dependence will be discussed in a moment. A certain fraction of that flux reaches the cigarette. Upon finding that fraction and integrating over y, it is found that the radiation loss of the cigarette, when in the presence of a substrate, is cut down from the usual expression to

$$\phi_{c,r} \cong \epsilon_c\left[\sigma T_c^4 - \frac{0.7}{\epsilon_s}\Delta\phi\right] - \epsilon_c\phi_a \tag{156}$$

where T_c is assumed to be independent of θ. (See Appendix F). The approximate factor 0.7 is the result of a large number of simplifications and numerical integrations. One of the assumptions is that $p = \sigma_y$.

In the $T_s(0) = T_a$ limit, equation (156) is approximately correct, since $\sigma T_c^4 >> \phi_a$, the deviation from exactitude is negligible. For higher temperatures $T_s(0)$, the flux ϕ_{cr} decreases, as it should, and is still a substantial fraction of σT_c^4 for the upper limit, $T_s(0) = T_c$.

Equation (156) can be written as

$$\phi_{c,r} \approx \epsilon_c^* \sigma T_c^4 - \epsilon_c \phi_a \tag{157}$$

where

$$\epsilon_c^* \equiv \epsilon_c \left[1 - \frac{0.7 \Delta\phi}{\epsilon_s \sigma T_c^4} \right] \tag{158}$$

Finally, this must be generalized to include the dependence on x and t. Just as was done for the convective part, the simplest (although crude) way to do this is to generalize ε_c* by fiat to ε_c*(x,t), where

$$\epsilon_c^*(x,t) \equiv \epsilon_c \left[1 - \frac{0.7\, \Delta\phi(x,t)}{\epsilon_s \sigma T_c^4(x,t)} \right] \tag{159}$$

and

$$\Delta\phi(x,t) \equiv \epsilon_s \sigma T_s^4(x,0,t) - \phi_a \tag{160}$$

CIGARET can then be run without explicitly introducing the substrate temperature by using h*(x,t) and ε_c*(x,t) as the model heat transfer coefficient and cigarette emissivity. These are easily computed at each time step, in CIGARET.

In summary, explicit expressions for the transverse dependence of the cigarette and substrate fluxes have been found, which supplement the longitudinal dependencies. Thus, if the longitudinal dependence on the cigarette surface is known, the flux ϕ(x,y,t) can be found.

Fluid Flow Effects. Quite independently of any possible "competition" from the substrate for oxygen (that is, for oxidative reactions), access to air is somewhat restricted from below because of the presence of the substrate. Thus, the effect of having the substrate there is equivalent to limiting the indrawn-oxygen rate to what it would be in the open, but with $y_a < 0.23$. This effect is incorporated in running CIGARET through the appropriate value for y_a being supplied by the user in the input file.

In order to see what a small reduction in y_a produces, CIGARET was run with the same input parameters as yielded the results shown in Figures 22 and 23, but one: y_a was taken as 0.21. The result, however, was that the simulated cigarette extinguished after a few seconds. [The criterion used to declare the cigarette "extinguished" is that the peak surface temperature falls below 700 K (427 °C)]. Yet, when the cigarette surface temperature history of the $y_a = 0.23$ run was translated into a flux, and the substrate described in Section II.E was exposed to this flux, the substrate ignited in 22 seconds. Clearly, these are contradictory results, and the effective value of y_a to be used for this cigarette lying on this substrate should be between 0.21 and 0.232. It will probably not be very different for other cigarette/substrate combinations.

V. ACKNOWLEDGEMENTS

The authors wish to thank Dr. Thomas J. Ohlemiller for the many insightful discussions on various aspects of the work, Dr. Richard G. Gann for his careful and helpful reading of the manuscript, and the Consumer Products Safety Commission for sponsoring this work.

VI. REFERENCES

Ames, W.F. (1969) *Numerical Methods for Partial Differential Equations*, Barnes and Noble, New York.

Baker, R. (1975) "Temperature Variation Within a Cigarette Combustion Coal During the Smoking Cycle," High Temperature Science 7, p.236.

Baker, R.R., and Crellin, R.A. (1977) "The Diffusion of Carbon Monoxide Out of Cigarettes," Beiträge zur Tabakforschung **9**, No.3 (October), p.131.

Belytschko, T. (1983) "An Overview of Semidiscretization and Time Integration Procedures," Chapter 1 in *Computational Methods for Transient Analysis*, edited by T. Belytschko and T.J.R. Hughes, North-Holland.

Bird, R.B., Stewart, W.E., and Lightfoot, E.N. (1960) *Transport Phenomena*, Wiley, NY.

Brandrup, J., and Immergut, E.H., eds. (1990) *Polymer Handbook*, 3rd ed., Wiley, NY.

Carslaw, H.S., and Jaeger, J.C. (1959) *Conduction of Heat in Solids*, 2nd ed; Oxford University Press.

Childs, G.E., Ericks, L.J., and Powell, R.L. (1973) "Thermal Conductivity of Solids at Room Temperature and Below," NBS Monograph 131, National Bureau of Standards, Gaithersburg, MD.

Clausing, A.M. (1969) "Numerical Methods in Heat Transfer" in *Advanced Heat Transfer*, Ed. B.T. Chao, University of Illinois Press, Urbana, IL.

Cohen, N. (1961) "Boundary-Layer Similar Solutions and Correlation Equations for a Laminar Heat Transfer Distribution in Equilibrium Air and Velocities up to 41,000 Feet per Second," NASA Technical Report R-118.

Conte, S.D. and de Boor, C. (1972) *Elementary Numerical Analysis*, McGraw-Hill, NY.

Croft, D.R., and Lilley, D.G. (1977) *Heat Transfer Calculations Using Finite Difference Equations*, Applied Science Publishers Ltd., London.

Egerton, A., Gugan, K., and Weinberg, F.J. (1963) "The Mechanism of Smoldering in Cigarettes," *Combustion and Flame* 7, p.63.

Gann, R.G., Harris, R.H. Jr, Krasny, J.F., Levine, R.S., Mitler, H.E., and Ohlemiller, T.J. (1988) "The Effect of Cigarette Characteristics on the Ignition of Soft Furnishings," NBS Technical Note 1241, National Bureau of Standards, Gaithersburg, MD.

Gugan, K. (1966) "Natural Smoulder in Cigarettes," *Combustion and Flame* **10**, p.161.

Hilsenrath, J., Beckett, C.W., Benedict, W.S., Fano, L., Hoge, H.J., Masi, J.F., Nuttall, R.L., Touloukian, Y.S., and Woolley, H.W. (1955) *Tables of Thermal Properties of Gases*, NBS Circular 564, National Bureau of Standards, Gaithersburg, MD.

Holman, J.P. (1981) *Heat Transfer* (5th ed.), McGraw-Hill, New York.

Kakaç, S., Shah, R., and Aung, W., eds. (1987) *Handbook of Single-Phase Convective Heat Transfer*, Wiley/Interscience, New York.

Kashiwagi, T., and Nambu, H. (1992) "Global Kinetic Constants for Thermal Oxidative Degradation of a Cellulosic Paper," *Combustion and Flame* **88** p.345.

Kunii, D. (1961) *Kagaku Kogaku* [Chem. Eng. (Japan)] **25** p.891.

Larkin, B.K. (1964) "Some Stable Explicit Difference Approximations to the Diffusion Equation," *Mathematics of Computation* **18** p.196.

Lawson, J.R. (1993) National Institute of Standards and Technology, unpublished data.

Lendvay, A.T., and Laszlo, T.S. (1974) "Cigarette Peak Coal Temperature Measurements," *Beiträge zur Tabakforschung* **7**, p.63.

Miller, A.L. (1991) "Where There's Smoking There's Fire," *NFPA Journal*, p.86.

Mitler, H.E., and Davis, W.D. (1987) "Computer Model of a Smoldering Cigarette," Annual Conference on Fire Research, National Bureau of Standards, Gaithersburg, MD, Nov. 1987.

Mitler, H.E., and Walton, G. (1992) "A Computer Model of the Smoldering Ignition of Furniture," NISTIR 4973, National Institute of Standards and Technology, Gaithersburg, MD.

Peyret, R., and Taylor, T.D. (1983), *Computational Methods for Fluid Flow*, Springer-Verlag, New York.

Moussa, N.A., Toong, T.Y., and Garris, C.A. (1977) "Mechanism of Smoldering of Cellulosic Materials," *Sixteenth Symposium (International) on Combustion*, The Combustion Institute, Pittsburgh, PA, p.1447.

Muramatsu, M., Umemura, S., and Okada, T. (1979) "A Mathematical Model of Evaporation-Pyrolysis Processes Inside a Naturally Smoldering Cigarette, *Combustion and Flame* **36**, p.245.

Muramatsu, M. (1981) "Study of Transport Phenomena Which Occur During Unforced Smoldering of Cigarettes," Res. Report No. 123 of the Japan Tobacco and Salt Monopoly (in Japanese).

Ohlemiller, T.J. (1985) "Modeling of Smoldering Combustion Propagation," *Progress in Energy and Combustion Science* **11**, p.277.

Ohlemiller, T.J. (1991) "Smoldering Combustion Propagation on Solid Wood," in *Fire Safety Science, Proceedings of the Third International Symposium* (Eds., G. Cox and B. Langford); Elsevier Publishing Co., London, p.565.

Ohlemiller, T.J. (1991) unpublished results.

Ohlemiller, T.J., Villa, K., Braun, E., Eberhardt, K.R., Harris Jr., R.H., Lawson, J.R., and Gann, R.G. (1993) "Test Methods for Quantifying the Propensity of Cigarettes to Ignite Soft Furnishings," Special Publication 851, National Institute of Standards and Technology, Gaithersburg, MD.

Özisik, M.N. (1980) *Heat Conduction*, Wiley-Interscience, New York, 1980.

Parker, W.J. (1985) "Prediction of the Heat Release Rate of Wood," *Fire Safety Science - Proceedings of the First International Symposium* (Eds., C.E. Grant and P.J. Pagni); Hemisphere Publishing Corp, p.207.

Parker, W.J. (1988) "Prediction of the Heat Release Rate of Wood," Ph.D. Thesis, George Washington University, Washington, DC.

Quintiere, J.G., Harkleroad, M.F., and Walton, W.D. (1983) "Measurement of Material Flame Spread Properties," *Combustion Science and Technology* **32** p.67.

Quintiere, J.G., and Harkleroad, M.F. (1985) "New Concepts for Measuring Flame Spread Properties," *Fire Safety Science and Engineering*, ASTM STP 882, T.Z. Harmathy, ed., ASTM, Philadelphia, PA, p.239.

Quintiere, J.G. (1988) "The Application of Flame Spread Theory to Predict Material Performance," *J. of Res. of Nat'l Bur. of Standards* **93**(1), p.61.

Raznjevic, K. (1976) *Handbook of Thermodynamic Tables and Charts*, Hemisphere Pub. Co., New York.

Samfield, M. (1986) private communication.

Sandusky, H.W. (1976) "A Computer-Simulated Cigarette Model for Use in the Development of Less Hazardous Cigarettes," Ph.D. Thesis, Princeton University, Princeton, NJ.

Schneider, P.J. (1973) "Conduction," *Handbook of Heat Transfer*, 1st Ed., Eds. W.M. Rohsenow, & J.P. Hartnett, McGraw-Hill, New York.

Siegel, R., and Howell, J.R. (1981) *Thermal Radiation Heat Transfer*, 2nd ed., McGraw-Hill, NY.

Sparrow, E.M., and Cess, R.D. (1978) *Radiation Heat Transfer*, McGraw-Hill, NY.

Summerfield, M., Ohlemiller, T.J., and Sandusky, H.W. (1978) "A Thermophysical Mathematical Model of Steady-Draw Smoking and Predictions of Overall Cigarette Behavior," *Combustion and Flame* **33**, p.263.

Szekely, J., Evans, J., and Sohn, H. (1976) *Gas-Solid Reactions*, Academic Press, New York.

Thomas, P.H. (1957) "Some Conduction Problems in the Heating of Small Areas on Large Solids," *Quart Journ. Mech. and Applied Math.*, Vol. X, Pt. 4.

Torrance, K.E. (1985) "Numerical Methods in Heat Transfer," *Handbook of Heat Transfer Fundamentals*, 2nd Ed., Eds. W.M. Rohsenow, J.P. Hartnett, and E.N. Gacic, McGraw-Hill, New York.

Touloukian, Y.S., Powell, R.W., Ho, C.Y., and Klemens, P.G. (1970) *Thermophysical Properties of Matter*, Vol.2, Thermal Conductivity, Nonmetallic Solids, IFI/Plenum.

Treybal, R.E. (1955) *Mass-Transfer Operations*, McGraw-Hill, New York.

Weast, R.C., Ed. (1976) *Handbook of Chemistry and Physics*, CRC Press, Cleveland, OH.

Wichmann, I.S. (1991) "On the Use of Operator-Splitting Methods for the Equations of Combustion," *Combustion and Flame* **83**, p.240.

APPENDIX A

CONDUCTION ALGORITHM TESTS

A computer program called TEMPSUB was developed as part of the earlier investigation into the ignition of furnishings by smoldering cigarettes (Gann *et al.*, 1988). This program modeled heat transfer in furniture, or in a "substrate," using a simple finite difference approximation (FDA) for a homogeneous substrate with uniform and constant properties. The research indicated that this program would have to be expanded to include a two-layer model (fabric + padding), pyrolysis of each layer, an asymmetric flux input, and a variable grid.

These features have been implemented in SUBSTRAT by using a slightly different approach to the FDA than was used in TEMPSUB. The original approach was to convert the differential equation for heat transfer into an FDA by a Taylor's series approximation. The new approach is based on the conservation of energy within a control volume. It is based on physical reasoning and is usually easy to apply. It is most useful for variable grids, convective boundary conditions, odd-shaped regions, etc. It is more difficult to obtain accuracy estimates for the control volume approach than for the Taylor's series approach. For simple cases involving uniform grids and homogeneous materials the two approaches lead to identical FDA's. See Torrance (1985) or Croft and Lilley (1977) for further details.

Since there is a considerable increase in the desired capabilities of the upgraded program, it was decided to develop a program which would allow extensive testing of the FDA. This program is called CTEST3 (Conduction TEST - 3 dimensional) which has the ability to model simple boundary conditions (constant temperature, heat flux, or convection coefficient) on any of the six faces of the region.

The FDA used in CTEST3, the explicit Euler method, has been checked against several heat transfer problems which have analytic solutions. The first few tests involve various combinations of constant temperature, heat flux, and convection coefficient boundary conditions with analytic solutions from the classic text by Carslaw and Jaeger (1959).

Several of these analytic solutions involve the error function which is defined by

$$\mathrm{erf}(x) = \frac{2}{\sqrt{\pi}} \int_0^x e^{-\xi^2} d\xi \tag{A1}$$

so that $\mathrm{erf}(0) = 0$,

$\mathrm{erf}(\infty) = 1$,

and $\mathrm{erf}(-x) = -\mathrm{erf}(x)$.

The complementary error function is also used. It is defined as

$$\mathrm{erfc}(x) = 1 - \mathrm{erf}(x) = \frac{2}{\sqrt{\pi}} \int_x^\infty e^{-\xi^2} d\xi \tag{A2}$$

so that $\mathrm{erfc}(0) = 1$,

and $\mathrm{erfc}(\infty) = 0$.

Repeated integrals of the error function are also useful in conduction problems. These are defined by the recursive relationships

$$i^n\mathrm{erfc}(x) = \int_x^\infty i^{n-1}\mathrm{erfc}(x)\,dx \qquad n=1,2,... \tag{A3}$$

or

$$i^0\mathrm{erfc}(x) \equiv \mathrm{erfc}(x) \tag{A3a}$$

$$\mathrm{ierfc}(x) \equiv i^1\mathrm{erfc}(x) = \frac{e^{-x^2}}{\sqrt{\pi}} - x\,\mathrm{erfc}(x) \tag{A3b}$$

$$2ni^n\mathrm{erfc}(x) = i^{n-2}\mathrm{erfc}(x) - 2x\,i^{n-1}\mathrm{erfc}(x) \qquad n=2,3,... \tag{A3c}$$

See Appendix II of Carslaw and Jaeger (1959) for further details on error functions. Computer subroutines were written implementing these functions for the computation of the analytic solutions of the heat transfer tests.

Test 1: One-Dimensional Steady-State Conduction

CTEST3 has been tested for steady-state conduction with constant thermal properties and uniform grid spacing. This test sets opposite faces on a cubic region to different temperatures and makes the remaining faces adiabatic. After a sufficient number of time steps the temperature within the region should vary linearly from the hot to the cold face:

$$T(x) = T(0) + \frac{x}{L}[T(L) - T(0)] \tag{A4}$$

This has been confirmed in all three directions.

Test 2: One-Dimensional Transient Conduction, Constant Heat Flux Boundary Condition

This test was used in the development of the original substrate model. The analytic case for a constant flux involves a homogeneous solid occupying the semi-infinite region $x > 0$. The solid is initially at zero temperature throughout. At time $t = 0$, a constant heat flux, q, is applied to the $x = 0$ surface. The temperature within the region is given by Carslaw and Jaeger (1959), p. 75, equation (6):

$$T(x,t) = \frac{q\sqrt{4\alpha t}}{\kappa}\,\mathrm{ierfc}\left(\frac{x}{\sqrt{4\alpha t}}\right) \tag{A5}$$

Preliminary testing (again using a uniform grid and constant thermal properties) indicated that as Δt and Δx decreased, there was a uniform approach to the analytic solution. As for the accuracy to be expected, for $\Delta x = 1$ mm and $\Delta t = 0.5$ s, the error (after the first three time steps) was < 1 percent. We note that the results of test did not agree with results from the original TEMPSUB model. Further investigation indicated an error in the TEMPSUB boundary conditions subroutine. Correcting this error brought results from the two programs into complete agreement.

Tests show that reducing the grid size along with corresponding reduction of the time step cause the FDA solution to approach the analytic solution. Therefore, the FDA is consistent. Reducing the time step without changing the grid size does not improve the accuracy of the solution. In fact, it is best to operate as close to the stability limit as possible for both accuracy and execution time. Use of the variable grid gives results consistent with the uniform grid at the surface. The error in the calculated surface temperature goes down as time increases.

Test 3: One-Dimensional Transient Conduction, Constant Convection Coefficient Boundary Condition

This test represents a slab of a homogeneous solid of thickness 2L in the x direction and infinite extent in the y and z directions which is initially at unit temperature throughout. At time t = 0 the temperature of the fluid on both sides of the slab is changed to zero and heat is convected from the slab through a constant convection coefficient. Because of symmetry this problem is equivalent to a slab of thickness L with one adiabatic surface at x = 0 and a convective surface at x = L. The temperature within the region is given by Carslaw and Jaeger (1959), p. 122, equation (12):

$$T(x,t) = \sum_{n=1}^{\infty} \frac{2B\cos(\delta_n x/L)}{[B^2+B+\delta_n^2]\cos\delta_n} e^{-\delta_n^2 F} \qquad \text{(A6)}$$

where $B = hL/\kappa$ (Biot number),
$F = \alpha t/L^2$ (Fourier number), and
δ_n are the solutions of the transcendental equation $\delta_n \tan\delta_n = B$.

In order to check the calculation of this complicated analytic solution, the solution to a related problem was also computed. This is the temperature in a semi-infinite slab with the convective boundary condition (Carslaw and Jaeger (1959), p. 72, equation (5)):

$$T(x,t) = \text{erfc}\left(\frac{x}{\sqrt{4\alpha t}}\right) - \exp\left(\frac{h}{\kappa}(x+\alpha h t/\kappa)\right)\text{erfc}\left(\frac{x}{\sqrt{4\alpha t}} + \frac{h}{\kappa}\sqrt{\alpha t}\right) \qquad \text{(A7)}$$

where x is now the distance from the convective surface into the region. There is good agreement between the FDA and analytic solutions. Again, the error in the calculated temperature goes down as time increases.

Test 4: Three-Dimensional Transient Conduction, Constant Surface Temperature Boundary Condition

This test represents a block of a homogeneous solid in the region defined by -a < x < a, -b < y < b, and -c < z < c which is initially at unit temperature throughout. At time t = 0 the temperatures of the surfaces of the block are reduced to zero, and the block begins to cool. The temperature within the region is given by Carslaw and Jaeger (1959), p.184, equation (5):

$$T(x,y,z,t) = \frac{64}{\pi^3} \sum_{l=0}^{\infty} \sum_{m=0}^{\infty} \sum_{n=0}^{\infty} \frac{(-1)^{l+m+n}}{(2l+1)(2m+1)(2n+1)} \times$$
$$\cos\left[\frac{(2l+1)\pi x}{2a}\right] \cos\left[\frac{(2m+1)\pi y}{2b}\right] \cos\left[\frac{(2n+1)\pi z}{2c}\right] \times \tag{A8}$$
$$\exp\left\{-\frac{\kappa\pi^2 t}{4}\left[\frac{(2l+1)^2}{a^2} + \frac{(2m+1)^2}{b^2} + \frac{(2n+1)^2}{c^2}\right]\right\}$$

This expression requires the summation of many terms at small values of time, but only a few terms at large values of time. The implementation of this complicated equation had to be checked against simpler analytic cases. The first case represents a homogeneous solid occupying the semi-infinite region, $x > 0$. The solid is initially at unit temperature throughout. At time $t = 0$ the temperature at $x = 0$ is instantly reduced to zero. The temperature within the region is given by Carslaw and Jaeger (1959), p.59, equation (3):

$$T(x,t) = \text{erf}\left(\frac{x}{\sqrt{4\alpha t}}\right) \tag{A9}$$

The second case involves a solid which occupies the region $x > 0$, $y > 0$, $z > 0$. It is initially at unit temperature and at time $t = 0$ the temperature at the $x = 0$, $y = 0$, and $z = 0$ surfaces is instantly reduced to zero. The temperature within the region is given by Carslaw and Jaeger (1959), p. 184, equation (1):

$$T(x,y,z,t) = \text{erf}\left(\frac{x}{\sqrt{4\alpha t}}\right) \text{erf}\left(\frac{y}{\sqrt{4\alpha t}}\right) \text{erf}\left(\frac{z}{\sqrt{4\alpha t}}\right) \tag{A10}$$

The temperatures near the corners of the block should be very similar to this.

There was good agreement (error $< 1\%$) for a test with $a = 30$ mm, $b = 20$ mm, $c = 10$ mm, and using a 1 mm uniform grid. The original variable grid model was found to be insufficiently accurate at points where the grid size changed. It was therefore replaced by the current uniformly increasing grid at a cost of some increase in code complexity; although the results are not quite as accurate as for the uniformly spaced grid, the difference is very minor.

Test 5: One-Dimensional Transient Conduction, Two Different Materials

This test consists of one material in the region 1 ($0 < z < L$) initially at unit temperature and another material in region 2 ($z > L$) initially at zero temperature. The boundary at $z = 0$ is adiabatic. At time $t = 0$ heat begins to be conducted between the two regions. The temperatures in the two regions are given by Özisik (1980), p. 328, equation (8-109):

$$T_1(x,t) = 1 - \frac{1-\delta}{2} \sum_{n=0}^{\infty} \delta^n \left\{ \text{erfc}\left[\frac{(2n+1)L-x}{\sqrt{4\alpha_1 t}}\right] + \text{erfc}\left[\frac{(2n+1)L+x}{\sqrt{4\alpha_1 t}}\right] \right\}$$

$$T_2(x,t) = \frac{1+\delta}{2} \sum_{n=0}^{\infty} \left\{ \text{erfc}\left[\frac{2nL+\mu(x-L)}{\sqrt{4\alpha_1 t}}\right] - \text{erfc}\left[\frac{(2n+2)L+\mu(x-l)}{\sqrt{4\alpha_1 t}}\right] \right\} \qquad \text{(A11)}$$

where

$$\mu = \sqrt{\frac{\alpha_1}{\alpha_2}}, \quad \beta = \frac{\kappa_1}{\kappa_2 \mu}, \quad \delta = \frac{\beta - 1}{\beta + 1} .$$

There was good agreement between the FDA and analytic solutions. It even worked well when the first layer was only one-half of a grid thick. This may be useful for thin fabric coverings.

Test 6: Three-Dimensional Transient Conduction, Constant Heat Flux Impinging on a Circular Area (Disk) on a Semi-Infinite Region.

The impinging flux is q, there is convective cooling from the surface, $h(T_s - T_a)$, and the disk radius is R. The temperature at the center of the heated area is given by Thomas (1957), equation (5):

$$T(t) = \frac{qR}{\kappa} \left\{ \sqrt{\frac{4\alpha t}{\pi R^2}} \left[1 - \exp\left(-\frac{R^2}{4\alpha t} \right) \right] + \text{erfc}\left(\frac{R}{\sqrt{4\alpha t}} \right) \right\} -$$

$$- \frac{2q}{h} \int_{\omega=0}^{\frac{h}{\kappa}\sqrt{\alpha t}} \left[1 - \exp\left(\frac{-h^2 R^2}{4k^2 \omega^2} \right) \right] \omega e^{\omega^2} \text{erfc}(\omega)\, d\omega \qquad \text{(A12)}$$

The first part of the above expression is the center point temperature if there is no convective cooling. Tests indicate that the accuracy of the FDA for this test is primarily dependent on how accurately the circular flux pattern is represented on the rectangular surface grid. A small grid and assigning cell heat gain according to the portion of the cell that is within the circle improve accuracy.

Note that tests 1 through 6 involve a step change, which should be the worst condition to simulate with the FDA. In all cases the maximum errors occurred at the first time step, and the error declined as time increased.

Test 7: Three-Dimensional Transient Conduction, Uniformly Moving Point-Source Heat Flux

This test consists of a point source of power Q moving in an infinite body at a constant velocity v in the x direction (Schneider (1973), pp.3-86, equation (78)):

$$\frac{\kappa r}{Q}(T - T_o) = \frac{1}{4\pi} \exp\left[-\frac{v}{2\alpha} (\xi + r) \right] \qquad \text{(A13)}$$

where $\xi = x - vt$ and $r = (\xi^2 + y^2 + z^2)^{1/2}$. Adjusting for a semi-infinite body with the point source moving along an adiabatic surface is done by replacing 4π by 2π in equation (A13). Generally good agreement was achieved for this test. Accuracy was limited by grid size near the point source and the fact the this is a quasi-steady case in that movement of the point source does not have a beginning point.

Larkin's Method

The FDA algorithm in CTEST3 was transferred directly into the new substrate model TMPSUB2. The addition of pyrolysis forced the use of a very small grid in the region of peak temperature for a satisfactory solution. This, combined with the stability requirement of the explicit Euler method, forced a very small time step and therefore a very long execution time. A different FDA algorithm had to be found to achieve a program fast enough to be useful. Larkin's method was chosen because of its simplicity in that it uses the same spatial FDA as the original method while the new temporal FDA does not require the solution of simultaneous equations.

CTEST3 was not rewritten to run all of the test cases, but several tests were made with TMPSUB2 (some using a modified surface boundary condition) which indicate the accuracy of the method for different grid size and time step options. The results of these tests are shown in Tables A-1, A-2, and A-3.

Table A-1 gives the results of several tests which can be compared to equation (A5) to determine the effect of grid spacing. These tests use a region 40 mm thick to simulate a semi-infinite body which is shown to be appropriate by having negligible heat flux at the constant temperature surface at Z=40 mm. Comparisons are made based on the temperature of the surface (Z=0 mm).

> Test 2a: Using a constant 1 mm grid spacing the temperature after 100 seconds is 0.33% less than the exact value.
>
> Test 2b: Using a constant 0.5 mm spacing gives a surface temperature 0.18% below the theoretical value.
>
> Tests 2c through 2f use variable grid spacing to reduce the number of cells and execution time at the cost of some loss of accuracy.

Table A-2 gives the results of several tests where the parameters that control the time step while maintaining a constant grid spacing, are varied. These parameters are the maximum time step, dtmax, and the maximum temperature change, dTmax. (Whenever $T_{n+1} - T_n$ exceeds dTmax, the time step is halved.) Obviously the greatest accuracy should be achieved with small values for these two parameters, but execution time is reduced by using large values. There is no obvious optimum; the user must choose values appropriate for results he wishes to achieve.

Table A-3 shows tests of different grid spacings for full three-dimensional heat conduction from a stationary spot heat flux. These tests use representative thermal properties for the fabric and padding. Various combinations of cell spacings are used to select the best grid.

Table A-1. Grid Spacing Tests

Thermal diffusivity: 2e-07 m^2/s Thermal conductivity: 0.1 W/mK
Surface heat flux: 1e+04 W/m^2 Distance from surface: 0 m

time	Texact	Test2a	Test2b	Test2c	Test2d	Test2e	Test2f
0.000	0.0000	0.000	0.000	0.000	0.000	0.000	0.000
0.125	17.8412	5.000	9.319	9.319	9.319	9.319	9.319
0.250	25.2313	9.643	16.889	16.889	16.889	16.889	16.889
0.375	30.9019	13.970	23.331	23.331	23.331	23.331	23.331
0.500	35.6825	18.298	28.916	28.916	28.916	28.916	28.916
0.625	39.8942	22.252	33.840	33.840	33.840	33.840	33.840
0.750	43.7019	26.206	38.035	38.035	38.035	38.034	38.034
0.875	47.2035	29.838	42.229	42.229	42.229	42.229	42.229
1.000	50.4627	33.469	45.757	45.757	45.757	45.757	45.757
1.250	56.4190	40.170	52.366	52.366	52.366	52.366	52.366
1.500	61.8039	46.383	58.208	58.208	58.208	58.208	58.208
1.750	66.7558	52.167	63.496	63.496	63.496	63.496	63.496
2.000	71.3650	57.577	68.361	68.361	68.361	68.361	68.361
2.250	75.6940	62.656	73.042	73.042	73.041	73.041	73.041
2.500	79.7885	67.445	77.173	77.173	77.173	77.173	77.171
2.750	83.6828	71.859	81.305	81.305	81.304	81.304	81.302
3.000	87.4039	76.273	85.049	85.049	85.048	85.047	85.044
3.500	94.4070	84.279	92.243	92.243	92.242	92.240	92.233
4.000	100.9253	91.625	98.911	98.909	98.908	98.904	98.893
4.500	107.0474	98.433	105.154	105.152	105.149	105.143	105.125
5.000	112.8379	104.796	111.046	111.042	111.038	111.030	111.002
6.000	123.6077	116.456	121.976	121.970	121.962	121.946	121.894
7.000	133.5116	127.018	132.004	131.993	131.981	132.050	131.966
8.000	142.7299	136.650	141.315	141.300	141.283	141.309	141.188
9.000	151.3880	145.711	150.034	150.014	149.991	149.993	149.830
10.000	159.5769	154.229	158.272	158.248	158.219	158.201	157.994
15.000	195.4410	191.150	194.315	194.266	194.208	194.109	193.654
20.000	225.6758	221.986	224.670	224.600	224.514	224.343	223.631
25.000	252.3132	249.025	251.396	251.307	251.195	250.960	249.998
30.000	276.3953	273.438	275.472	275.367	275.235	274.852	273.660
35.000	298.5410	295.758	297.599	297.487	297.339	296.828	295.425
40.000	319.1538	316.566	318.155	318.040	317.879	317.378	315.771
45.000	338.5137	336.042	337.525	337.408	337.234	336.650	334.844
50.000	356.8248	354.491	355.815	355.694	355.509	354.928	352.929
60.000	390.8820	388.738	389.887	389.758	389.550	388.899	386.532
70.000	422.2008	420.206	421.230	421.093	420.862	420.147	417.431
80.000	451.3517	449.479	450.409	450.262	450.010	449.235	446.188
90.000	478.7307	476.960	477.816	477.660	477.388	476.556	473.195
100.000	504.6265	502.943	503.740	503.574	503.282	502.397	498.738
cells:		41	81	35	25	18	12
steps:		153	154	154	154	153	153

TEST2A: dz=1.0mm, nz=41, nc=41, r=1.000, dtmax=1.0, dTmax = 5.0
TEST2B: dz=0.5mm, nz=81, nc=81, r=1.000, dtmax=1.0, dTmax = 5.0
TEST2C: dz=0.5mm, nz=35, nc=4, r=1.055, dtmax=1.0, dTmax = 5.0
TEST2D: dz=0.5mm, nz=25, nc=4, r=1.115, dtmax=1.0, dTmax = 5.0
TEST2E: dz=0.5mm, nz=18, nc=4, r=1.234, dtmax=1.0, dTmax = 5.0
TEST2F: dz=0.5mm, nz=12, nc=4, r=1.628, dtmax=1.0, dTmax = 5.0

Table A-2. Time Step Control Tests

Thermal diffusivity: 2e-07 m^2/s Thermal conductivity: 0.1 W/mK
Surface heat flux: 1e+04 W/m^2 Distance from surface: 0 m

time	Texact	Test2b	Test2g	Test2h	Test2J
0.000	0.0000	0.000	0.000	0.000	0.000
0.125	17.8412	9.319	9.093		
0.250	25.2313	16.889	16.685	20.000	20.000
0.375	30.9019	23.331	23.148		
0.500	35.6825	28.916	28.750	31.538	31.538
0.625	39.8942	33.840	33.688		
0.750	43.7019	38.035	38.107	39.690	39.690
0.875	47.2035	42.229	42.125		
1.000	50.4627	45.757	45.801	47.841	47.841
1.250	56.4190	52.366	52.390		
1.500	61.8039	58.208	58.223	58.553	58.553
1.750	66.7558	63.496	63.506		
2.000	71.3650	68.361	68.368	69.264	69.264
2.250	75.6940	73.042	72.899		
2.500	79.7885	77.173	77.158	77.403	77.403
2.750	83.6828	81.305	81.191		
3.000	87.4039	85.049	85.028	85.542	85.542
3.500	94.4070	92.243	92.222		
4.000	100.9253	98.911	98.891	97.831	97.831
4.500	107.0474	105.154	105.136		
5.000	112.8379	111.046	111.029	110.120	110.120
6.000	123.6077	121.976	121.963	120.390	120.390
7.000	133.5116	132.004	131.993	130.660	130.660
8.000	142.7299	141.315	141.312	139.622	139.622
9.000	151.3880	150.034	150.053	148.583	
10.000	159.5769	158.272	158.312	156.621	157.545
15.000	195.4410	194.315	194.402	192.945	
20.000	225.6758	224.670	224.773	223.337	221.615
25.000	252.3132	251.396	251.504	250.229	
30.000	276.3953	275.472	275.656	274.420	
35.000	298.5410	297.599	297.855	296.726	
40.000	319.1538	318.155	318.512	317.415	313.420
45.000	338.5137	337.525	337.900	336.887	
50.000	356.8248	355.815	356.236	355.255	
60.000	390.8820	389.887	390.336	389.440	382.464
70.000	422.2008	421.230	421.690	420.860	
80.000	451.3517	450.409	450.870	450.093	442.530
90.000	478.7307	477.816	478.274	477.541	
100.000	504.6265	503.740	504.191	503.495	495.723
cells:		81	81	81	81
steps:		154	724	106	42

TEST2B: dz=0.5mm, nz=81, nc=81, r=1.000, dtmax=1.0, dTmax = 5.0
TEST2G: dz=0.5mm, nz=81, nc=81, r=1.000, dtmax=1.0, dTmax = 1.0
TEST2H: dz=0.5mm, nz=81, nc=81, r=1.000, dtmax=1.0, dTmax = 20.0
TEST2I: dz=0.5mm, nz=81, nc=81, r=1.000, dtmax=4.0, dTmax = 5.0
(Same results as test2b because dT > 2.5 at dt = 1.0)
TEST2J: dz=0.5mm, nz=81, nc=81, r=1.000, dtmax=4.0, dTmax = 20.0

Table A-3. 3-D Transient Conduction Tests

time	test3a	test3b	test3c	test3d	test3e
0.00	0.000	0.000	0.000	0.000	0.000
1.00	65.749	70.904	71.046	71.254	71.301
2.00	88.450	91.190	91.381	91.660	91.723
3.00	104.807	106.828	107.053	107.382	107.455
4.00	118.536	120.437	120.692	121.060	121.140
5.00	130.745	132.693	132.974	133.375	133.460
10.00	178.269	180.414	180.785	181.287	181.377
15.00	211.444	213.792	214.214	214.765	214.850
20.00	236.140	238.668	239.121	239.692	239.766
30.00	269.762	272.068	272.539	273.119	273.173
40.00	291.304	293.512	293.988	294.550	294.585
50.00	305.937	308.182	308.659	309.201	309.219
60.00	316.279	318.588	319.064	319.589	319.594
70.00	323.830	326.195	326.670	327.180	327.176
80.00	329.498	331.903	332.376	332.876	332.865
90.00	333.853	336.285	336.757	337.248	337.233
100.00	337.271	339.718	340.188	340.673	340.654
cells:	18081	18081	18081	19176	18375
steps:	152	154	154	154	154
time:	303.08	316.37	316.10	338.90	346.32

TEST3A: dx=0.5mm, nx=41, ny=21, nz = 21, nc = 4, yw=zw = 40,
rx=ry=1.167, rz=1.187, dtmax=1.0, dTmax = 5.0

TEST3B: dx=0.25mm, nx=41, ny=21, nz = 21, nc = 4, yw=zw = 40,
rx=ry=1.240, rz=1.240, dtmax=1.0, dTmax = 5.0

TEST3C: dx=0.25mm, nx=41, ny=21, nz = 21, nc = 4, yw=zw = 30,
rx=ry=1.210, rz=1.210, dtmax=1.0, dTmax = 5.0

TEST3D: dx=0.25mm, nx=47, ny=24, nz = 17, nc = 4, yw=zw = 30,
rx=ry=1.161, rz=1.326, dtmax=1.0, dTmax = 5.0

TEST3E: dx=0.25mm, nx=49, ny=25, nz = 15, nc = 4, yw=zw = 30,
rx=ry=1.149, rz=1.431, dtmax=1.0, dTmax = 5.0

APPENDIX B

TMPSUB2 AND SUBSTRAT USER'S GUIDE

General Information

SUBSTRAT and two helper programs are available on a diskette for IBM PC compatible computers. The distribution diskette includes both executable and source code for SUBSTRAT, executable code for the other two programs, and sample input files. The general relationship of programs and files is illustrated in Figure B-1. The TSDATA program is used to prepare data files for SUBSTRAT which in turn creates two types of output files. The plot file is used by the TSPLOT program to display contour plots of substrate temperatures. The list file includes a step-by-step record of the highest temperature in the substrate.

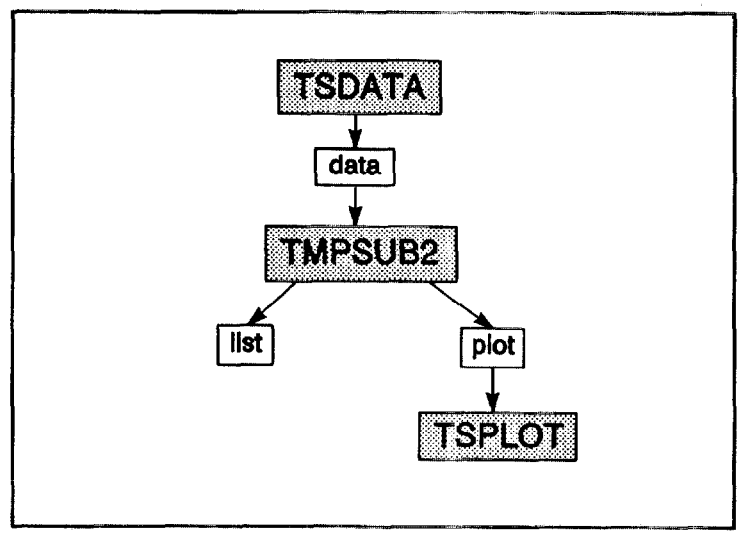

Figure B-1. TMPSUB2 Programs and Files

TSDATA and TSPLOT must be run using MS-DOS on IBM PC compatible computers with VGA graphics. SUBSTRAT requires a 386 class PC with math coprocessor or 486 class PC (no graphics needed) in order to achieve satisfactory performance. Typical execution times are 20 to 30 minutes on a 33Mhz 486 computer.

The SUBSTRAT source code (file SUBSTRAT.CCC) can be compiled using any ANSI C compiler. All SUBSTRAT input and output files are ASCII files. Therefore, SUBSTRAT can be recompiled and run on a different computer, while still using TSDATA and TSPLOT on a PC and transferring files between the computers. A different computer may allow SUBSTRAT to execute faster and/or handle more cells for more accurate simulation.

Be sure to inspect the README file on the distribution diskette. One way to read this file is to place the diskette in drive A: (or drive B:) and type

MORE < A:README (or MORE < B:README)

A permanent copy may be made with

PRINT < A:README

The README file contains a list of all files on the diskette, instructions for installing the necessary files on your hard disk, and information on any changes or additions to the program.

There should be at least 1,000,000 bytes available on your hard disk. It is best to create a single subdirectory for the executable programs and related data files. This will allow you to easily delete all

the files related to this program when you are finished with it. In general, when running on a PC, *keep all files in the current working directory.*

The following sections give details of the operation of SUBSTRAT, TSDATA, and TSPLOT.

SUBSTRAT

All input for SUBSTRAT must be placed in a data file. This file is read as the "standard input stream," so SUBSTRAT executes on MS-DOS and UNIX computers by redirecting the input file. For example, if there already exists an input data file, *e.g.*, TEST1.DAT, one can begin a run by typing

SUBSTRAT < TEST1.DAT

Note: SUBSTRAT can be aborted at any time by simultaneously pressing CTRL and C.

Sample run

If you have not already done so, install the SUBSTRAT program following the instructions in the README file. For example, from the directory on the hard disk where you want SUBSTRAT installed and with the diskette in drive A:, type

A:INSTALL A:

At the present time you only need to install in response to the first question you will be asked.

During installation a program will determine the "initial unallocated memory." If the required memory is greater than this amount, follow the instructions under memory requirements below before proceeding.

Should you wish to examine the directory at this point, a DIR command should indicate the presence of at least the following files: SUBSTRAT.EXE, TEST1.DAT, TEST2.DAT, and MEMREM.EXE. As mentioned above, begin the sample run by typing

SUBSTRAT <TEST1.DAT

SUBSTRAT will then (1) indicate that it is reading the data file, (2) echo the simulation title to the screen, (3) initialize the data in all cells, and (4) report the amount of unallocated memory. If there is "insufficient memory," an error message will be displayed and the run aborted. See the memory requirements section below for corrective action.

Every time SUBSTRAT completes a time step during the simulation, it displays the time (in seconds) and peak temperature (degrees C) on the screen. This allows you to monitor the progress of the simulation.

This same information is included on the list file, TEST1.LST, thus providing a permanent record of the primary value computed during the simulation. The list file also includes an echo of the input file which helps to identify the simulation and is especially useful in identifying any errors in the input which are also written to the list file.

The plot file, TEST1.PLT, contains all temperatures in the Y=0 and Z=0 planes at the times specified plus data to identify the simulation and the coordinate values.

Memory Requirements

SUBSTRAT has been written to handle an arbitrary number of cells up to some limit imposed by available memory or by the operating system. MS-DOS limits available random access memory (**RAM, not disk memory**) to 640,000 bytes which is shared by the program, the data in the program, a portion of the operating system, and perhaps various TSR (Terminate & Stay Resident) programs. TMPSUB allocates memory for its data arrays from available RAM. When there is insufficient memory to run a particular simulation, you must either make more memory available or reduce the memory required by the simulation. One way to make more memory available is to remove TSR programs, such as network connections. This usually requires rebooting the computer in such a manner that these programs are not automatically accessed. MS-DOS 5.0 uses somewhat less memory than previous versions. See your PC consultant for assistance. Run MEMREM to determine approximately the memory available for data.

The memory required by the simulation is determined primarily by the total number of cells which in turn is determined by the values on line 4 of the data file (see below). The total number of cells can be reduced to an arbitrarily small value, but accuracy will suffer. If you must search for the number of cells than can be run on your machine, begin with a relatively small number and increase it until the unallocated memory reported by SUBSTRAT is small.

With minimal other uses of memory, SUBSTRAT is limited to less than 20,000 cells under MS-DOS. The only way to simulate more cells is to recompile SUBSTRAT for a different operating system and/or a different computer.

Contents of SUBSTRAT Data File

line	variables	brief description
1	LIST	Name of the output file
2	PLOT	Name of the plot file
3	TITLE	Project title; echoed to output
4	NX NY NZ	number of cells in the X, Y, and Z directions (total number of cells = NX × NY × NZ)
5	NCX DX0 XW X0	X-coordinate data[1]: NCX number of constant length nodes in both directions from X0 DX0 length [mm] of constant length nodes XW total length [mm] of X axis X0 location of center of region of constant length nodes = initial position of peak flux from cigarette
6	NCY DY0 YW	Y-coordinate data[1]: NCY number of constant width nodes from Y = 0 DY0 width [mm] of constant width nodes YW total width [mm] of Y axis
7	NCZ DZ0 ZW FT	Z-coordinate data[1]: NCZ number of constant depth nodes from Z = 0 DZ0 width [mm] of constant depth nodes ZW total depth [mm] of Z axis FT fabric thickness [mm][2]
8	SEP	Width of air gap between fabric and padding [mm]
9	E TM NCF	Fabric data: E emittance TM maximum temperature[3] [°C] NCF number of data points for T, K, C (NCF <= 10)
10	T K C	Fabric thermal properties[4]: T temperature [°C] K conductivity [W/mK] C specific heat [kJ/kgK] Repeat line 10 up to NCF times.
11	DV DC DA	Densities: DV virgin material [kg/m^3] DC char [kg/m^3] DA ash [kg/m^3]
12	A N1 N2 T H	Fabric non-oxidative pyrolysis data: A reaction rate coefficient [1/min] N1 fabric mass exponent N2 oxygen concentration exponent (must be zero) T activation temperature [K] H heat of pyrolysis [kJ/kg]
13	A N1 N2 T H	Fabric oxidative pyrolysis data: A reaction rate coefficient [1/min] N1 fabric mass exponent N2 oxygen concentration exponent T activation temperature [K] H heat of pyrolysis [kJ/kg]

14	A N1 N2 T H	Fabric char pyrolysis data (similar to 13)
15	E TM NCP	Padding data: E emittance TM maximum temperature[3] [°C] NCP number of data points for T, K, C (NCP <= 10)
16	T K C	Padding thermal properties[4]: T temperature [°C] K conductivity [W/mK] C specific heat [kJ/kgK] Repeat line 16 up to NCP times.
17	DV DC DA	Densities: DV virgin material [kg/m^3] DC char [kg/m^3] DA ash [kg/m^3]
18	A N1 N2 T H	Padding non-oxidative pyrolysis data (similar to 12)
19	A N1 N2 T H	Padding oxidative pyrolysis data (similar to 13)
20	A N1 N2 T H	Padding char pyrolysis data (similar to 13)
21	BC TA T0 OX	Boundary & initial conditions: BC 0 = adiabatic outer boundaries[5], 1 = constant temperature outer boundaries TA ambient temperature [°C] T0 initial substrate temperature [°C] OX oxygen concentration [fraction]
22	Q0 V Y X+ X-	Moving radiant flux distribution on surface: Q0 peak flux [kW/m^2] V velocity [mm/min] Y standard deviation in Y direction [mm] X+ std dev in positive X direction [mm] X- std dev in negative X direction [mm]
23	HC HG	Heat transfer coefficients[6] HC for quiescent air [W/m^2K] HG for impinging air [W/m^2K]
24	dt DT TT	Simulation control: dt maximum time step [s] DT maximum temperature change [°C] TT total simulation time [s]
25	LIST I J K	Debug reports (SUBSTRAT compiled with DEBUG defined): LIST 1 = activate data dumps (default 0) I J K are the indices of the cell to be studied
26	PLOT	Time at which to write temperatures to the plot file; repeat line 26 up to 10 times.

Notes:

[1] The relationship between the number of nodes, number of constant size nodes, size of constant size nodes and total length of an axis must be such that the variable width nodes are increasing in size.

[2] The fabric thickness and the depth of the constant depth cells are related: the fabric/padding boundary must be halfway between two cells. Therefore, the fabric thickness must be 0.5, or 1.5, or 2.5, etc., times the depth of the constant depth cells, or the constant depth cells must be 2, or 2/3, or 2/5, etc. times the thickness of the fabric. The boundary between the fabric and padding must be within the region of constant depth cells.

[3] When the temperature of any fabric (or padding) cell reaches the "maximum" fabric (or padding) temperature, the simulation is terminated.

[4] The way that k(T) and c(T) are input is by entering the values for each at a number of temperatures; the program then carries out a cubic spline fit to those points, to obtain the values at any other temperature. Even if k(T) and c(T) are given by explicit equations, this is still the way that the program "knows" the values.

[5] The "outer boundaries" of the substrate consist of the X = 0, X = XW, Y = YW, and Z = ZW planes (see items 5, 6, & 7).

[6] These coefficients refer to cases A and B in Section II.B.6. When using HC set HG to zero and vice versa.

The contents of the data file are described further in the description of the TSDATA program. It will generally be easier to check a data file by processing it with TSDATA, than to compare it line by line with the description given above.

TSDATA

The SUBSTRAT data file can be created with any ASCII line editor. However, the contents of the file are quite cryptic and thus prone to error; far better is to use TSDATA. TSDATA is an interactive program for creating data files. Because it is interactive, it uses certain commands which restrict its operation to IBM PC compatible computers. It includes extensive checking of the input data. TSDATA is especially useful for creating a data file which is only slightly different from another data file. This is useful in performing the parametric studies for which SUBSTRAT was designed.

Two special files are used by TSDATA. The help file, TSDATA.HLP, contains the text of the interactive help messages. Help is activated by pressing the F1 function key. If the help file is not available in the current working directory, no interactive help will be available. The configuration file, TSDATA.CFG, sets the colors of the display. The file included on the distribution diskette assumes that a standard VGA monitor is being used. If the configuration file is not in the current working directory, a set of default colors will be used. A new configuration file can be made by using the MAKECFGT program. See the README file for instructions.

The operation of TSDATA is explained on the following pages which show the messages and input screens which will appear as the program is run. After reading through these pages, try using TSDATA with one of the sample data files. Begin the program by typing TSDATA. Abort the program by pressing CTRL and C.

Sample Runs

At this point the following files should be available in the current working directory: TSDATA.EXE, TSDATA.HLP, TSDATA.CFG, and TEST1.DAT. If they are not, use the INSTALL procedure.

First use TSDATA to view the contents of the TEST1.DAT file. Type:

TSDATA

Press ENTER until the main menu appears; press ENTER again to set up the file information. Enter TEST1.DAT as the name of the previous data file. Press ENTER to cycle through file names (respond Y to the warning message about a duplicate file). Press ESC to return to the main menu. Press ENTER to view each section of data in turn; press ESC to return. When you reach the Save option, press CTRL and C to abort the program. This process will not have changed TEST1.DAT.

Now create a new data file, TEST3.DAT, similar to TEST1.DAT but with a peak flux of 20kW/m^2. Proceed as above until you reach "Name of new data file:". At this point move the cursor to the "1" in the file name and press 3 and then press ENTER. Revise the other two file names and the title accordingly. Press ESC to return to the main menu, and move to the boundary conditions option. Press ENTER and move (using cursor keys) to the peak heat flux. Change the value to 20, press ENTER, press ESC. Now enter the save option, and respond Y to save the file TEST3.DAT. Then enter the exit option, respond Y to exit, and respond Y to create a batch file. After this you should have exited TSDATA. Now type RUN to start SUBSTRAT using TEST3.DAT as input data.

TSDATA Input Screens and Help Messages

Standard title page with disclaimer at start of TSDATA program.

```
=====================================================

   TSDATA -- interactive program to prepare data files for SUBSTRAT

                          Version 1.0

        Developed at the National Institute of Standards and Technology.
                     Program author:  George Walton

    This program is furnished by the government and is accepted by any
    recipient with the express understanding that the United States
    Government makes no warranty, expressed or implied, concerning the
    accuracy, completeness, reliability, usability, or suitability for
    any particular purpose of the information and data contained in
    this program or furnished in connection therewith, and the United
    States shall be under no liability whatsoever to any person by reason
    of any use made thereof.  This program belongs to the government.
    Therefore, the recipient further agrees not to assert any proprietary
    rights therein or to represent this program to anyone as other than
    a government program.

=====================================================
```

General description of input process:

```
=====================================================
    This program assists you in preparing input data files for the SUBSTRAT
    program.  It operates best by reading an existing SUBSTRAT data file
    which is then modified to create a new data file.  A sample data file
    is distributed with the program.  It can also be used to enter data
    from scratch.  Several data files can be created in one TSDATA session.

    Data are processed interactively through a system of data entry menus.
    Keyboard input is required from the user whenever the cursor is in
    a data entry field.  A data entry field is designated by a special
    color as is shown in the lower right corner of this screen.  This is
    a standard pause allowing the user to read the screen.  Pressing any
    key in response will allow the program to continue.

    While the cursor is in a data entry field, it will often be possible
    to get help by pressing the F1 function key.  Help is intended to
    give additional information about the data.  For help to work, the
    TSDATA.HLP file must be in the same directory as the TSDATA.EXE file.
    Program execution may be terminated when the cursor is in a data
    entry field by pressing CTRL and C simultaneously.

=====================================================
```

General description (continued):

```
=======================================================
    There will usually be several data entry fields on a single screen.
    The field may be blank or it may present a default response.  The
    contents of a data entry field (even all blank) may be edited.
    That is, characters may be overwritten, deleted, or inserted.
    It may or may not be necessary to make an entry depending on context.

    These fields are ordered from top to bottom and left to right.
    Pressing the tab key or the down-arrow key moves the cursor to the
    next field to the right/down;  The shifted-tab or up-arrow moves
    to the previous field to left/up.  Control-home or page-up moves the
    cursor to the first field on the screen.  Control-end or page-down
    moves to the last field.  Movement between fields can be done only
    if an entry is not required and no other keys have been pressed.

    Data entry begins in the exchange mode, i.e., the value of the key
    pressed replaces the character at the cursor.  Pressing the insert
    key will switch to the insert mode (and from insert to exchange).
    The delete key will remove the character at the cursor.  Control-x
    will clear the entire data entry field.  Move the cursor left with
    the left-arrow, control-left-arrow, or home keys.  Move the cursor
    right with the right-arrow, control-right-arrow, or end keys.  When
    the data is satisfactory, press the ENTER key.

=======================================================

    Various checks are usually made on each data entry.  These may produce
    a warning or error message at the bottom of the screen.  The first line
    of this message indicates the nature of the problem.  The second line
    indicates the severity of the problem, the file and line in the TSDATA
    source code where the error message originated, and whether some help
    may be available by pressing the F1 key.

    Most errors will return you to the data entry field to correct the input.
    Such errors include invalid characters or numeric values outside certain
    situation-dependent limits.

    Some problems may generate a question:

       Question? (y/n) ▓

    The user can press the Y and then ENTER keys to indicate a positive (yes)
    response or N and then ENTER to indicate a negative (no) response.

    Some errors are fatal causing the program to terminate.
=======================================================
```

Screen 1: (primary menu)

```
======================================================

SUBSTRAT data preparation:

   ▒  File information

   ▒  Geometry description

   ▒  Fabric data

   ▒  Padding data

   ▒  Boundary conditions

   ▒  Simulation control

   ▒  Save this data file

   ▒  Exit data preparation

Use cursor keys to move between menu selections.
Press ENTER to activate the menu selection at the X.
Press ESC to return from a selection.  Press F1 for help.
======================================================
```

General help message:

```
This program assists you in preparing input data files for the SUBSTRAT
program.

This is the main menu.  It directs you to the different data
preparation subsections.

Begin each data file by entering the "file information".

Data relating to the geometry, fabric, padding, or boundary conditions
may be entered or changed in any order.

The data file is not created until you "save this data file".

Multiple data files can be created in one interactive session.
Terminate the session by entering "exit data preparation".
```

Note:
An X appears in the selection designator: ▒.

Screen 2:

```
=====================================================
  File information:                  press ESC when done;  press F1 for help.

Copy data from previous data file named:

Name of new data file:

Name of list file:

Name of plot file:

Title for this simulation:

Files previously defined in this session:
 data files   list files   plot files   titles (first 40 characters)
 ----------   ----------   ----------   ---------------------------

=====================================================
```

General help message:

The data files you create are stored in the current directory. If you want to make a data file which is similar to a previous data file, enter the name of the previous file. That file must also be in the current local directory.

SUBSTRAT creates two files when it is run:
(1) the list file (which echoes the input, saves any error messages, and notes the peak temperature of the substrate during the simulation),
(2) the plot file (which becomes the input file to the plotting program used to view the temperature distribution in the substrate).

Files should generally have different names. For example, consecutive SUBSTRAT runs with the same plot file names will save only the plot file from the last run (which will have replaced the previous plot files). Use identical names if you definitely want to replace existing files, including data files.

The title that you enter here is echoed in the list and plot files. Use the title as a reminder of the special features of a particular run.

Up to 10 data files created previously in this session are recorded at the bottom of the screen for your convenience.

Help messages in response to error messages:

(1) could not open file:

The file which you specified was not found. A typing error is the most likely problem, or the file is not in the current directory.

(2) duplicate file names:

This message indicates that a file name matches one in the local directory, or one previously set in this session, or that you have not pressed ENTER at each of the file names to complete the check of file names.

If you have copied an existing data file, the "new" file names are the ones that appeared in the existing data file.

Files should generally have different names. For example, consecutive SUBSTRAT runs with the same plot file names will save only the plot file from the last run (which will have replaced the previous plot files). Use identical names if you definitely want to replace existing files, including data files.

You may use a duplicate file name by responding 'Y' to the question about writing over the previous file.

Notes:

An entry for the previous data file causes its data to be copied.

The new data file will be created when "save this data file" is executed at the main menu. This save adds the new data, list and plot file names to the list displayed at the bottom of this screen.

There should be no duplicate file names. That would cause files to be overwritten during simulation. The program checks for duplicates.

The simulation title is echoed in the output files.

Note that upon entering the "Title for this simulation," the cursor jumps back to the first box and blanks it out. This is done only so that if the user has changed his mind (or an error has been made), new (or corrected) entries can be made immediately. If there has been no error, then simply press ESC.

Screen 3:

```
=====================================================
  Geometric description:              press ESC when done;  press F1 for help.

Fabric thickness:            mm

Width of air gap:            mm

X-coordinate data:
            Number of grid points:                        Rx = 1.xxx
         Total length of substrate:            mm
     Size of constant length cells:            mm
   Number of constant length cells:

Y-coordinate data:
            Number of grid points:                        Ry = 1.xxx
          Half-width of substrate:            mm
     Size of constant width cells:            mm
   Number of constant width cells:

Z-coordinate data:
            Number of grid points:                        Rz = 1.xxx
          Total depth of substrate:            mm
     Size of constant depth cells:            mm
   Number of constant depth cells:

                                                  cells: xxxxx

=====================================================
```

General help message:

```
The substrate consists of a thin fabric, padding, and possibly an
air gap between them.  An air gap width of 0.0 indicates no gap.

The X direction is along the cigarette; the Y direction is along the
fabric; the Z direction is into the padding.

A variable grid is used.  It consists of several constant width cells
near the point of peak incident heat flux followed by increasingly
larger cells out to the boundaries of the substrate.  For example:

   |  |  |  |  |  |   |    |     |      |       |
Y=0                                             Y=width

Each variable width cell is R times longer than the preceding cell.
Simulation is most accurate when R is only slightly greater than one.
A value of R less than about 1.25 should be sufficiently accurate.
Simulation will generally involve a trade-off of accuracy and run time.

The fabric thickness and the depth of the constant depth cells are
related:  the fabric/padding boundary must be halfway between two cells.
Therefore, the fabric thickness must be 0.5, or 1.5, or 2.5, etc., times
the depth of the constant depth cells.
```

Other help messages:

```
For the X-axis the following conditions should apply:
    4 * NCX < NX   and   (NX - 1) * DX0 <= XW
where NX = number of grid points, XW = total length of substrate,
DX0 = size of const length cells, & NCX = number of const length cells.

For the Y-axis the following conditions should apply:
```

```
    2 * NCY < NY    and    (NY - 1) * DY0 <= YW
where NY = number of grid points, 2YW = total width of substrate,
DY0 = size of const width cells, & NCY = number of const width cells.
Because of the assumed bilateral symmetry of the flux, it is only necesary
to make calculations between y = 0 and y = YW (half the width).  The number
of constant-width cells is that in the half-width section.

For the Z-axis the following conditions should apply:
    2 * NCZ < NZ    and    (NZ - 1) * DZ0 <= ZW
where NZ = number of grid points, ZW = total depth of substrate,
DZ0 = size of const depth cells, & NCZ = number of const depth cells.

The fabric thickness and the depth of the constant depth cells are
related:  the fabric/padding boundary must be halfway between two cells.
Therefore, the fabric thickness must be 0.5 or 1.5 or 2.5, etc., times
the depth of the constant depth cells, or the constant depth cells must
be 2 or 2/3 or 2/5, etc. times the thickness of the fabric.

The boundary between the fabric and padding must be within the region
of constant depth cells.
```

Notes:

"Rx", "Ry", and "Rz" are the geometric progression rates. The sample problems have a relatively high value in the Z direction. Tests have indicated this is satisfactory because the low conductivity of the padding permits less heat transfer in this direction.

"cells:" gives the total number of cells used to model the substrate. It equals NX × NY × NZ. This value is critical to the total memory required for a simulation.

The following figure illustrates the substrate coordinate system and the variable grid:

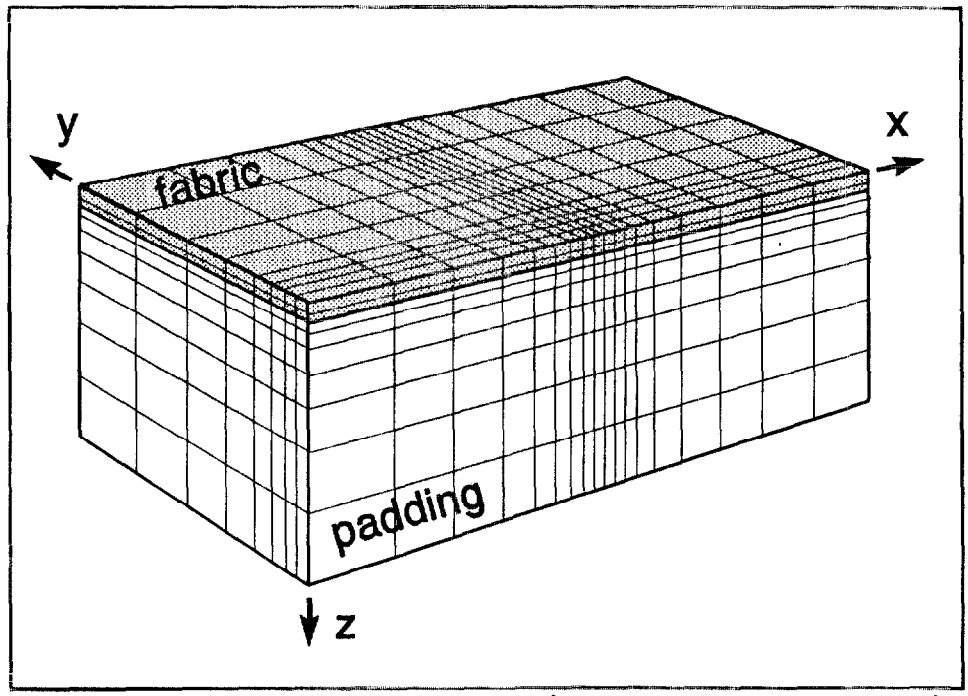

Figure B-2. Substrate Coordinate System and Variable Grid

Screen 4:

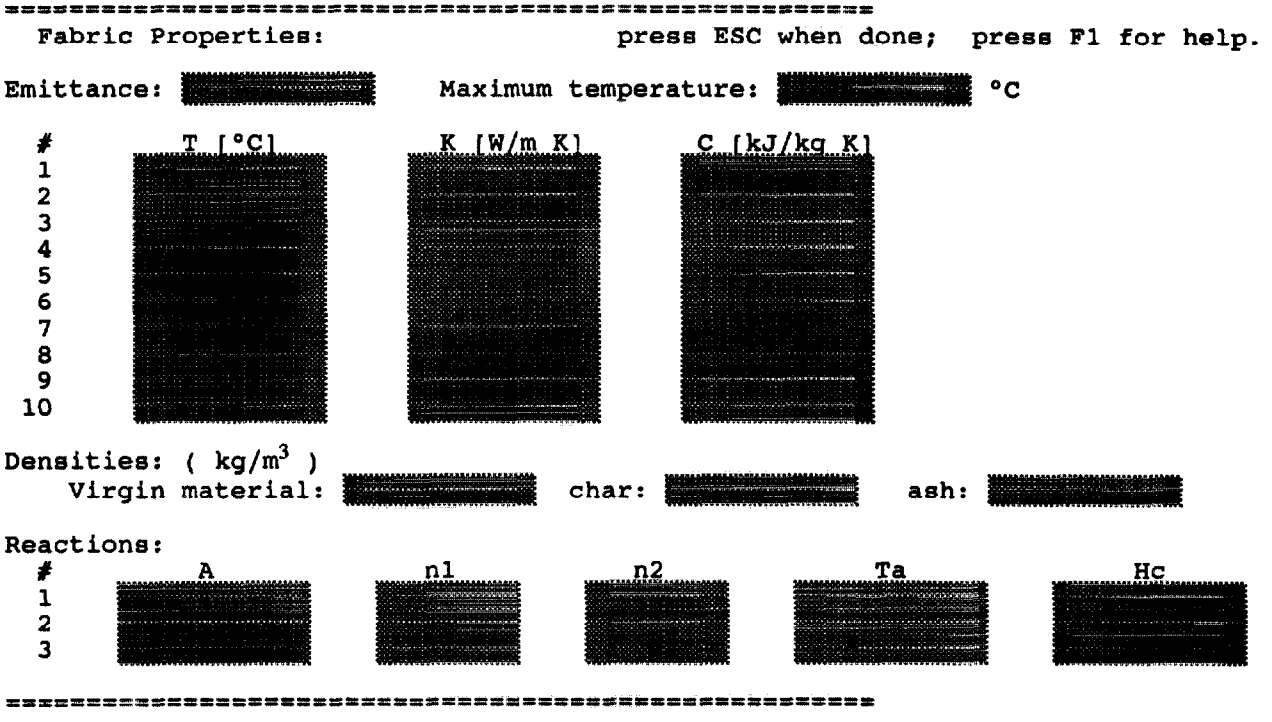

General help message:

Emittance is used in computing radiant heat loss from the fabric to ambient and radiant heat transfer across the air gap.

The simulation stops when the temperature of any fabric cell reaches the prescribed maximum temperature.

Thermal conductivity (K) and heat capacity (C) can be specified at up to 10 temperatures. SUBSTRAT uses a cubic spline curve fit for K and C. As fabric mass is lost by pyrolysis, K is also reduced in proportion to the current density. Values are required at least two temperatures even if K and C are constant.

A two-stage, three-reaction pyrolysis model is used: the virgin material is converted to char in stage 1 and then to ash. The char density is the value for completely converting the virgin material to char with no conversion to ash. The ash density is what's left after total pyrolysis.

The pyrolysis equations are of the form:

$$R = A * Dm^{n1} * Cx^{n2} * \exp(Ta/T) \quad \text{and} \quad Q = R * Hc$$

where
- R = rate of pyrolysis
- A = reaction coefficient [1/min]
- Dm = density of material (virgin or char)
- n1 = related exponent
- Cx = oxygen concentration
- n2 = related exponent
- Ta = activation temperature [K]
- T = current cell temperature [K]
- Hc = heat of pyrolysis [kJ/kg]

```
The first reaction is thermal degradation (n2 = 0 and Hc < 0) of virgin
material.  The second reaction is oxidation of the virgin material.
These two reactions produce char.  The third reaction is oxidation
of the char to produce ash.
```

Help message in response to error message:

```
Temperatures must be given in increasing order.
The lowest temperature should be several degrees less than any
possible substrate temperature.  The highest temperature should
be several degrees higher than the maximum temperature.
```

```
==========================================================
Screen 5:
==========================================================
  Padding Properties:                  press ESC when done;  press F1 for help.

Emittance:                  Maximum temperature:                  °C

  #      T [°C]          K [W/mK]          C [kJ/kgK]
  1
  2
  3
  4
  5
  6
  7
  8
  9
 10

Densities: ( kg/m3 )
    Virgin material:                char:                ash:

Reactions:
  #          A              n1              n2              Ta              Hc
  1
  2
  3

==========================================================
```

Padding help messages are similar to fabric messages.

Screen 6:

```
=====================================================
  Boundary Conditions:                press ESC when done;  press F1 for help.

At X=0, X=Xmax, Y=Ymax, Z=Zmax: (*) adiabatic
                                ( ) constant temperature

 Initial substrate temperature:                  °C

           Ambient temperature:                  °C

         Oxygen mass fraction:

Heat transfer coefficients:
                 Quiescent air:                  W/m²K
                 Impinging air:                  W/m²K

Moving heat flux pattern from the cigarette:
               Peak heat flux:                   kW/m²
    Initial X position of peak:                  mm
                  +X velocity:                   mm/min
     ±Y standard deviation (A):                  mm
     +X standard deviation (B):                  mm
     -X standard deviation (C):                  mm

=====================================================
```

General help message:

Select the condition of the outer boundaries (X=0, X=length, Y=width, Z=depth) by pressing ENTER in the appropriate place.

The incident heat flux from the cigarette is represented by a moving flux distribution on the surface of the substrate. This distribution has the shape of non-symmetric Gaussian curve which is described by six parameters:

(1) the X coordinate at the peak of the curve at the start of the simulation { the initial position of the peak is (Xo, 0, 0) },
(2) the speed, S, at which the peak moves along the X axis { the position P of the peak at time t is (Xo+S*t, 0, 0) },
(3) the maximum heat flux at the peak { at position (P, 0, 0) },
(4) the width of the curve in the Y direction { at position (P, ±A, 0), the heat flux is 0.37 times the flux at the peak },
(5) the width of the curve in front of the peak { at position (P+B, 0, 0), the heat flux is 0.37 times the flux at the peak }, and
(6) the width of the curve behind the peak { at position (P-C, 0, 0), the heat flux is 0.37 times the flux at the peak }.

Screen 7:

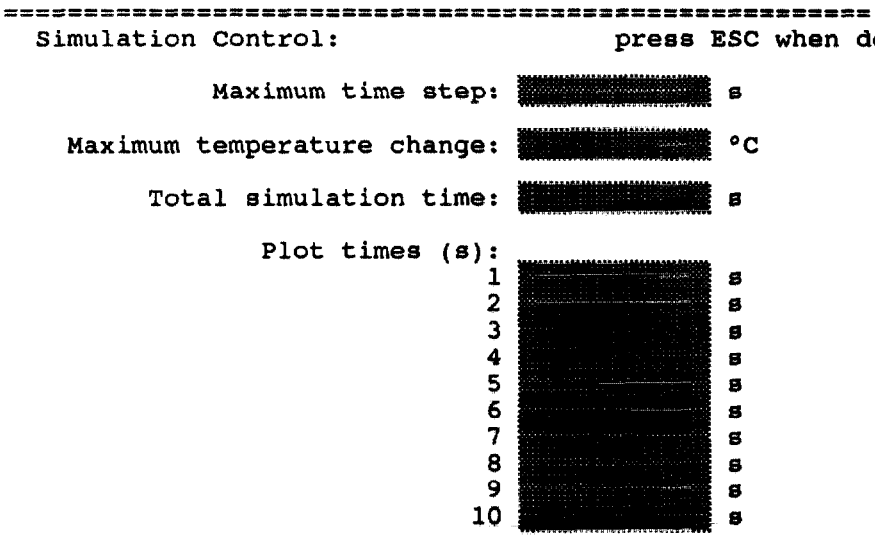

General help message:

SUBSTRAT uses a variable time step which is chosen so as not to exceed the maximum time step given and so that the maximum temperature change in any cell is not greater than the maximum given. This allows the program to run quickly when the temperatures are not changing rapidly. Smaller values for these two parameters will lead to more accurate simulations at the cost of longer execution times.

The simulation will stop at the total simulation time unless it has already stopped by exceeding a maximum fabric or padding temperature.

Plot times are entered in increasing order. When the simulation reaches a plot time, substrate temperatures are copied to the plot file. Leave later positions blank if you do not want to use all 10 times. A plot is automatically written when the simulation stops. The last plot time should be greater than the simulation time to satisfy a requirement in the SUBSTRAT program.

Screen 8:

```
=====================================================

Save this data file? (y/n) ▓

display any error message(s).

=====================================================
```

General help message:

```
    If you entered this area accidentally and are not ready to stop
    preparing the current data file, respond "N" to this question.
    This will return you to the main menu.
```

Help messages in response to error message:

(1) check data.

```
    Data in the indicated section may be incomplete or incorrect.
    Enter that section and check the data.
```

(2) temperature problem.

```
    The lowest temperature for fabric or padding thermal properties must
    be several degrees lower than either the initial or ambient temperature.
    You need to change (at least) one of those values.
```

(3) files limit.

```
    No more SUBSTRAT data files can be created in this session.
    You probably should exit TSDATA now.  You may replace one of the
    data files already created.
```

Screen 9:

```
==================================================

Exit data preparation? (y/n) ▌                    (1)

display error messages, if applicable             (2)

prepare DOS batch file to run all cases (y/n)? ▌  (3)

==================================================
```

Help messages:

(1) initial message.

```
If you entered this area accidentally and are not ready to stop
preparing data files, answer "N" to this question.
```

(2) error messages.

```
This warning indicates that TSDATA may have data which you have not saved.
If you respond "Y" to the question about checking this data file, you
are returned to the main menu where you can check and then save the file.
If you respond "N", you will continue to exit the TSDATA program.
```

(3) batch file message.

```
A positive response will create a file RUN.BAT resembling:

SUBSTRAT <datafile.1
SUBSTRAT <datafile.2
SUBSTRAT <datafile.3
SUBSTRAT <datafile.4

This file can be used to run SUBSTRAT on computers using MS-DOS.
```

Notes:

Message (1) appears automatically.

Error message (2) may appear.

Message (3) appears after a Y to question (1).

TSPLOT

The TSPLOT program will display contour plots of substrate temperatures on the screen. It is an interactive program which uses the plot file from SUBSTRAT as input. Because it is interactive and graphic, it uses certain commands which restrict its operation to IBM PC compatible computers. A plot file contains the substrate surface (Z = 0 plane) and center-plane (Y = 0 plane, see Figure B-2) temperatures at various times set in the input data file.

Three special files are used by TSPLOT. The CHRSET.VGA file contains the bit patterns for the graphic display. This file is required. The help file, TSPLOT.HLP, contains the text of the interactive help messages. Help is activated by pressing the F1 function key. If the help file is not available in the current working directory, no interactive help will be available. The configuration file, TSPLOT.CFG, sets the colors of the display. The file included on the distribution diskette assumes that a standard VGA monitor is being used. If the configuration is not in the current working directory, a set of default colors will be used. These colors may not provide satisfactory contour plots. A new configuration file can be made by using the MAKECFGG program. See the README file for instructions.

The operation of TSPLOT is briefly explained on the following page. Because the screen interface is similar to TSDATA and relatively few options are available, a detailed description should not be necessary. After reading this description, try using TSPLOT with the sample plot files. Begin the program by typing TSPLOT. Abort the program by pressing CTRL and C.

Sample Run

At this point the following files should be available in the current working directory: TSPLOT.EXE, CHRSET.VGA, TSPLOT.HLP, TSPLOT.CFG, TEST1.PLT, and TEST2.PLT. If they are not, use the INSTALL procedure. If you ran TEST1 or TEST2 and aborted before completion, use INSTALL to replace the plot files with the original complete versions.

Type TSPLOT. Press ENTER until the main menu appears; press ENTER again to get the plot file. Enter TEST1.PLT as the name of the plot file. After returning to the main menu, press ENTER to display the next plot. Note that this plot is for t = 1 second, and the pattern is rather small. After viewing this plot, press any key to return to the main menu. Move (use cursor keys) to the set display parameters option and press ENTER. Change the Xmin value from "0" to "10", press ENTER, change Xmax from "60" to "50", press ENTER, and press ESC. Now press ENTER to display the prior plot. The limits of the display have been changed, and the heated area appears larger. Press ENTER to alternate between the main menu and the next plot. In the later plots note the discontinuity in the profiles in the padding caused by the air gap. After the last plot you will arrive at the exit option. Instead of exiting, move to the get plot file option, press ENTER, and enter TEST2.PLT as the name of the plot file. Return to the main menu and display the next plot which is the first plot from TEST2.PLT. Note that the limits of the X-axis have not been reset for this new plot. As you continue by displaying successive plots note how the point of peak temperature is moving along the X-axis. When you reach the exit option, press ENTER, and respond Y to exit the program.

TSPLOT Main Menu

This is the main menu screen. It directs you to the different options.

```
==================================================

TSPLOT program:

   ▒  Get plot file

   ▒  Display next plot

   ▒  Redisplay

   ▒  Set display parameters

   ▒  Exit


Use cursor keys to move between menu selections.
Press ENTER to activate the menu selection at the X.
Press ESC to return from a selection.  Press F1 for help.
==================================================
```

The first option is "Get plot file". You must get a (enter the name of an existing) plot file before any plots can be displayed.

The plot file is read sequentially. You may display the data at the next plot time (option two), or you may redisplay the last plot shown (option three).

The graphic display consists of three parts: the temperature scale (in °C) to the right, the substrate surface temperature contours in the upper left of the screen, and the center-plane temperatures in the lower left. In other words, the temperature contours for the Z=0 and Y=0 planes are displayed together as if they have been folded along the X-axis so as to both be flat on the screen. The display also shows the time and the X-axis with coordinates at the left and right edges and tic marks every millimeter.

The fourth option lets you reset the display parameters. You may set the coordinates of the left and right edges of the display. These values change both the position and the scale of the regions being displayed thus enlarging or shrinking the plot. The initial limits of the X-axis are for the entire region simulated. You may also change the temperature contours which are initially set at 25 °C intervals. Changes must be made so that each temperature is always less than the one above and more than the one below. You will then probably want to redisplay the last plot.

After displaying one set of plots, you may get a new plot file without exiting this program. This is the only way to go back in time on the plot file: get the plot file again and start at the beginning.

When you reach the end of the plot file, TSPLOT automatically takes you to the exit option.

APPENDIX C

ANALYSIS OF NUMERICAL ERRORS PRODUCED BY A RUNAWAY REACTION RATE

We have made an effort to make a fine grid in the region where the fluxes and flux gradients are high. Nevertheless, when the reaction rates become very high, the gradients will become so steep that the approximation of constant temperature and constant reaction rate within a cell becomes questionable. In this appendix, we examine the magnitude of the errors thus committed by discretization. This analysis can also serve to make appropriate corrections in the program; this has not been done here, partly because the analysis should first be generalized to the non-symmetric case. (See the assumptions made just below equation (C1).

Consider the heat diffusion equation, equation (95). Suppose we have the (correct) temperature distribution T(x,y,z,t), with a peak at (x_o,y_o,z_o); the reaction rate is given by an expression such as equations (108) or (110). Let us simplify this form and assume that

$$R_p = R_\infty \exp(-T_A/T(r)) \tag{C1}$$

where all the preexponential factors are lumped together as the factor R_∞ and $\mathbf{r} \equiv (x,y,z)$ is the position vector. Consider the terms in equation (12); we simplify the analysis by assuming that the temperature peak lies at the cell center (*i.e.*, at $\mathbf{r}_o$), and that the distribution is symmetric fore-and-aft. Then, since calculating R_p in that cell means calculating it at the center, and therefore the peak, that means we **overestimate** the reaction rate, since the rate falls off at the faces of the cell.

Symmetry implies that

$$\nabla\cdot(\kappa\nabla T) \approx \kappa\left(\frac{\partial^2 T}{\partial x^2}+\frac{\partial^2 T}{\partial y^2}+\frac{\partial^2 T}{\partial z^2}\right) \approx 3\kappa\frac{\partial^2 T}{\partial x^2} \tag{C2}$$

A second-order approximation to this derivative is

$$\nabla\cdot(\kappa\nabla T) \approx 3\kappa\frac{T_{i-1}-2T_i+T_{i+1}}{(\Delta x)^2} \tag{C3}$$

Because of the assumed symmetry, $T_{i-1} = T_{i+1}$, so that we finally have

$$\nabla\cdot(\kappa\nabla T) \approx 6\kappa\frac{T_{i-1}-T_i}{(\Delta x)^2} \tag{C4}$$

Inserting this into equation (12), that equation becomes

$$\rho c\frac{\Delta T_{i,j,k}}{\Delta t} \approx H_c R_p(r) - 2\kappa\frac{T_{i,j,k}-T_{i-1,j,k}}{(\Delta x)^2} - \ldots \tag{C5}$$

minus similar terms in Δy and Δz (as indicated by the ellipsis). Suppose further, for the sake of simplicity, that the temperature profile is Gaussian:

$$\theta(x,y,x,t) = \theta_m \exp\left[-\frac{(x-x_o)^2+(y-y_o)^2+(z-z_o)^2}{\sigma^2}\right] \tag{C6}$$

where $\theta = T - T_a$

and T_a = ambient (reference) temperature.

If we redefine the origin to be at (x_o,y_o,z_o), then

$$\theta(x,y,x,t) = \theta_m \exp(-r^2/\sigma^2) \tag{C7}$$

where $r^2 = x^2 + y^2 + z^2$.

Then if $x^2/\sigma^2 << 1$ everywhere within the cell, we can expand (C7). At the center of the cell,

$$\theta_i = \theta(r_0) = \theta_{max} \equiv \theta_m \tag{C8}$$

and

$$\theta_{i-1} = \theta_m \exp[-(\Delta x/\sigma)^2] \approx \theta_m[1-(\Delta x/\sigma)^2]. \tag{C9}$$

Define $\xi = (\Delta x/\sigma)^2$. Then

$$T_i - T_{i-1} = \theta_i - \theta_{i-1} \approx \theta_m \xi \tag{C10}$$

so that equation (C5) becomes

$$\rho c \frac{\Delta\theta}{\Delta t} \approx H_c R_p - \frac{2\kappa}{(\Delta x)^2}\left[\theta_m \frac{(\Delta x)^2}{\sigma^2}\right] - \ldots \tag{C11}$$

Assuming three-fold symmetry, the other two terms in (C11) are the same, and thus

$$\rho c \frac{\Delta\theta}{\Delta t} \approx H_c R_p - 6\kappa \frac{\theta_m}{\sigma^2} \tag{C12}$$

Note that the dependence on Δx has dropped out. Indeed, the last term is the exact diffusive loss rate, resulting from the distribution (C7).

Now let us examine the magnitude of the error made by using a <u>finite</u> value of Δx. From equation (C7),

$$\Delta\theta \equiv \theta_i - \theta_{i-1} = \theta_m[1 - \exp(-\xi)] \tag{C13}$$

Then expanding to the next higher order than was done in (C9),

$$\Delta\theta \approx \theta_m \xi(1 - \xi/2) \tag{C14}$$

and the second term in (C5) becomes

$$\frac{2\kappa\Delta\theta}{(\Delta x)^2} \approx \frac{2\kappa\theta_m}{\sigma^2}(1 - \xi/2) \tag{C15}$$

Thus the numerical calculation <u>underestimates</u> the loss rate. Since the correct heat loss rate is

$$\mathcal{L} = 6\kappa\theta_m/\sigma^2 \tag{C16}$$

and we have

$$L \equiv \frac{6\kappa\theta_m}{(\Delta x)^2}[1-\exp(\xi)], \tag{C17}$$

we multiply **L** by the ratio

$$F = \frac{\xi}{[1-\exp(-\xi)]} \approx \frac{1}{1-\xi/2} \tag{C18}$$

in order to get the correct loss rate $\mathcal{L}$.

As the temperature "runs away," the distribution becomes increasingly peaked, and σ declines. As it does so, ξ increases, and so, therefore, does F; this helps to slow down, or moderate, the runaway. ξ is readily found to be

$$\xi = \ln(\theta_i/\theta_{i-1}) \tag{C21}$$

Next, consider the source term in equations (C5) and (C12), again. Define

$$f(x,y,z) = \exp[-T_A/T(x,y,z)] \tag{C22}$$

The correct power output in the elemental volume ΔV is, from equation (C1),

$$R_p \Delta V = 8R_\infty \int_0^{\Delta x/2} dx \int_0^{\Delta y/2} dy \int_0^{\Delta z/2} f(x,y,z)\, dz \tag{C21}$$

where we have again translated (x_o,y_o,z_o) to be at the origin, and have taken advantage of the 3-fold reflection symmetry. Again assume equation (C7) to hold. If $\xi << 1$, then within the cell we can Taylor expand and write

$$f(x,y,z) = \exp(-T_A/T_m) + x\left(\frac{\partial f}{\partial x}\right)_0 + \frac{x^2}{2}\left(\frac{\partial^2 f}{\partial x^2}\right)_0 + \ldots \tag{C22}$$

plus similar terms in y and z. Since the peak is at the origin,

$$\left(\frac{\partial f}{\partial x}\right)_0 = \left(\frac{\partial f}{\partial y}\right)_0 = \left(\frac{\partial f}{\partial z}\right)_0 = 0, \tag{C23}$$

and dropping the higher-order terms,

$$f(x,y,z) \approx \exp(-T_A/T_m) + \frac{x^2}{2}\left(\frac{\partial^2 f}{\partial x^2}\right)_0 + \frac{y^2}{2}\left(\frac{\partial^2 f}{\partial y^2}\right)_0 + \frac{z^2}{2}\left(\frac{\partial^2 f}{\partial z^2}\right)_0 \tag{C24}$$

We find that

$$\left(\frac{\partial^2 f}{\partial x^2}\right)_0 = -\frac{2T_A}{T_m^{\,2}}\frac{\theta_m}{\sigma^2}\exp(-T_A/T_m) \tag{C25}$$

Thus

$$f(x,y,z) \approx \exp(-T_A/T_m)\left[1 - \frac{T_A\theta_m}{T_m^{\,2}\sigma^2}r^2\right] \tag{C26}$$

and integration over the cell yields

$$R_p \Delta V \approx (\Delta x)^3 R_\infty f(0) \left[1 - \frac{T_A \theta_m}{4 T_m^2} \xi^2 \right] \tag{C27}$$

This is only valid for $\Delta x/\sigma << 1$. In that limit, however, (C26) is well approximated by

$$\bar{R}_p \approx R_\infty \exp(-T_A/T_m) \exp\left[-\frac{T_A \theta_m}{4 T_m^2} \xi^2 \right] \tag{C28}$$

which is a reasonable first approximation to the correct integral, even when $\Delta x/\sigma$ is not very small.

The numerical approximation is

$$R_p = R_p(r_0) \approx R_\infty \exp(-T_A/T_m) \tag{C29}$$

Thus (C28) shows that we must multiply this approximation by $\exp\left[-\frac{T_A \theta_m}{4 T_m^2} \xi^2 \right]$ in order to get a still better approximation to the source term.

APPENDIX D

ANALYSIS OF IGNITION EXPERIMENT

Among the things we wish to extract from this experiment is the heat transfer coefficient to the surface, h. Figure D-1 shows the total heating fluxes to the gauge, as a function of the power input, with and without a purging flow of nitrogen. Consider the 18 kW/m^2 case. **Without** the purge flow, the heating flux is purely radiative, and is measured to be $\phi_{rad}^* \approx 10$ kW/m^2. With the purge flow on, there is considerable convective heating of the surface as well, and the measured flux is $\phi_{tot} \approx 18$ kW/m^2, suggesting that the convective flux is $\phi_{con} = \phi_{tot} - \phi_{rad} = 18 - 10 = 8$ kW/m^2. However, when the purge flow is turned on, it cools off the heating element somewhat. How much it does so, however, is unknown. Assume that the purge flow reduces the hot-surface temperature such that ϕ_{rad} is reduced to some fraction F of the original. Then

$$\phi_{rad} \approx 10F \tag{D1}$$

and

$$\phi_{con} \approx 18 - 10F \tag{D2}$$

At the point P, on the heater axis but at the surface being heated (5.4 mm below), the heater subtends a solid angle such that the view factor is Ω. Hence the impinging radiative flux is

$$\phi_{rad} = \Omega \epsilon_d \sigma T_d^4 + (1-\Omega)\sigma T_a^4 \tag{D3}$$

where ϵ_d is the emissivity of the device surface. For the particular case that was carried out, the standoff distance is 5.4 mm, while the diameter of the glowing filament is 13 mm. According to Siegel and Howell (1981), Appendix C, the view factor for a disk of radius R, at a point a distance H along the axis normal to the disk, is

$$\Omega = \left(\frac{H^2}{R^2} + 1\right)^{-1} \tag{D4}$$

Hence $\Omega = 0.592$. We also assume that $T_a = 25$ °C ≈ 298 K, and that $\epsilon_d \approx 0.85$. It follows from equations (D1) and (D3) that

$$T_d^4 = \frac{10F}{\Omega \epsilon_d \sigma} - \frac{(1-\Omega)T_a^4}{\Omega \epsilon_d} \tag{D5}$$

If F = 1, this yields $T_d \approx 493$ °C, while F = 0.9 yields $T_d = 472.5$ °C. The device surface cannot be much colder than 500 °C, since it is observed to glow red. If $T_d = 472.5$ °C, then $\phi_{rad} \cong 9$ kW/m^2.

We will assume that the factor F remains constant for all irradiations. Thus for the case $\phi_{tot} = 25$ kW/m^2, $\phi_{rad}^* \approx 16$ kW/m^2, and equation (D5) implies that $T_d = 840.3$ K = 567.1 °C.

We proceed the same way for all four cases, and obtain the values in the first six columns of Table D-1 (with fluxes given in kW/m^2). Column 6, marked ϕ_c, is the convective flux, found as the difference between ϕ_{tot} and ϕ_{rad}. These values of ϕ_c are plotted vs ϕ_{tot} and a smooth curve passed through these points, including the point at the origin. That yields the smoothed convective fluxes ϕ_c, given in column 7.

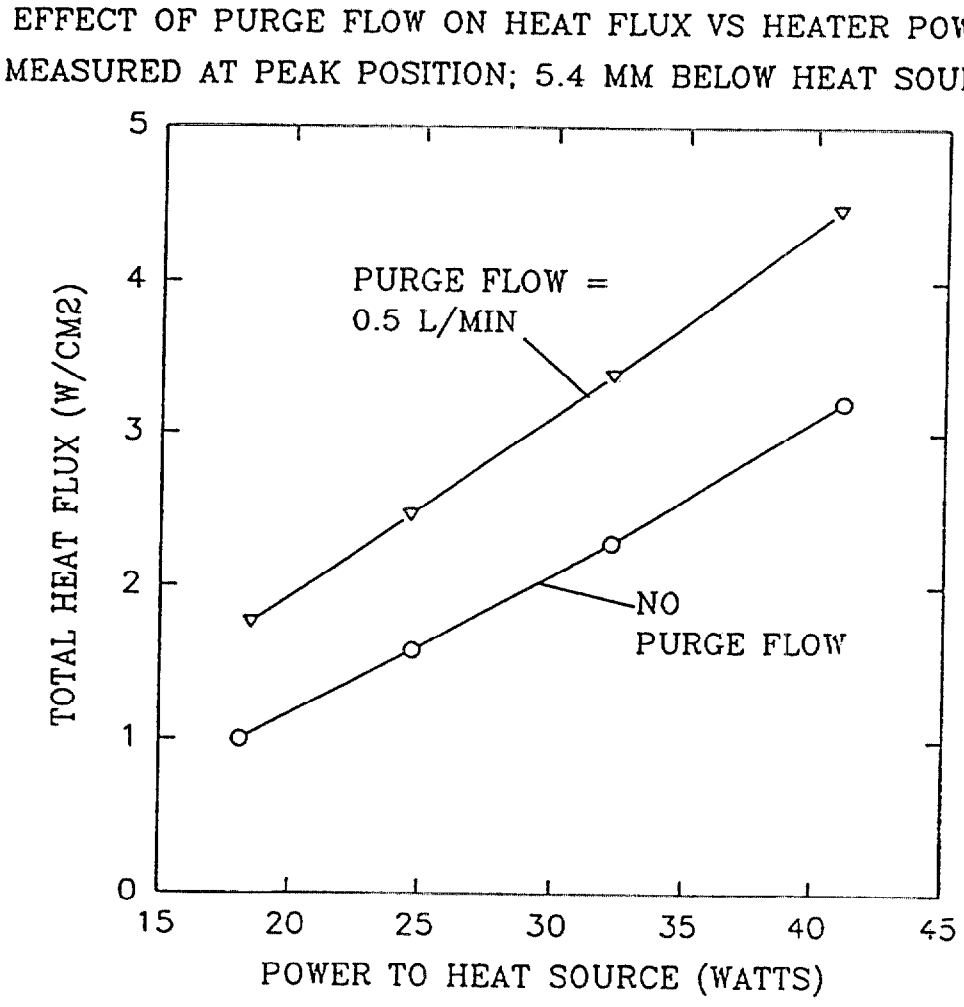

Figure D-1. Total heat flux impinging on gauge, with and without purge flow

Table D-1. Measured and Inferred Quantities From the Ignition Experiments

ϕ_{tot}	ϕ_{rad}/F	$T_d(K)$	$T_d(°C)$	ϕ_{rad}	ϕ_c	$\bar{\phi}_c$	hf	$T_g(K)$	h	f
18	10	745.7	472.5	9.0	9.0	8.9	19.67	698	22.0	0.893
25	16	840.3	567.1	14.4	10.6	10.7	19.56	760	22.9	0.854
34.5	23	921.0	647.8	20.7	13.2	13.0	20.71	837	23.9	0.865
44	32	1000.9	727.7	28.8	15.2	15.2	21.48	907	24.8	0.866

The convective flux can be written in the form

$$\phi_c = h(T_g - T_c) \tag{D6}$$

where T_g is the purge gas temperature, and T_c is the (cold) gauge temperature. In order to make progress we make one further plausible assumption: the purging gas takes up a (constant) fraction of the total energy delivered to the device. We can express this as

$$\theta_g = f\theta_g \tag{D7}$$

where Θ is the temperature referred to the gauge temperature:

$$\theta_i \equiv T_i - T_c \ . \tag{D8}$$

Thus, equations (D6) and (D7) yield

$$\phi_c = h\theta_g = fh\theta_d \tag{D9}$$

Since we have T_d (column 4) and ϕ_c (column 7), we readily infer the factor fh from equation (D9). This is given as column 8.

Next, we must find the heat transfer coefficient h for stagnant flow. The purge air comes down, strikes the fabric, and must move away radially. This configuration is approximated by the standard problem of stagnant flow. The heat transfer coefficient for this case is given in Kakaç *et al.* (1987). Their equation (2.176) on page 2-59 gives the Nusselt number:

$$\left(\frac{Nu}{Pr^{0.4}\sqrt{Re}}\right)_w = 0.767\left(\frac{\mu_e \rho_e}{\mu_w \rho_w}\right)^{0.43} \tag{D10}$$

which was found by Cohen (1961). The subscripts w and e, above, stand for "wall" and "edge" (of the boundary layer), respectively. The second factor on the right-hand side is approximately one, in this case. The Reynolds number is

$$Re = \frac{u_\infty \ell_c}{\nu} \tag{D11}$$

where ℓ_c is the characteristic length. One might think that the characteristic length here is the diameter of the opening. In fact, however, Cohen (1961) gives **Re** in the form

$$Re = \frac{du_\infty}{dx}\frac{\ell_c^2}{\nu} \tag{D12}$$

Since the (vertical) velocity goes from u_∞ to zero in the distance δ, we may write

$$\frac{du_\infty}{dx} \approx \frac{u_\infty}{\delta}; \tag{D13}$$

then equation (D12) indicates that the proper ℓ_c to use here is δ. u_∞ is readily inferred from the volumetric flow, dV/dt = 0.5 l/min. Thus

$$\dot{V} = \frac{\pi r^2 u_\infty \rho_g}{\rho_a} = \frac{\pi d^2 u_\infty T_a}{4T_g} \tag{D14}$$

which yields

$$u_\infty = 6.28(T_g/T_a) \qquad \text{cm/sec} \tag{D15}$$

The Nusselt number is given by

$$Nu = \frac{h\delta}{\kappa} \tag{D16}$$

where δ is the stand-off distance between the heater and the substrate, 5.4 mm. Combining these, and knowing $\kappa(T)$ and $\nu(T)$ for air, we obtain $h(T_g)$, as shown in Figure D-2. Note that this is independent of any estimates of F, the radiative and convective fluxes, etc.

We now proceed as follows: we guess a value for T_g; corresponding to this we have $h(T_g)$, and we then find $h(T_g)(T_g - T_a) \equiv \phi^*$. We must do this until $\phi^* = \phi_c$, as given in Table D-1. This procedure converges quite rapidly, and we find the values of T_g and $h(T_g)$ shown in columns 9 and 10. Finally, dividing hf by the now-known values of h, we obtain the values of f shown in column 11. There are two things to be noted about f: it is almost as large as it can get (*i.e.*, close to unity), and it is approximately independent of ϕ_{tot}.

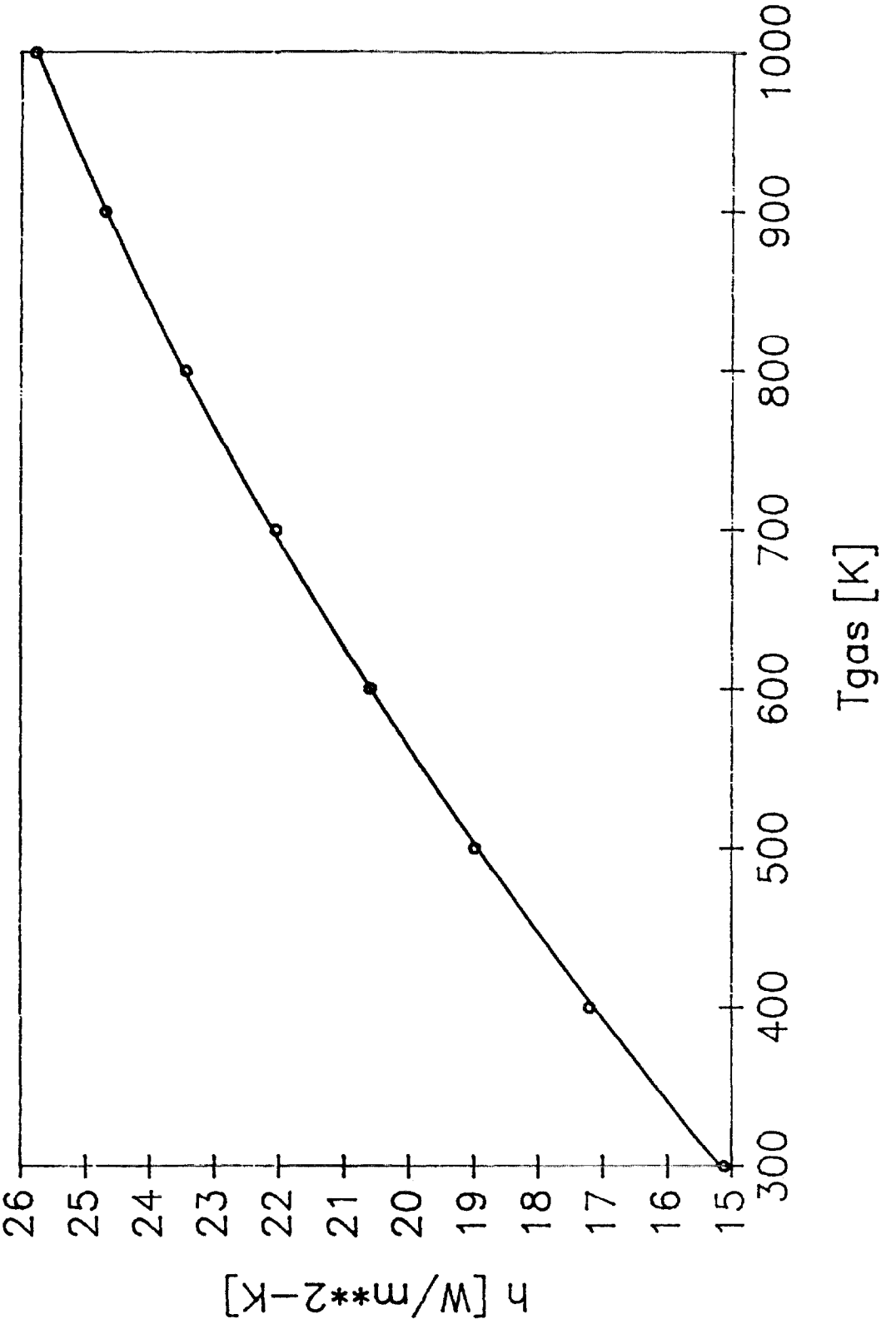

Figure D-2. Calculated heat transfer coefficient, as a function of the temperature T_g of the impinging purge gas jet

APPENDIX E

THERMOPHYSICAL DATA FOR COTTON

The fabric is a weave of cotton fibers. Cotton itself is a flexible, hollow tube of cellulose; the central channel is called the lumen, and occupies a fraction η of the total volume. Thus we would expect that the density of cotton is about

$$\rho(\text{cotton}) = (1-\eta)\rho_s,$$

where ρ_s is the density of the solid (largely α-cellulose). Measurements yield $\eta = 0.2 - 0.4$. However, Brandrup and Immergut (1989) gives the following data on page V-122. (The references given there to the original authors are omitted here for brevity):

Material	Density (g/mℓ)
Cellulose I	1.582-1.630
Cellulose II	1.583-1.62
Cellulose III	1.61
Cotton	1.545-1.585

Thus, the density of cotton appears to be very nearly the same as that of the solid (cellulose) implying that $\eta \approx 0$. We will hereafter ignore the apparently small difference between α-cellulose and cotton, and take the (mean) density to be $\rho_s = 1.565 \pm 0.02$ g/mℓ.

For many polymers, there is only a weak dependence of the thermal conductivity on T, between 100 and 300 K (see Siegel and Howell (1981) Figure 68). One can get an idea of the variability of the thermal conductivity of cotton and of cotton fabrics from Figures AA-AC, in Kakaç *et al.*

Measurements at NIST by J.R. Lawson (private communication) have shown that the density of #10 duck is $\rho \approx 0.6$ g/cm^3, that of #6 duck is 0.72 g/cm^3, and that of all the other cotton duck fabrics measured is

$$\rho_f = \rho(\text{fabric}) = 0.62 \text{ g/cm}^3 = 620 \text{ kg/m}^3.$$

The "void fraction" of the fabric is Φ. With $\rho_s = 1.565$, $\rho_f = 0.62$, and with ρ_a = density of air at STP = 1.774×10^{-3} g/cm^3, the relationship

$$\rho_f = (1 - \Phi)\rho_s + \Phi\rho_a$$

yields $\Phi = 0.6045$.

Next, consider the specific heat. Again, the values given in Brandrup and Immergut (1989) are:

Material	Specific Heat (J/g K)
Cellulose	1.34
Cotton	1.22
	1.15-1.18 (0-34 °C)
	1.32 (0-100 °C)
	1.327-1.251
	1.273-1.35

Where the temperature range is not listed, it is assumed to be the ambient (20 or 25 °C). We will thus not be far wrong it we take $c_s = 1.3$ J/g-K,

where the subscript "s" stands for "solid" (cotton or α-cellulose). We expect that, just as was the case for density,

$$c_f = c(\text{fabric}) = \Phi c_{air} + (1 - \Phi)c_s.$$

Hence

$$c_f \approx 1.122 \text{ J/g-K}, \qquad \text{at } T \approx 300 \text{ K}.$$

This author has not been able to find the **temperature dependence** $c_s(T)$; we will defer that question for the moment.

Finally, we come to the thermal conductivity, κ. This is a quantity which is notoriously difficult to obtain accurately. Figure E-1, from Childs *et al.* (1973), shows the large variations in thermal conductivity depending on measuring conditions. Many of the low values (nos. 5, 6, and 8, for example) were measured in a vacuum. Numbers 4 and 9, on the other hand, were similar specimens, measured in air at 25 °C. However, #9 had over three times the density of #4 and would therefore have been expected to have a substantially higher thermal conductivity.

We list here four sources for the thermal conductivity:

a. The apparently most consistent data from Childs *et al.* (1973): curves 1, 2, and 3, and point 7, give

$$\kappa \approx 0.0365 \text{ W/m K} \quad \text{at } T = 306 \text{ K} = 33 \text{ °C}$$

b. We have the following data for cotton paper, from Brandrup and Immergut (1989):

T (°C)	κ (W/m K)
30	0.049
40	0.071
50	0.084
60	0.090

A curve-fit to these points, if extrapolated, would predict that κ vanishes at (and below) $T \approx 10$ °C, which is nonsense.

c. Touloukian *et al.* (1970) give:

T (°C)	κ (W/m K)
0	0.056
20	0.058
100	0.067

The density of the material for these measurements is listed as 81 kg/m^3; hence $\Phi = 0.9493$. Then equation (14) gives

$$\kappa = 0.03408\kappa_s + 0.9828\kappa_g \qquad \text{(E1)}$$

while the tabular data are reasonably well fitted by

$$\kappa(T) = 0.056 + 1.1\text{x}10^{-4}T, \quad \text{with T in °C} \qquad \text{(E2)}$$

We have $\kappa_{air}(25\ °C) = 0.02624$ W/m K; now if the data in the table are the conductivities for the light cotton/air mixture, then at 20 °C, with $\kappa_g = \kappa_{air}$, equation (E1) yields $\kappa_s = 0.945$, which is an unreasonably large value. According to Kunii (1961), the value for the gas-phase thermal conductivity to be used in equation (14) is 1.7 times what it is in the ambient. If we use $\kappa_{gas} = 1.7\text{x}0.02624 = 0.04461$, the resulting value of κ_s is $\kappa_s = 0.415$ W/m K, still very large. If, on the other hand, the listed values are for κ_s, then $\kappa_s = 0.058$ and $\kappa_g = \kappa_a$ imply that $\kappa = 0.0278$, while for $\kappa_g = 1.7\kappa_a$, $\kappa = 0.0458$. Thus none of the combinations is plausible.

d. Ohlemiller has made measurements of the thermal conductivity of the (#12) cotton duck; the apparatus only works properly when the sample is thermally thick, however. Therefore he carried out a series of measurements, with an increasing number of layers of the fabric. It was then possible to infer the asymptotic value which would be reached if the number of layers had been increased to a very large number: It was assumed that

$$\kappa(n) = \kappa_\infty[1 - \exp(-n\Theta)],$$

where Θ = dimensionless thickness of one layer, and n = number of layers. The data were:

n	κ
0	0
6	0.050
12	0.077
18	0.099

The Asymptotic value of the series at the left is 0.9. That is $\kappa_\infty = 0.13$ J/m K.

$\kappa = 0.13$ is about twice the value (0.056) found in the Handbook, as quoted in c., just above. Recall that for this fabric, the void fraction is 0.6045. With $\Phi = 0.6045$, equation (14) gives

$$\kappa = 0.28505\kappa_s + 0.84554\kappa_{gas}$$

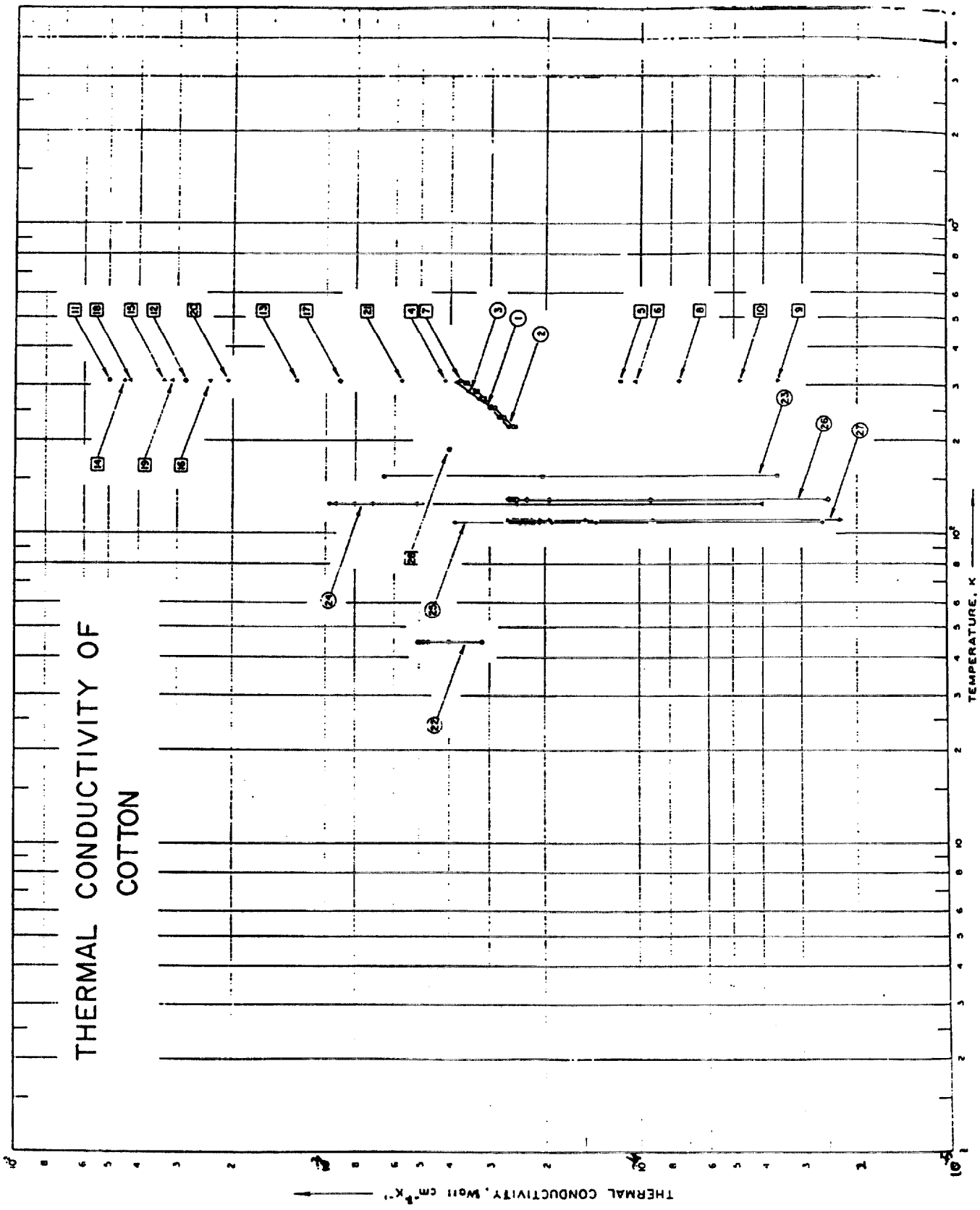

Figure E-1. Thermal conductivity of cotton as a function of temperature, as measured by different workers

If we use $\kappa_{gas} = \kappa_{air}$, we would then infer that $\kappa_s = 0.378$, which is an order of magnitude greater than the earlier estimates. If we use $\kappa_{gas} = 1.7\kappa_{air}$, then $\kappa = 0.13$ implies $\kappa_s = 0.324$, only a little smaller. The latter value is not too different from the 0.415 found in source c., above.

We thus take $\kappa_a \equiv \kappa_s(T_a = 25\ °C) \approx 0.324$ W/m K

and $\kappa(T_a) \approx 0.13$ W/m K

Assuming that the temperature dependence is like that given by eqaution (E2), we find that

$$\kappa(T) = 0.125 + 2.457\text{x}10^{-4}\,T, \qquad \text{(E3)}$$

with T in °C. Alternatively, we might use equation (14) in its more general form, that is, including the temperature dependence

$$\kappa(T) = 0.28505\kappa_s(T) + 0.84554(1.7)\kappa_{air}(T) \qquad \text{(E4)}$$

For air, $\kappa(T)$ is given by equation (52) in Childs *et al.* For the solid, a reasonable assumption is that the conductivity is proportional to the absolute temperature, and that it is also proportional to the density. Thus $\kappa_s(T)$ is given by

$$\kappa_s(T) = \kappa_s(T_a)\,\rho T/\rho_a T_a \cong 0.3237\,\rho T/\rho_a T_a \qquad \text{(E5)}$$

We now turn to the question of the **temperature dependence** of c_f. For a number of materials, the thermal diffusivity is relatively insensitive to T. This is, in particular, the case for **wood** (see Parker 1985, 1987) which consists, to a significant extent, of cellulose and related compounds. If we assume that to be the case for cotton, then we could write

$$\kappa(T) = \alpha\rho c(T); \qquad \text{(E6)}$$

c(T) is generally much easier to measure than $\kappa(T)$, and this would be a relatively good way to obtain $\kappa(T)$; the irony is that we do not have c(T) for cotton or cellulose.

If we take $\kappa_f = 0.13$ for the fabric at ambient temperature, we now find that

$$\alpha \equiv \kappa/\rho c \approx 0.13/(620)(1122) = 1.87\text{x}10^{-7}\ m^2/s$$

We therefore have, finally,

$$c(T) = \kappa/\rho\alpha \approx \kappa(T)/620(1.87\text{x}10^{-7}) = 8630\kappa(T)\ \text{J/kg K}$$

where $\kappa(T)$ is given by equation (E3), or by (E4), if preferred.

APPENDIX F

HEAT TRANSFER COEFFICIENT IN THE PRESENCE OF A SUBSTRATE

It is first assumed that there is no x-dependence of cigarette or substrate temperature. Now refer to Figure F-1; we need to know how the losses from point P on the cigarette to the substrate surface depend on θ. For the convective losses, it is clear that for small θ, they will depend on the substrate temperature in the neighborhood of P. In fact, for each angle θ, we may identify a mean value y associated with it. For $\theta = \pi/2$, buoyant convection carries gases directly away from the surface, so that the associated value of y is $y = \infty$, and the convective losses are precisely as they would be for the free cigarette. In general, we may write

$$\phi_c(\theta) \approx h_s(y)\,[T_c(\theta) - T_s(y)] \tag{F1}$$

where we have explicitly assumed that T_c may vary around the circumference.

It is now necessary to integrate this around the circumference, to obtain the total (convective) energy loss rate (per unit length). An expression was found relating θ and y; in order to enable explicit calculations to be carried out, it was assumed that $T_s(y)$ can be approximated by the expression

$$T_s(y) \sim T_o + \Delta T\, e^{-y^2/s^2} \tag{F2}$$

with

$$\Delta T \equiv T_s(y=0) - T_o\ . \tag{F3}$$

The integration is carried out in two steps. First, suppose that T_c does **not** vary around the circumference; the flux can then be integrated, with the result

$$\begin{aligned}\int_0^{\pi} \phi_c(\theta)\,d\theta \approx\ & \pi\left[h_o + \frac{\Delta h}{2}\, e^{\eta}\, erfc\sqrt{\eta}\,\right](T_c - T_o) \\ & - \frac{\pi}{2}\Delta T\left[h_o e^{\zeta}\, erfc\sqrt{\zeta} + \Delta h\, e^{\eta+\zeta}\, erfc\sqrt{\eta+\zeta}\right]\end{aligned} \tag{F4}$$

where

$$\sqrt{\eta} \equiv R/\sigma_y \qquad \text{and} \qquad \sqrt{\zeta} \equiv R/s \tag{F5}$$

Assuming s = R, $\sigma_y = 0.8R$, $h_o = 10$, and $\Delta h = 61$, equation (F4) yields

$$\int_o^{\pi} \phi_c\, d\theta \approx \frac{\pi}{2}\left[42.437(T_c - T_a) - 20.923\,\Delta T\right] \tag{F6}$$

Next, the variation in surface temperature around the circumference was taken into account. It was assumed that

$$T_c(\theta) \approx \begin{cases} T_c(\pi/2) - \tau(1 - 2\theta/\pi) & -\pi/2 \le \theta \le \pi/2 \\ T_c(\pi/2) & \pi/2 < \theta \le 3\pi/2 \end{cases} \tag{F7}$$

where

$$\tau \equiv T_c(\pi/2) - T_c(0) \tag{F8}$$

Note that $T_c(\theta=0)$ is the minimum temperature around the circumference. Hence we may write $T_c(\theta=0) \equiv T_{c,min}$. We will shortly see that τ is in fact a function of x and t. The time dependence of $T_c(\theta)$ has been suppressed for brevity. Assuming that the T_c used earlier is the maximum temperature, a simple integration around θ shows that $\pi(18.0366)\tau/2$ must be subtracted from the above result. Hereafter, T_c will always mean the peak temperature around the circumference.

We want to run the cigarette program with model input values of h, T_c, and/or T_a such that the "isolated" cigarette will have the indicated energy loss *via* convection. This can be achieved, for example, by using an effective heat transfer coefficient h*, such that

$$\int_0^{\pi} \phi_c(\theta) d\theta = \int_0^{\pi} h^*(T_c - T_a) d\theta = \pi h^*(T_c - T_a) \tag{F9}$$

Thus, from equation (F6),

$$h^* = 21.22 - 10.47\left(\frac{T_s - T_a}{T_c - T_a}\right) - 9.02\left(\frac{T_c - T_{c,min}}{T_c - T_a}\right) \qquad \text{W/m}^2\text{K} \tag{F10}$$

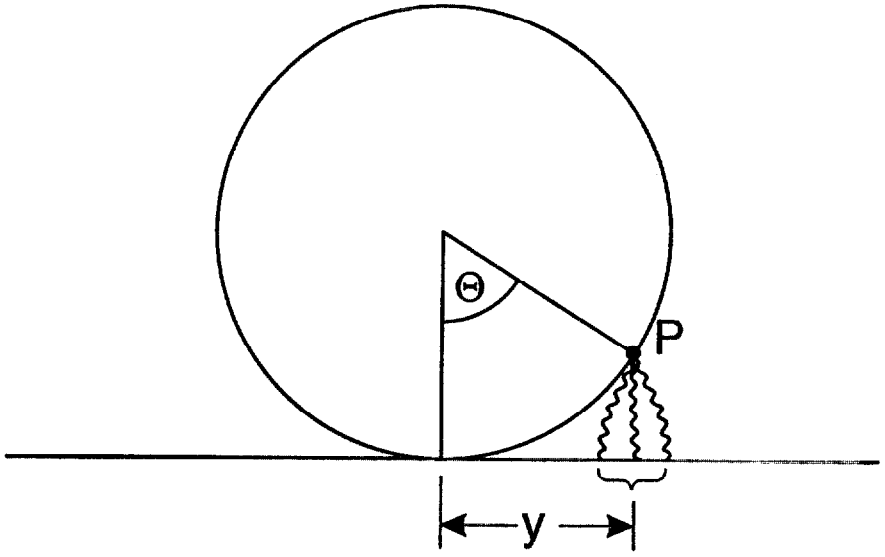

Figure F-1. Schematic of the exchange of energy between point P on the cigarette surface and the substrate surface.

APPENDIX G

CALCULATION OF THE CONVECTIVE VIEW FACTOR

The conductive flux distribution in the transverse direction, $\phi_c(x,y,t)$, is calculated in Appendix 5-D of Gann *et al.* (1988). The approximate expression

$$\phi(0,y,0) \approx \phi(0,0,0)\,\frac{a^2}{a^2 + y^2} \tag{G1}$$

is derived there, where $\phi_c(0,0,0)$ is the (peak) initial conduction/convection flux along the line of contact; this flux falls rapidly with time. The parameter a is of the order R/2. Equation (G1) gives $\Omega_c(y)$ implicitly.

Experimental measurements (Gann *et al.* (1988), Section 4) have shown that the (total) flux from a cigarette can be fitted approximately with a distribution of the form

$$\phi_{in}(x,y,t) = \phi_{max} \exp\left[\left(\frac{x - x_o - vt}{\sigma_x}\right)^2 - \frac{y^2}{\sigma_y^2}\right] \tag{G2}$$

If expanded as a power series, this agrees with equation (G1), to lowest order in y^2. The total energy output from the distribution (B2) is

$$\dot{E} = \iint \phi(x,y)\,dx\,dy = \pi \sigma_x \sigma_y \phi_{max} \tag{G3}$$

Reasonable agreement with experiment is obtained with $\sigma_x = 0.6$ cm and $\sigma_y \approx 0.32$ cm. This suggests that the above implicit expression for $\Omega_c(y)$, equation (G1), be modified to be a Gaussian. That is, the coefficient in equation (139) is

$$h_s(y) = h_o + \Delta h\, e^{-y^2/\sigma_y^2} \tag{G4}$$

where

h_o = background $\approx$ 10 W/m^{2}K and $\Delta h = h_c - h_o \approx 61$ W/m^{2}K.

APPENDIX H

LONGITUDINAL DEPENDENCE OF RADIATION FLUX TO THE SUBSTRATE

If the cigarette surface were at the uniform temperature T_c, and the view factor for the cigarette for some point P on the substrate were Ω (the fraction of energy emitted by the given substrate area which would be intercepted by the cylinder), one might think that the radiation flux reaching P is

$$\phi_p = \Omega \phi_c + (1 - \Omega)\phi_a \tag{H1}$$

where

$$\phi_c \equiv \epsilon_c \sigma T_c^4 \tag{H2}$$

is the flux from the cigarette and

$$\phi_a \equiv \sigma T_a^4$$

is the ambient flux. If one properly considers the reflections between cigarette and substrate, however, then with the further assumption that the surface temperature of the substrate, T_s, is also uniform, one finds that the correct expression would be

$$\phi_p = \frac{\Omega \phi_c + (1 - \Omega)\phi_a}{1 - a\Omega} + \frac{(1 - \epsilon_c)\Omega^2 \phi_s}{1 - a\Omega^2}, \tag{H3}$$

where

$$\phi_s \equiv \epsilon_s \sigma T_s^4 \tag{H4}$$

and

$$a \equiv (1-\varepsilon_s)(1-\varepsilon_c). \tag{H5}$$

Equation (H3) reduces to (H1) in the case $\epsilon_c = 1$. The more general case, where neither T_s nor T_c are uniform over the surfaces, involves some very complex integrations which can generally not be carried out analytically.

Indeed, T_c is in fact **not** uniform, but highly peaked. The longitudinal (*i.e.*, parallel to the axis) net radiation flux distribution from the surface of the freely smoldering cigarette,

$$\phi_r(x) = \epsilon_c \sigma \left[T_c^4(x) - T_a^4\right] \tag{H6}$$

can be again be approximated by a Gaussian:

$$\phi_r(x) \approx \epsilon_c \sigma (\Delta T)^4 \exp\left[-\frac{(x - x_o)^2}{s^2}\right] \tag{H7}$$

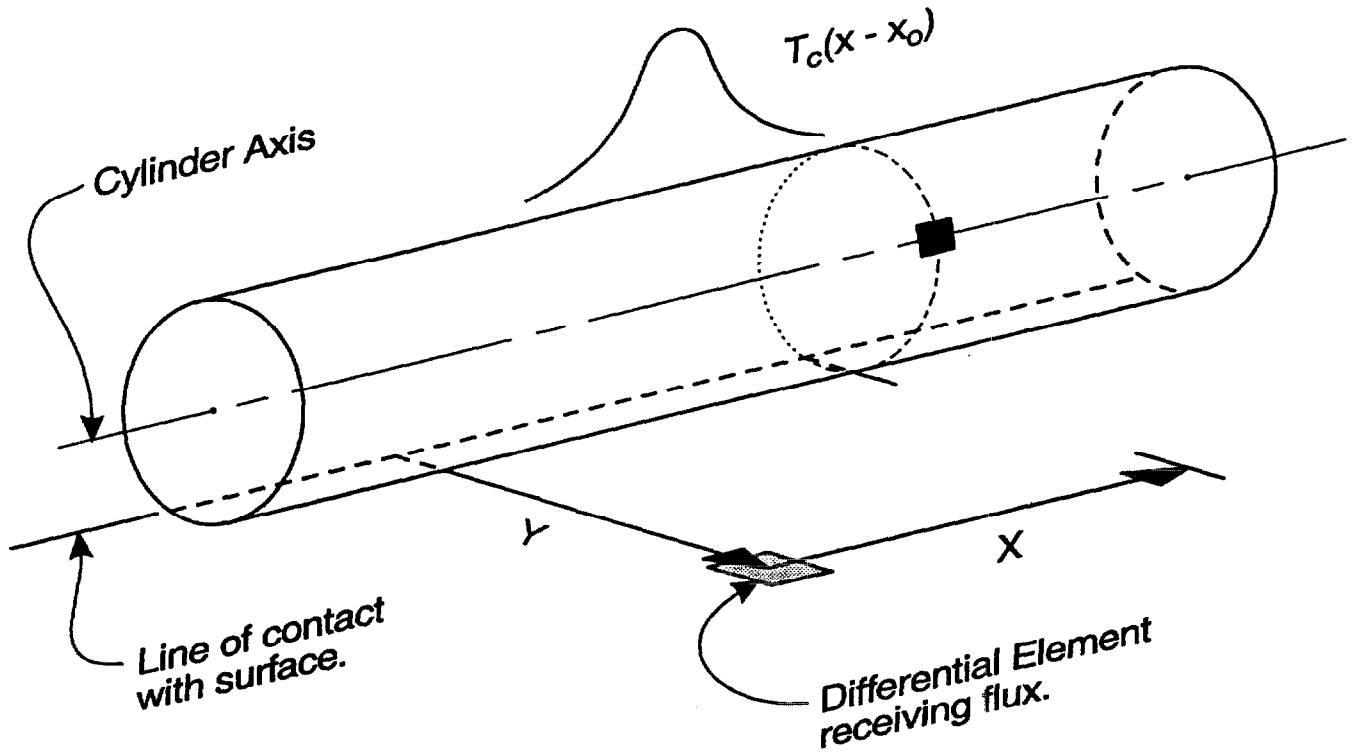

Figure H-1. The geometric relationship between a general point on the cigarette and another on the substrate. The profile above the cigarette is its surface temperature, with its peak at x_o.

Thus the peak flux from, and peak temperature on, the cigarette surface both occur at $x = x_o$; equation (H7) gives the peak flux, and equation (H8) defines ΔT:

$$T_{max}^4 = T_c^4(x_o) = T_a^4 + (\Delta T)^4 \tag{H8}$$

Thus, even if we had had the simple approximation (H1) rather than (H3), it must be generalized to

$$\phi_p = \epsilon_c \int \sigma T_c^4(x) d\Omega + (1 - \Omega)\phi_a \tag{H9}$$

where

$$\int d\Omega = \Omega$$

and where $d\Omega$ is the view factor from a differential element on the plane to the differential cylindrical shell of width dx, a distance x in the axial direction and a distance y in the orthogonal direction, as shown in Figure H-1. (See reference [20] in Siegel and Howell (1981).) However, we do not have an analytic expression for $d\Omega$.

Two alternative approximations were investigated: in one, the cylindrical shell is approximated (for $y > R$) as a wall of height $a \sim 2R$. In another, the Gaussian distribution (38a) was approximated by a band of constant (peak) temperature, of equivalent width. That is,

$$\int_{-\infty}^{\infty} \phi_{max} e^{-x^2/s^2} dx = \sigma \phi_{max} \tag{H10}$$

This equation yields

$$\sigma = \sqrt{\pi}\, s \tag{H11}$$

Thus, if $s = \sigma_x$, then with $\sigma_x \approx 6.1$ mm, $\sigma \approx 1$ cm. Neither of these approximations was satisfactory.

Although obtaining the **general** expression for Ω is a task of daunting complexity, we may obtain a crude approximation as follows: It is clear that the flux at (x,y) is most strongly determined by the cigarette temperature at the nearest points. These are just the points at x -- that is, on the normal to the cigarette at x. Carrying this through to its logical conclusion, we may assume that the flux at any point (x,y) depends <u>only</u> on the local temperature, $T_c(x)$. This achieves an enormous simplification.

In fact, since each point on the substrate receives radiation from other points on the cigarette as well, the actual distribution will have a slightly larger half-width than that on the cigarette. The effect can be expected to be small, however.

Thus at any given distance y from the contact line, the flux distribution over the substrate surface (along the x coordinate) obtained this way will be similar to the distribution on the cigarette surface, only scaled down appropriately, as we shall now see. There then remains the task of determining how the flux falls off with distance y from the cigarette surface.

From Sparrow and Cess (1978), we find that for a thin but infinitely long strip on the substrate, parallel to the cylinder axis and a distance y from it, the configuration (view) factor $F_{sc} \equiv \Omega$ is

$$\Omega(y) = \frac{R^2}{R^2 + y^2} \tag{H12}$$

where R is the cylinder radius. This is precisely of the same form as the factor for conduction. (See equation (B1).) This is a one-dimensional calculation; clearly, for the two-dimensional case, the flux will fall off faster. A simple expression which falls off faster but has the same y-dependence for small y is the Gaussian dependence $\exp(-y^2/R^2)$. More generally, the variance of the distribution may be somewhat different from R (though it may be expected to be *proportional* to R); call it σ_y. Thus we will use

$$\Omega(y) = e^{-y^2/\sigma_y^2} \tag{H14}$$

Since we found above that $\sigma_y \approx 3.2$ mm for R = 4mm, we may take, in general,

$$\sigma_y = 0.8R \tag{H14}$$

The improvement (over simply assuming that the heat flux profile is Gaussian in the y direction) which would be obtained by carrying out the formidable integrations indicated above, hardly justifies the effort. This holds even more strongly for the more complete expression, equation (H3). We thus use

$$\Omega_c(y) \approx \Omega(y) \approx \exp\left(-y^2/\sigma_y^2\right) \tag{H15}$$

for the sake of simplicity.

Now consider the **net** flux from the cigarette to the substrate: along the line of contact, $\Omega = 1$; therefore equation (H3) yields

$$\phi_{net,rad} = \frac{\epsilon_s \epsilon_c}{1-a}\sigma\left(T_c^4 - T_s^4\right) \tag{H16}$$

where a is given by equation (H5).

The radiation flux is treated in the same way as the convective flux, that is,

$$\phi_{net,r} = \epsilon_r \Omega \sigma(T_c^4 - T_s^4) - (1-\Omega)\epsilon_s \sigma(T_s^4 - T_a^4), \tag{H17}$$

where ε_r is given by equation (142), and this is split into an effective radiation from cigarette to substrate,

$$\phi_{cig,r} = \epsilon_r \Omega \sigma\left(T_c^4 - T_a^4\right) \tag{H18}$$

while the substrate radiates away at the rate

$$\phi_{sub,r} = \left[\epsilon_r \Omega + \epsilon_s(1-\Omega)\right]\sigma\left(T_s^4 - T_a^4\right) \tag{H19}$$

Note that we have taken the reflections from the cigarette partially into account, by using ε_r rather than ε_c; however, we have not made the fuller analysis, as in getting equation (H3).

All of the above holds for $0 \leq x \leq L$.

APPENDIX I

TRANSIENT DEPRESSION OF CIGARETTE TEMPERATURE UPON DEPOSITION ON A SUBSTRATE

As noted above, finding $T_{c,min}(t)$ is a very complex problem; a simple approximation is possible, however: this problem has been solved for the special case of two semi-infinite solid slabs (homogeneous, isotropic, uniform) of different temperatures, coming into contact (Carslaw and Jaeger (1959), Section 2.15). In the vicinity of the contact line, and for a short period, this solution will be approximately (and locally) valid.

It is assumed there that there is perfect thermal contact between the two surfaces, so that the temperatures at the interface immediately reach the mean value

$$\bar{T} = \frac{T_a + T_c}{1 + r} \tag{I1}$$

where r is the ratio of the thermal inertias of the materials:

$$r \equiv \sqrt{\frac{(k\rho c)_s}{(k\rho c)_c}} \tag{I2}$$

The temperature of the substrate varies with z and t according to

$$T_s(z,t) = T_a + \bar{T}\, erfc\left[\frac{z}{2\sqrt{\alpha_s t}}\right] \tag{I3}$$

where z is to be taken as positive into the substrate, and α_s is the thermal diffusivity of the substrate. The temperature of the other "slab" (the bottom of the cigarette) is

$$T_c(z,t) = \bar{T}\left[1 + r\, erf\left(\frac{z}{2\sqrt{\alpha_c t}}\right)\right] - T_a \tag{I4}$$

Since the thermal contact between cigarette and substrate is **not** perfect, their actual surface temperatures correspond to small finite depths z, in equations (I3) and (I4).

For a common fabric/foam substrate, the thermal properties are (Section II.D.2): k_s = 0.1435 W/mK, ρ_s = 620 kg/m^3, and c_s = 1122 J/kg K. Hence α_s = 2.063 x 10^{-7} m^2/s and the thermal inertia = 316 Ws$^{1/2}$/m^{2}K. For a cigarette, we find (Mitler, 1988) k_c = 0.316 W/mK, ρ_c = 620 kg/m^3, and c_c = 1043 J/kg K. Hence α_c = 1.165 x 10^{-6} m^2/s and the thermal inertia = 293, not very different from that of the substrate. With these two values, we find r = 1.0795. With T_c = 600 °C and T_a = 20 °C, equation (I1) yields $\langle T \rangle \approx$ 298 °C.

For this cotton fabric/foam, the temperature fall in a couple of seconds is estimated to be 50-70 °C at the flux peak, at the side of the cigarette; that is, at $\theta = \pi/2$. Hence the assumption made above that the cigarette temperature is unaffected at the side is not quite correct. At θ = 0, in fact, the temperature fall

was greater than 200 °C; the precise temperature could not be measured. Thus, $\delta T_{max} \approx 200$ °C. Then from equation (I4) we find that $erf(x/2\sqrt{\alpha_c t}) \approx 0.38$, for t ≈ 2 s. Assuming that the thermal diffusivities do not vary a great deal among cigarettes, we may take this term to be a constant. In general, then, assuming that $x/2\sqrt{\alpha_c t} \approx const.$, we may write, from equation (I4),

$$\delta T_{max} \approx T_c + T_a - [1 + 0.38\, r]\, \bar{T}$$

or

$$\delta T_{max} \approx 0.62\, r\, \bar{T} \qquad \text{(I5)}$$

Glass, as a substrate, is a more effective heat sink than a cotton fabric. Indeed, we find that the thermal inertia for ordinary glass is about 1690; hence in this case, r = 1690/316 = 5.35, and with T_c = 600 °C and T_a = 20 °C,

$$\bar{T} = \frac{620}{1 + r} = 97.7\ ^\circ C$$

and

$$\delta T_{max} \approx 324\ ^\circ C$$

APPENDIX J

MASS TRANSFER COEFFICIENTS

Baker and Crellin (1977) measured the diffusion of CO through cigarette paper. For CO in nitrogen, $D_o = 0.21$ cm^2/s, while for oxygen in nitrogen, $D_o = 0.199$ cm^2/s. These are close enough that we may take the results for CO to be valid for oxygen. They found the relationship:

$$D_p = A\sqrt{Z} \tag{J1}$$

between the diffusion coefficient of CO through the inherently porous cigarette wrapping paper, and the permeability Z of the paper, to hold. Here:

D_p is in 10^{-3} cm^2/s

and Z is in units of cm^3/min (10 cm^2 10 cm water)$^{-1}$

The value of A is 0.57, in the appropriate units. Permeabilities range between 16 and 2000, in these units, so D_p ranges between 1 and 22, with many of the papers in the region about:

$$D_p = 7 \times 10^{-3} \text{ cm}^2/\text{s}.$$

Cigarette paper thickness is $\delta = 43 \pm 5$ μm. Taking the mean, this yields:

$$\gamma_p = D_p/\delta \approx 1.6 \text{ cm/s}$$

For $\gamma_g = \gamma_b$, the boundary-layer value, we use equation (118). Then at the peak surface temperature ($T_s \approx 600$ °C), the mean value of temperature to be used in equation (118) is 310 °C = 583 K. We then get:

$$\gamma_b \approx 3.3 \text{ cm/s}.$$

According to these results, the resistance to diffusion through the paper is only about twice that through the boundary layer. The combined value, according to equation (122), is

$$\gamma \approx 1.1 \text{ cm/s}.$$

APPENDIX K

NOMENCLATURE

B = Biot number
C_g = specific heat of the gases
C_s = specific heat of the solid
D_e = diffusion coefficient for oxygen
D_{io} = diffusion coefficient for species i in the background "o" [equation (26)]
D_p = mean pore diameter
E_p = activation energy for the pyrolytic reaction
g = acceleration of gravity
h = heat transfer coefficient
h_{in} = mean convective heat transfer coefficient between cigarette and surface
h_q = heat transfer coefficient between cigarette and quiescent air
h_c = convective heat transfer coefficient; heat of combustion per unit mass
h_e = convective heat transfer coefficient (at the end)
h_r = heat transfer coefficient for radiation; see equations (15) and (106)
H_c = molar heat of combustion
k = thermal conductivity of the cigarette (see Section III.D.1, assumption #8)
k_g = thermal conductivity of the gas
k_{op} = normalized reaction rate (in min^{-1})
k_s = thermal conductivity of the solid shreds
l_c = a characteristic dimension [see equation (34)]
L = length of tobacco column
m = mass of tobacco column
n_A = no. of grams of ash yielded by the burning of one gram of char
n_c = no. of grams of char produced by the pyrolysis of one gram of tobacco
n_{O2} = no. of grams of oxygen which react with one gram of char
Nu = Nusselt number
Pr = Prandtl number
Q_{co} = energy released from char oxidation (lower heat of combustion)
Q_p = energy absorbed in (endothermic) pyrolysis
$\dot{Q}_i$ = energy loss rates: see Section III.B.7
$\dot{Q}$ = mean power produced during combustion
r = radial coordinate; ratio of thermal inertias [see equation (I2)]; stoichiometric fuel/oxygen ratio
R = universal gas constant; cigarette radius
Ra = Rayleigh number
Re = $u_o l_c/\nu$ = Reynolds number
R_p, R_{op} = pyrolysis rate (in $gm/cm^3 s$)
R_{co} = char oxidation rate
Sc = Schmidt number (Sc = ν/D)
S_i = source/sink term [equation (26)]
T = absolute temperature
$T_{c,min}$ = cigarette surface temperature at contact line
T_{cig} = cigarette surface temperature
T_s = surface temperature of the substrate
u_r = radial (convective) gas velocity

V = total volume of the cigarette
V_s = total volume occupied by the solids in the cigarette
x = coordinate; axis of cylinder representing cigarette
X_{ox} = volume fraction of oxygen
y = oxygen mass fraction
Y_s = surface value of y
y_a = ambient value of y
y_o = "local" ambient (inside cigarette); used in heterogeneous models
y_s = value of y at cigarette (or shred) surface
y_T = tobacco mass fraction
Z_p = pre-exponential factor in reaction rate equation (108)
Z_{CO} = pre-exponential factor in reaction rate equation (110)

Greek Symbols

α = thermal diffusivity of gas
β = volumetric coefficient of (gas) expansion; parameter in equation (56)
γ = mass transfer coefficient for air + paper
γ_b = mass transfer coefficient for air (the boundary layer) alone
δ = characteristic penetration depth
ϵ = emissivity of the fabric (assuming that α, the absorptivity, = ε)
ε_A = emissivity of the (paper) ash
ε_{cig} = emissivity of cigarette
ε_T = emissivity of the shreds
ε_s = emissivity/absorptivity of the substrate (assumed constant)
θ = e-folding distance in equations (40)-(43)
κ = thermal conductivity of the substrate
κ_s, κ_g = solid and gas-phase thermal conductivities, respectively
ν = kinematic viscosity of air
ρ_g = mass density of the gases
ρ_T = tobacco density
ρ_s = mass density of the solid
σ = Stefan-Boltzmann constant
τ = total duration of the smolder
ϕ = void fraction in the cigarette (*i.e.*, the volume fraction of gas, rather than of tobacco shreds)
Φ = total void fraction (including the void space in the shreds, and is therefore larger than ϕ)
ϕ_a = ambient radiation flux = σT_a^4
ϕ_c = radiation flux from cigarette; convective flux (substrate)
ϕ_c^* = model convective heating flux from cigarette (see equation (9))
ϕ_{in} = heating flux reaching the substrate surface
ϕ_{net} given by equation (6)
ϕ_{out} = surface heat loss of the surface to the ambient, for the areas away from the cigarette
ϕ_r = radiation flux (substrate)
Ω = $\Omega(r)$ = radiation view factor of the cigarette as seen by the substrate at the point r
Ω_c = fraction giving influence of convection at a given point

Subscripts

a = ambient; ash
c = convection; cigarette; char
g = gas
m = maximum
o = original; ambient
p = pyrolysis; peak
r = radial; radiation; effective
s = surface; substrate; solid
t = tobacco; total
x = in x-direction (axial)

NIST-114
(REV. 9-92)
ADMAN 4.09

U.S. DEPARTMENT OF COMMERCE
NATIONAL INSTITUTE OF STANDARDS AND TECHNOLOGY

MANUSCRIPT REVIEW AND APPROVAL

(ERB USE ONLY)
ERB CONTROL NUMBER: W93-1417
DIVISION: 864
PUBLICATION REPORT NUMBER: NIST/SP 852
CATEGORY CODE: 240
PUBLICATION DATE: August 1993
NUMBER PRINTED PAGES: 169

INSTRUCTIONS: ATTACH ORIGINAL OF THIS FORM TO ONE (1) COPY OF MANUSCRIPT AND SEND TO: THE SECRETARY, APPROPRIATE EDITORIAL REVIEW BOARD.

TITLE AND SUBTITLE (CITE IN FULL)

Modeling the Ignition of Soft Furnishings by a Cigarette

CONTRACT OR GRANT NUMBER

TYPE OF REPORT AND/OR PERIOD COVERED: Final

AUTHOR(S) (LAST NAME, FIRST INITIAL, SECOND INITIAL)

Mitler, H. E., and Walton, G. N.

PERFORMING ORGANIZATION (CHECK (X) ONE BOX)

- [xX] NIST/GAITHERSBURG
- [ ] NIST/BOULDER
- [ ] JILA/BOULDER

LABORATORY AND DIVISION NAMES (FIRST NIST AUTHOR ONLY)

Building and Fire Research Laboratory, Fire Safety Engineering Division

SPONSORING ORGANIZATION NAME AND COMPLETE ADDRESS (STREET, CITY, STATE, ZIP)

RECOMMENDED FOR NIST PUBLICATION

- [ ] JOURNAL OF RESEARCH (NIST JRES)
- [ ] J. PHYS. & CHEM. REF. DATA (JPCRD)
- [ ] HANDBOOK (NIST HB)
- [X] SPECIAL PUBLICATION (NIST SP)
- [ ] TECHNICAL NOTE (NIST TN)
- [ ] MONOGRAPH (NIST MN)
- [ ] NATL. STD. REF. DATA SERIES (NIST NSRDS)
- [ ] FEDERAL INF. PROCESS. STDS. (NIST FIPS)
- [ ] LIST OF PUBLICATIONS (NIST LP)
- [ ] NIST INTERAGENCY/INTERNAL REPORT (NISTIR)
- [ ] LETTER CIRCULAR
- [ ] BUILDING SCIENCE SERIES
- [ ] PRODUCT STANDARDS
- [ ] OTHER

RECOMMENDED FOR NON-NIST PUBLICATION (CITE FULLY) [ ] U.S. [ ] FOREIGN

PUBLISHING MEDIUM

- [X] PAPER
- [ ] CD-ROM
- [ ] DISKETTE (SPECIFY)
- [ ] OTHER (SPECIFY)

SUPPLEMENTARY NOTES

ABSTRACT (A 1500-CHARACTER OR LESS FACTUAL SUMMARY OF MOST SIGNIFICANT INFORMATION. IF DOCUMENT INCLUDES A SIGNIFICANT BIBLIOGRAPHY OR LITERATURE SURVEY, CITE IT HERE. SPELL OUT ACRONYMS ON FIRST REFERENCE.) (CONTINUE ON SEPARATE PAGE, IF NECESSARY.)

This paper describes the user-friendly computer models CIGARET and SUBSTRAT. CIGARET calculates the time-dependent behavior of a cigarette smoldering quietly in the air, away from surfaces. The model incorporates diffusion and convection of gases, as well as the kinetics of char oxidation. It calculates the internal heat fluxes, as well as the internal distributions of temperature, gas velocity, and oxygen concentration. SUBSTRAT determines whether a two-layer solid (with an air gap in between), exposed to a moving heating flux such as is produced by a cigarette, will ignite. Among the processes taken into consideration are three-dimensional heat conduction in the substrate and its pyrolysis. This model has successfully simulated the thermal runaway signifying smoldering ignition of the substrate when it is exposed to a set of external heating fluxes. SUBSTRAT and CIGARET have been designed to work in tandem to simulate the most frequent cause of fatal fires: cigarette ignition of upholstered furniture and bedding. Users' guides are included.

KEY WORDS (MAXIMUM 9 KEY WORDS; 28 CHARACTERS AND SPACES EACH; ALPHABETICAL ORDER; CAPITALIZE ONLY PROPER NAMES)

cigarettes; cigarette model; computer model; free smolder; furniture fires; ignition; mathematical modeling; modeling; pyrolysis; simulation; smoldering; substrates

AVAILABILITY

- [X] UNLIMITED
- [ ] FOR OFFICIAL DISTRIBUTION. DO NOT RELEASE TO NTIS.
- [X] ORDER FROM SUPERINTENDENT OF DOCUMENTS, U.S. GPO, WASHINGTON, D.C. 20402
- [X] ORDER FROM NTIS, SPRINGFIELD, VA 22161

NOTE TO AUTHOR(S) IF YOU DO NOT WISH THIS MANUSCRIPT ANNOUNCED BEFORE PUBLICATION, PLEASE CHECK HERE. [ ]

ELECTRONIC FORM

U.S. Department of Commerce
National Institute of Standards and Technology
Gaithersburg, MD 20899